Title
A structural, geophysical, isotopic and geochemical appraisal of the CSA deposit, Cobar, Australia : implications for the deformation of the Cobar Basin and mineral potential.

Author
Jeffrey, S

Bibliographic citation
Jeffrey, S (1994). A structural, geophysical, isotopic and geochemical appraisal of the CSA deposit, Cobar, Australia : implications for the deformation of the Cobar Basin and mineral potential.. University Of Tasmania. Thesis. https://doi.org/10.25959/23211689.v1

Is published in:

A STRUCTURAL, GEOPHYSICAL, ISOTOPIC AND GEOCHEMICAL APPRAISAL OF THE CSA DEPOSIT, COBAR, AUSTRALIA: IMPLICATIONS FOR THE DEFORMATION OF THE COBAR BASIN AND MINERAL POTENTIAL.

STUART JEFFREY

DEDICATED TO MARGOT.

YOUR ASSISTANCE WAS INSPIRATIONAL.

YOUR TOLERANCE REMARKABLE.

THANK YOU.

TABLE OF CONTENTS

LIST OF FIGURES

LIST OF TABLES

LIST OF MAPS

ABSTRACT

Since the discovery of base and precious metals in Cobar during the latter part of last century much time and effort has been spent researching the geological origins of and factors influencing the Cobar style of deposit. Models have taken three forms, epigenetic, syngenetic, and structural. Problems faced by those working in the Cobar District include

1) relating structures to mineralisation and mineralising events,
2) understanding the source of sulfides and quartz veining, and the relationship between the two, and
3) using geophysics to enhance the knowledge of the basin.

The first of these problems has been clarified by the author conducting detailed surface and underground mapping of the CSA deposit and comparing the results with those of previous workers. The structural mapping showed a pattern consistent with other Cobar deposits and identified structural elements not previously recorded. As a result the timing relationships of these structures was redefined such that three deformation events were identified, D1 being basin closure, D2 being sulfide injection into pipe like fracture zones formed by sinistral deformation, and D3 being simultaneous strike slip west block up movement and quartz injection.

The problem of the significance of quartz veining has been resolved by review of a range of isotopic and geochemical data. Isotopic and geochemical data confirmed sulfide remobilisation by

D3, a metamorphic origin for the quartz, but either a sedimentary or igneous origin for the sulfides. Previous work had suggested the sulfides to be of metamorphic origin based on their being hosted by quartz filled structures. However the structural reinterpretation clearly demonstrates that the quartz occupies structures that displace and hence post date mineralisation.

Regional and local gravity models presented are based on the recovery of an old gravity survey not previously compiled and systematically interpreted. It is shown through the models that it is possible for the mineralised systems to have a relief of more than 2km given certain geological parameters, some of which are based on assumption. Consequently, there is still a need to review and refine the models and assumptions used as there is likely to be more than one valid geological solution to the Cobar Basin geometry. Future use of this data, coupled with some increase in coverage may well change existing regional assumptions about the Cobar Basin.

CHAPTER 1

INTRODUCTION

The Cobar mining field is located in central western New South Wales, Australia, approximately 750km west of Sydney (Fig. 1.1). The field is defined by a narrow elongate belt of NNW trending deposits and mines that extend from the Elura deposit in the north to the Queen Bee deposit in the south. Geologically the field is located within the NW portion of the Lachlan Fold Belt (Fig. 1.2) defined as a Cambrian to Carboniferous rock succession that has been multiply deformed by numerous orogenic events.

Topographically, the area consists of low ridges and alluvial flats at approximately 250m asl. Isolated hills such as those at the CSA, New Cobar, Occidental, Peak and Queen Bee deposits usually represent resistant strata or altered rocks while others may be due to silcrete or ferricrete. Vegetation is scrubby given an annual rainfall of 350mm (which is highly variable) and an annual temperature range of $-5^{\circ}C$ to $50^{\circ}C$.

Since the discovery of base and precious metals at Cobar during the latter part of last century, much time and effort has been spent researching the geological origins of and factors influencing the Cobar style of deposit. Models have taken three forms, epigenetic (Andrews (1913)), syngenetic (Mulholland and Rayner (1958), Sullivan (1950, 1951), Rayner (1969), Robertson (1974), Brooke (1975), Gilligan and Suppel (1978), Adams and Schmidt (1980) and Schmidt (1983)) and structural (Glen (1990, 1988, 1987)). However a combination of these has not been seriously considered.

Consequently the problems the author address in relation to the CSA deposit and Cobar area in general are

1) recording and relating observed structural components of the CSA deposit to other deposits in the Cobar field, Robertson's (1974) work on the CSA deposit, and regional geology,
2) clarify the position relating to the source of the sulfides and quartz veins, and their relationship to structural components,
3) gain a better understanding of the Cobar area geology by reprocessing and using gravity survey data, and
4) propose a model for ore formation and basin deformation.

As for the problem of relating structural components of the basin to a genetic model, the author conducted a detailed structural analysis of the CSA deposit using data from

1) surface mapping (generated by the author and by verifying previous attempts to map the surface exposure),
2) mapping of underground workings developed from 1990 to 1993 between 9 and 11 Level (810m and 990m below surface), and
3) comparing the results of the underground and surface mapping with those of Robertson (1974) for the upper one third of the CSA deposit, and Glen (1990, 1988, 1987) and Hinman and Scott (1990) for other Cobar deposits and regional data.

In representing the isotopic work of Brill and Seccombe (unpub), Brill and Seccombe and Chivas (unpub), Seccombe (unpub) and Seccombe (1990) and their conclusions about the origins of the CSA deposit it will be demonstrated that there is more than one valid solution to the source of the sulfides. This will be expanded upon to suggest the source of the quartz veining as part of the new proposed genetic model. In the process, sulfide geochemical trends observed by Robertson (1982a, 1982b, 1983, 1984) in fresh rock are outlined and reinterpreted in light of this genetic model.

Finally, the author has attempted to reprocess and utilise a gravity survey conducted by Cobar Mines P/L between 1972 and 1974. By relating this information with old BMR data it is hoped that a regional basin model and local mine scale model can be produced which may assist in understanding structural models of the basin.

A summary of the regional geology is presented in Chapter 2 and a detailed overview of the CSA deposit is given by the author in Chapter 3. The authors structural and geophysical work is presented in Chapters 4 and 5 respectively while a discussion of isotopic and geochemical work is undertaken in Chapters 6 and 7 culminating in the suggestion of a modified ore genesis and basin deformation model in Chapter 8.

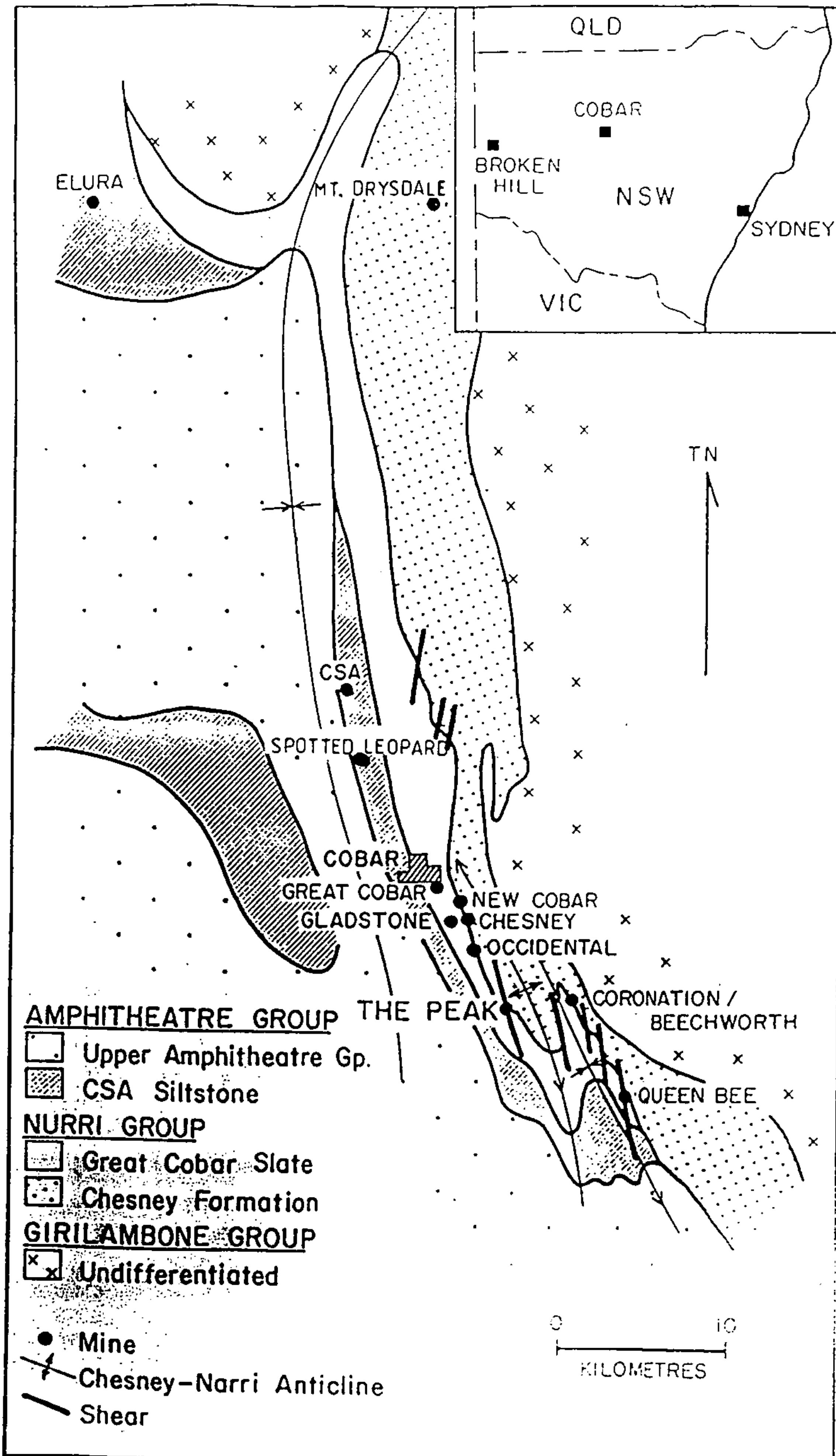

FIGURE 1.1 GEOLOGY OF THE COBAR MINING FIELD

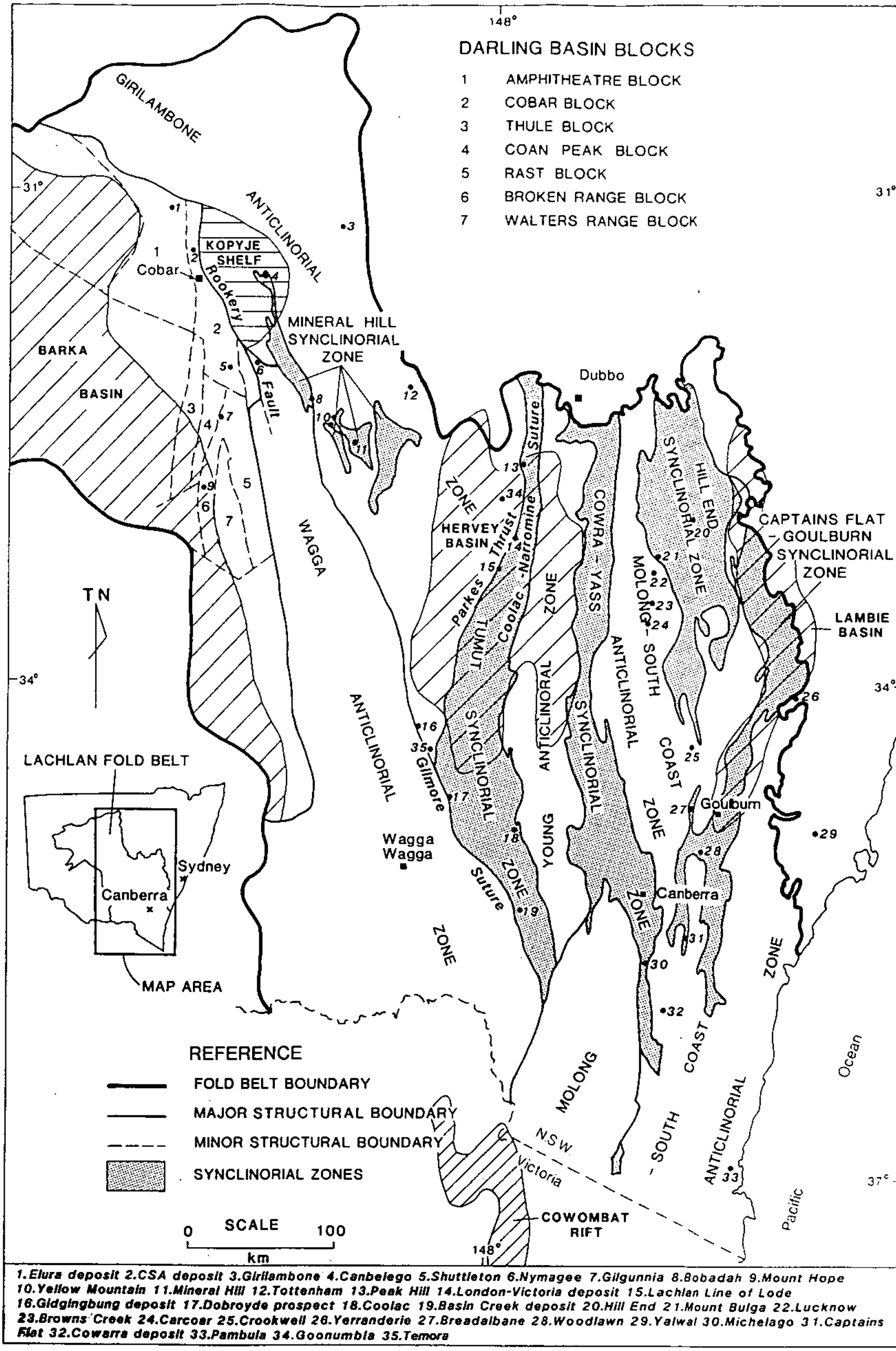

FIGURE 1.2 TECTONIC UNITS OF THE LACHLAN FOLD BELT. FROM SUPPEL AND SCHEIBNER (1990).

CHAPTER 2

REGIONAL GEOLOGY

2.1 STRATIGRAPHY

The stratigraphy of the Cobar area has been subject to much controversy due to poor outcrop and exposure, similarity of sedimentary units, lack of fossils, and the range of deformation visible in each unit. Consequently every published account of the stratigraphy has provided a different interpretation. Table 2.1 (Baker 1975) is a summary of the inferred stratigraphy from 1913 to 1975. The current accepted view is shown in Table 2.2.

Basement rocks below the Cobar Basin are unknown, but to the east and north basement is exposed as the Ballast Beds of the Girilambone Group. These are Cambrian - Ordovician (?) turbidite sequences containing Silurian volcanics and intrusives that deformed and metamorphosed the unit from lower to upper greenschist facies.

The remaining stratigraphic units, Table 2.2, belong to the Cobar Supergroup which is subdivided into the Kopyje, Narri and Amphitheatre Groups. (Pogson & Felton 1978, Glen 1982, Kirk 1983). Sediments of the supergroup were deposited in full or half grabens (Fig 2.1), with the Cobar Basin being a graben controlled to the west by the Myrt Fault and the east by the Rookery Fault. Later deformation reactivated these faults and metamorphosed the sediments to lower greenschist facies during the Carboniferous (Pogson & Felton 1978, Glen 1988). This deformation also overprinted the Ballast Beds.

The units of the Kopyje Group, also known as the Meryula Formation, were deposited on a shallow marine shelf to the east of the Cobar Basin (Fig 2.1). The units unconformably overlie the Ballast Beds and consist of siltstones, sandstone, a basal conglomerate, local limestone, and minor volcanics.

The Narri Group occurs along the eastern margin of the Cobar Basin and is divided into two units. The lower is the Chesney Formation, consisting of the basal Drysdale Conglomerate Member which fines upwards into sandstones and siltstones. The upper conformably overlying unit is the Great Cobar Slate which consists of shales and siltstones. Deposition of these units was by turbidite fans, with the material being derived from an eastern landmass (Baker 1975, Pogson & Felton 1978) (Fig 2.1).

The contact of the Chesney Formation and Great Cobar Slate is occasionally sheared or faulted as a result of the later deformation. These areas focused mineralised fluids that formed the New Cobar, Chesney, Occidental, Peak, Great Cobar, Dapville and Queen Bee deposits.

Conformably overlying the Narri Group is the Amphitheatre Group, sedimentary units of which are believed to be derived from the west (Fig. 2.1) and deposited in numerous turbidite sequences. The basal unit is the CSA Siltstone, host for the CSA and Elura deposits, and is composed of sandstone, greywacke and siltstone units defined by Bouma sequences. The upper unit of the Amphitheatre Group, including the Biddibirra Formation, is composed of coarser quartz rich sandstones with minor siltstone.

Intrusive rocks are also found within the basin, the most obvious one being the feldspar quartz porphyry at the Queen Bee deposit (Fig. 2.2). It is also found as dykes near the contact of the Chesney Formation and Great Cobar Slate in the same area (Trueman 1972). On petrographic evidence it is suggested that the porphyry is a near surface intrusion rather than a flow (Trueman 1972). The porphyry shows little evidence of being cleaved. Dykes have been located in the north of the basin near "Poon Boon" and are suggested to be equivalent to the Queen Bee porphyry (Baker 1978).

At the Peak Mine the core of the mineralised system is a flow banded rhyolite (Fig. 2.3) (M. Dufty pers. comm.) that is weakly cleaved. The rhyolite is surrounded by what is locally termed a volcanic breccia that has a pseudo-hyaloclastite appearance (Fig. 2.4). Hinman and Scott (1990) identify these volcanic units as Kopyje Group volcanic basement sheared into the basin (Fig. 2.5).

At the CSA Mine a fine grained siliceous unit with a conchoidal fracture has been suggested as being a tuff (B.L. Schmidt pers. comm.). However it could represent a highly altered sedimentary unit.

2.2 STRUCTURE

The basin into which sediments were deposited was opened by sinistral extensional tectonics and closed by dextral movement in the early Carboniferous (Glen 1990, Smith 1992, Smith and Marshall

1992). This deformation produced three structural zones within the basin, a high strain zone along the eastern edge of the basin (Zone 1 of Glen 1990) and a lower strain zone in the central and south western part of the basin (Zone 2 of Glen 1990) (Fig. 2.6). Little is known of Zone 3 except that it is a low strain zone.

Zone 1 is bounded by the Myrt Fault to the west and Rookery Fault to the east (Fig. 2.7) and contains a regional S1 cleavage that is subvertical. Changes in orientation and relationships of F1 and S1 are used by Glen (1990) to further subdivide Zone 1 into subzones. Unfortunately, Glen (1990) suggests that every major stratigraphic contact within Zone 1 is now a fault contact, something which is not seen in the exploration data generated to date.

Zone 2 to the west contains structures of two deformation events. Although there is an S1 cleavage developed it is weak compared to Zone 1 while the F1 folds have variable strike. The later D2 structures have a variable S2 cleavage and the F2 folds, which are upright, open and of variable plunge, refold F1 structures. Zone 2 is divided into blocks by a series of WNW trending D1 faults (Glen 1990).

Smith and Marshall (1992) essentially agree with the work of Glen (1990) however they do not advocate a detachment structure between Zones 1 and 2 but prefer a gradual westward decrease in D1 and D2 intensity over the entire basin.

2.3 METAL ZONATION

From north to south within the Cobar Mining Field there is evidence for regional metal zonation. The Elura mine to the north is Pb/Zn/Ag, further south the CSA is Cu/Pb/Zn/Ag, while the deposits to the south of Cobar are Cu/Au/Ag/Pb/Zn.

The deposits are subdivided into three groups (Glen 1987) based on their location. The Group 1 deposits either lie on or near the faulted contact of the Chesney Formation and Great Cobar Slate (Peak, Occidental, Chesney, New Cobar, Coronation/Beechworth and Queen Bee deposits). Group 2 deposits lie within the Great Cobar Slate along NNW trending quartz zones (Great Cobar, Dapville and Gladstone deposits), while the group 3 deposits (Elura and CSA deposits) lie within the CSA Siltstone.

However, if a section of the basin is drawn and the deposits placed on it (Glen 1988, Fig. 2.8) the metal zonation trend is E-W across the basin. This suggests that mineralisation is due to sedimentary source or proximity to some intrusive source, which is essentially what Connor (1985) suggested as being a controlling factor in Cobar type mineralisation (Fig. 2.9). Connor (1985) also suggested a vertical zonation to mineralisation.

Metal zonation is also visible on a deposit scale. Glen (1987) briefly summarises this zonation for the Cu/Au deposits south of Cobar based on drill core intersections. Each deposit may have more than one lens, each of different mineralogy, but broadly they can be divided into two types:

1) Copper rich ore, containing chalcopyrite, gold, pyrite, sphalerite and pyrrhotite

2) Zinc rich ore, containing sphalerite, pyrite, chalcopyrite, galena, pyrrhotite and gold.

The Elura deposit is also zoned (Fig. 2.10), but concentrically. The outer zone of siliceous ore contains quartz, pyrite, sphalerite and galena. The central zone is a core of pyrrhotite, containing monoclinic and hexagonal pyrrhotite, pyrite, siderite, sphalerite and galena. Intermediate between these zones is the pyrite ore containing pyrite, sphalerite, galena, quartz and siderite. (Seccombe 1990). Zonation of the CSA Mine is defined in Chapter 3.

TABLE 2.1 PREVIOUS COBAR STRATIGRAPHIC MODELS. FROM BAKER (1975).

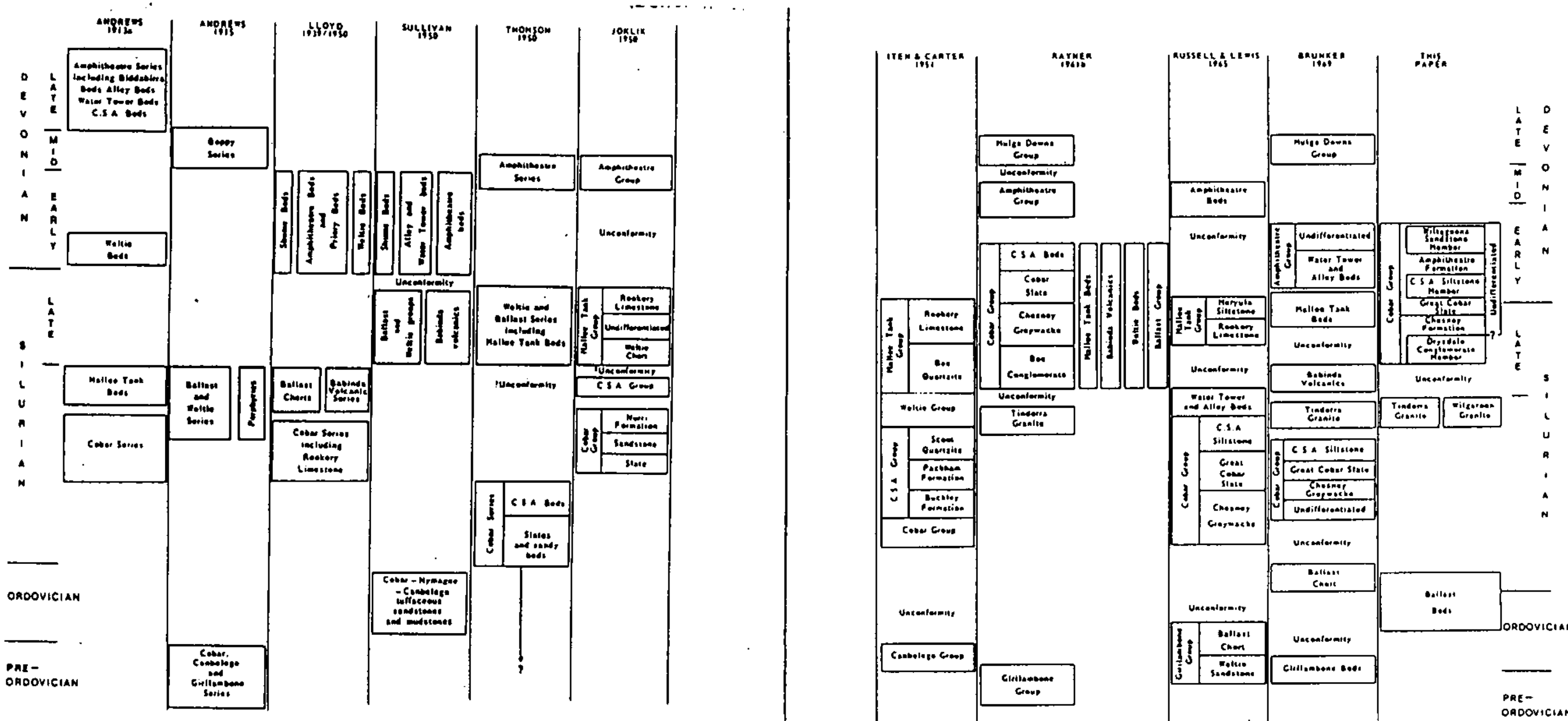

*Few of the ages are based on palaeontological evidence. Unconformities are shown where suggested or implied by the author

TABLE 2.2 CURRENT COBAR STRATIGRAPHIC MODEL.

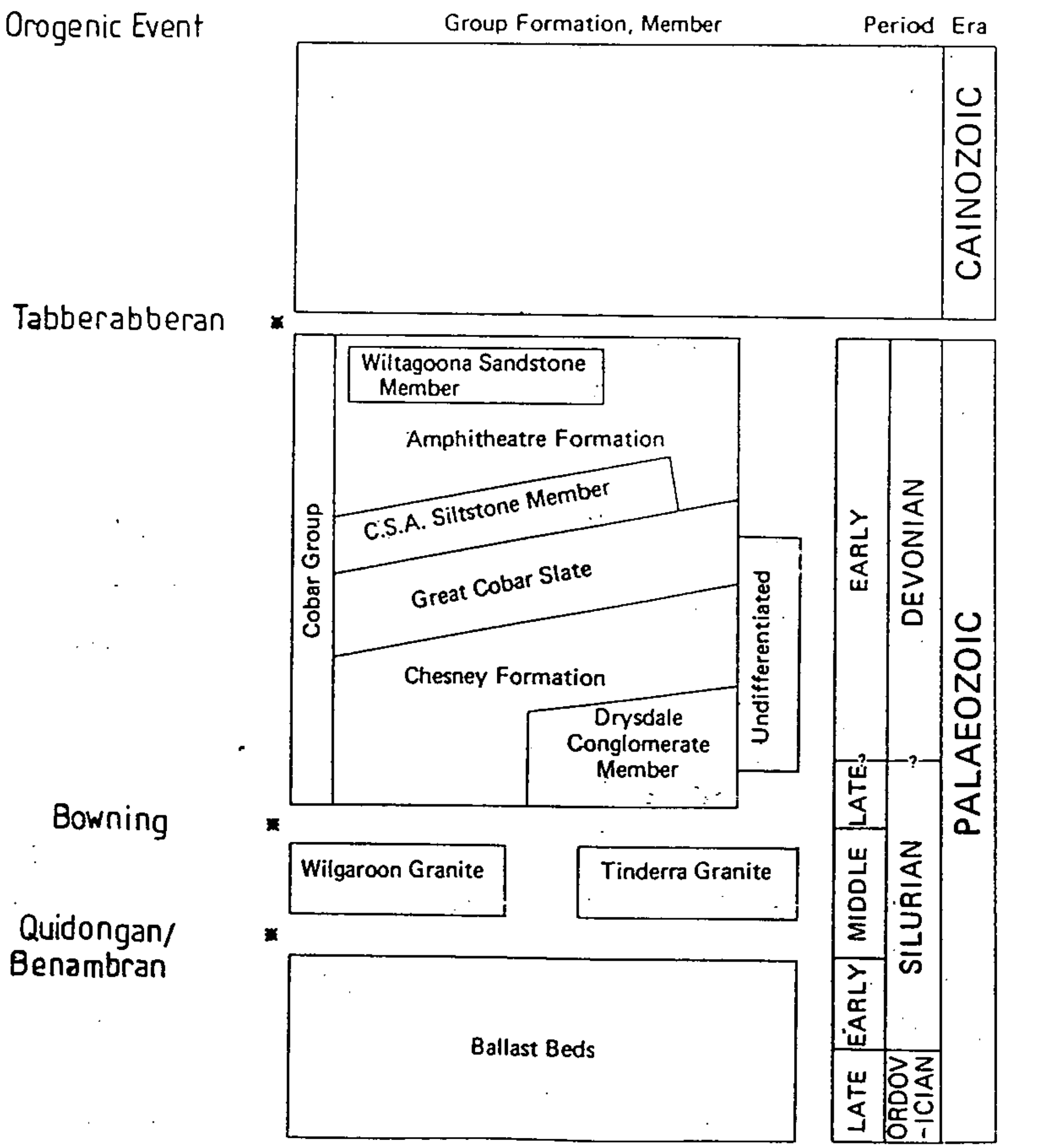

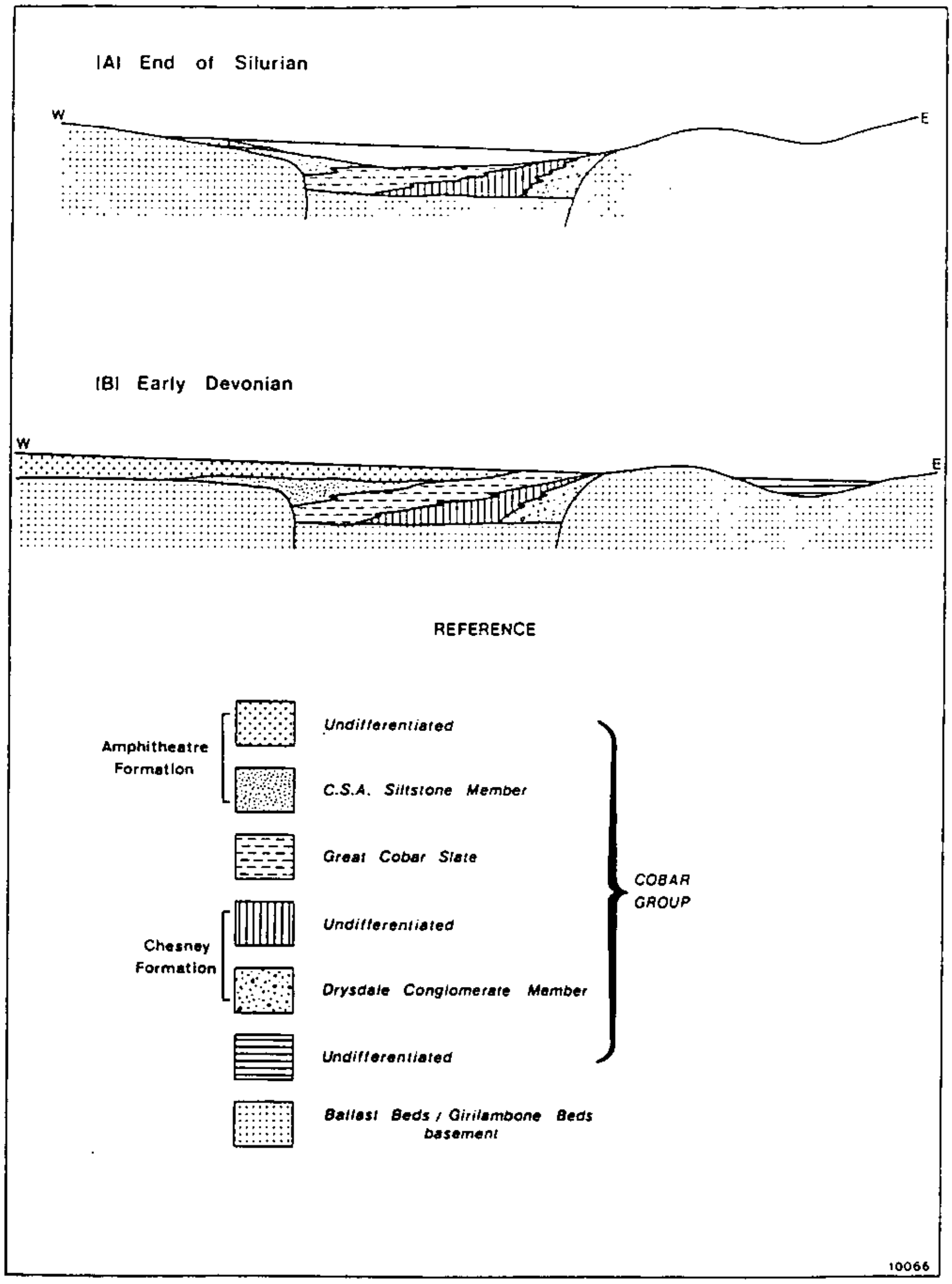

FIGURE 2.1 SCHEMATIC CROSS SECTION OF COBAR GROUP SEDIMENTATION. FROM BAKER (1975).

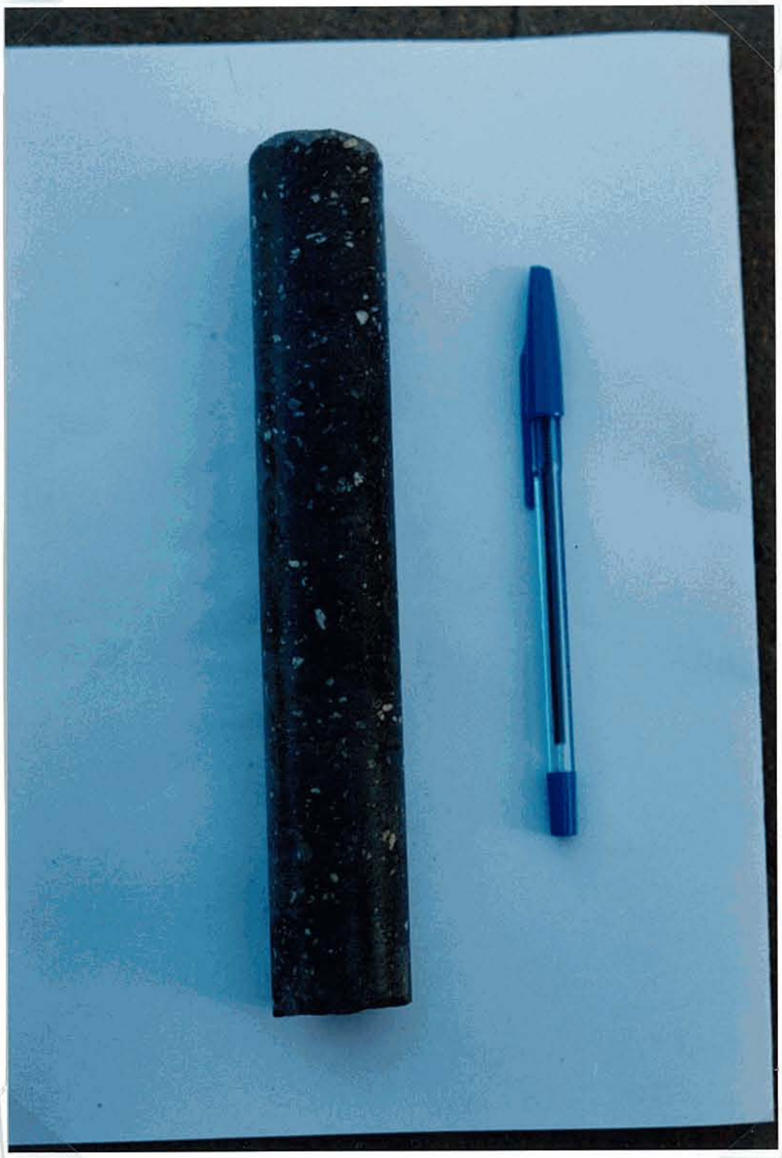

FIGURE 2.2 QUEEN BEE PORPHYRY

FIGURE 2.3 FLOW BANDED RHYOLITE FROM THE PEAK DEPOSIT

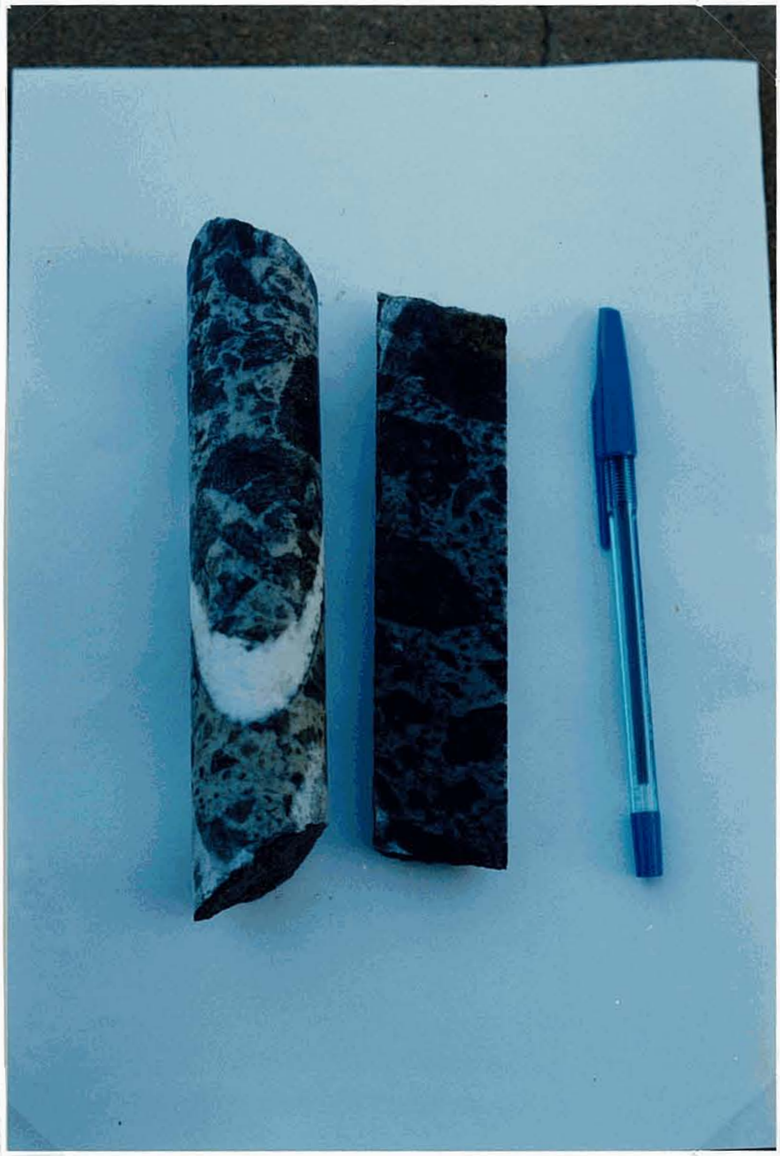

FIGURE 2.4 VOLCANIC BRECCIA FROM THE PEAK DEPOSIT

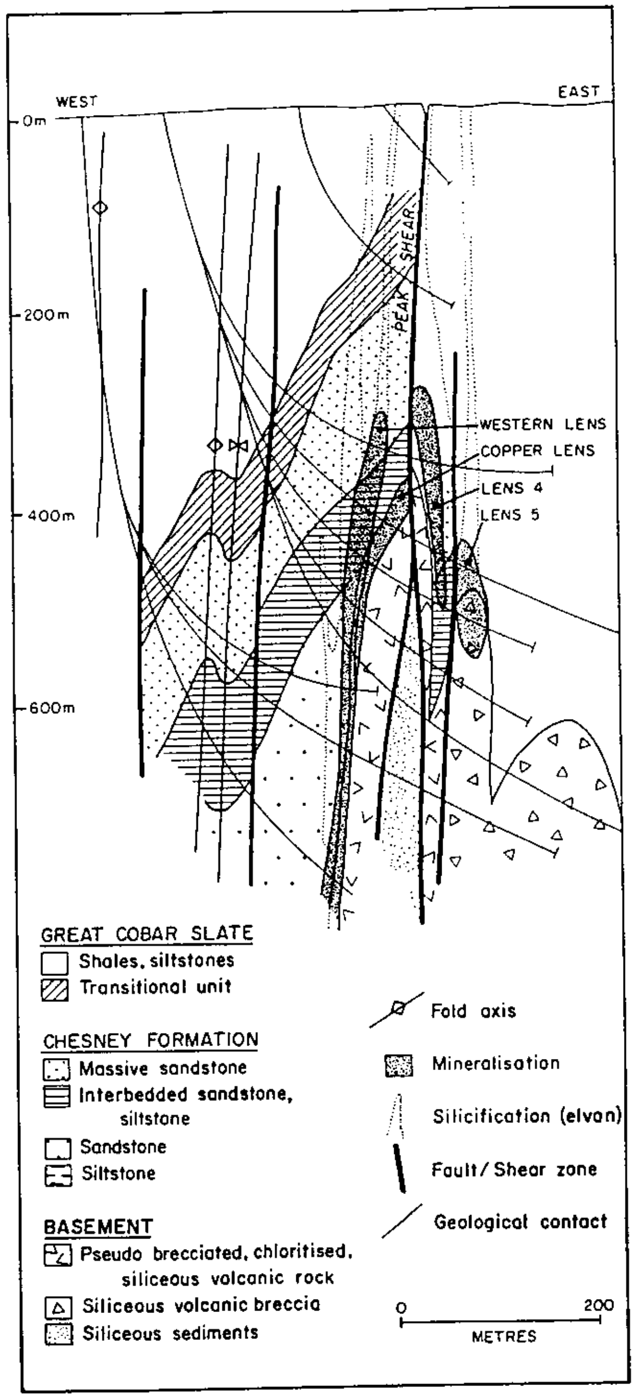

FIGURE 2.5 CROSS SECTION 10 530N THROUGH THE PEAK DEPOSIT LOOKING NORTH. FROM HINMAN AND SCOTT (1990).

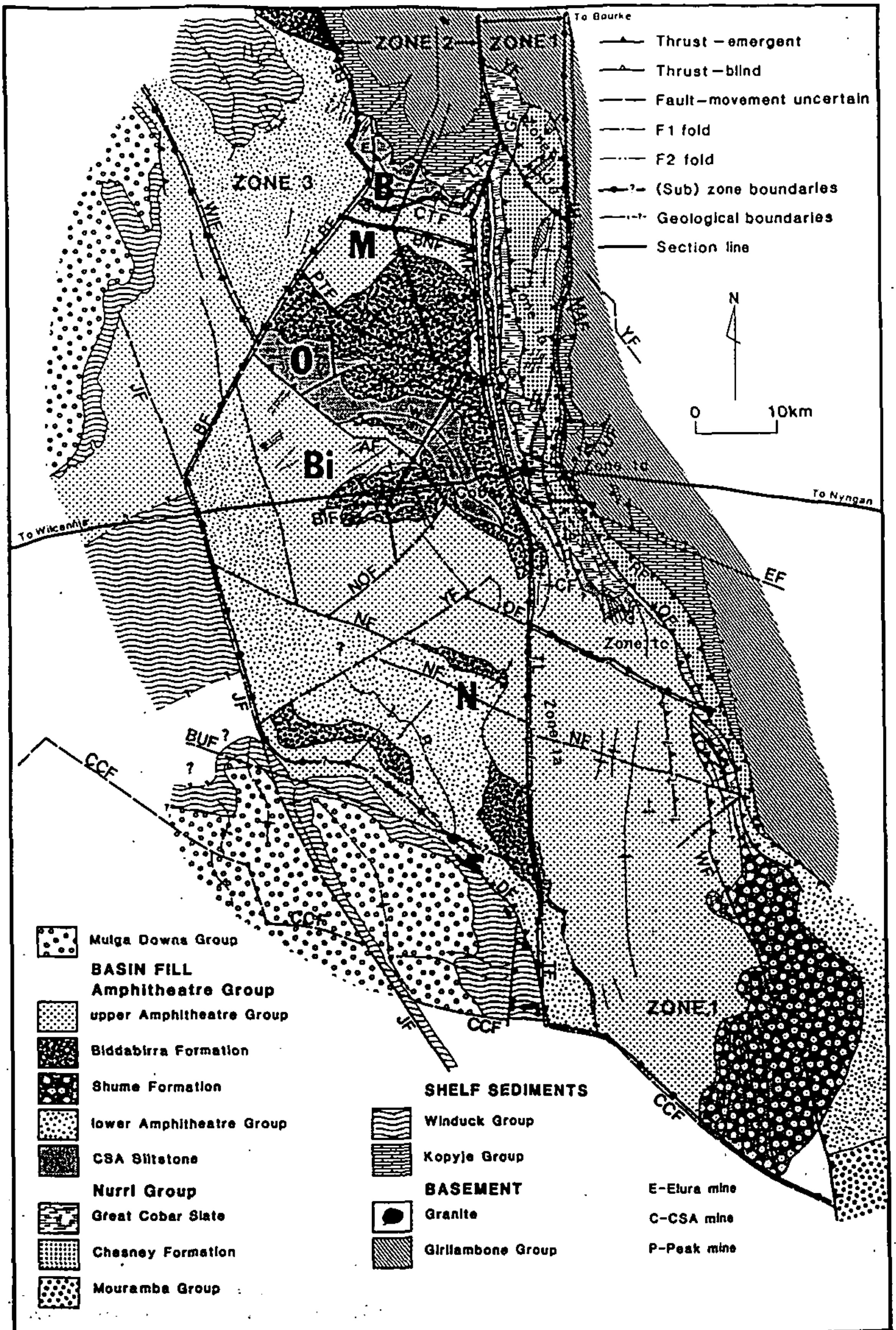

FIGURE 2.6 MAP OF INVERTED COBAR BASIN. FROM GLEN (1990)

Map of deformed Cobar Basin, showing stratigraphic units, subdivision into structural zones, subzones and blocks, regional folds and contractional faults. Abbreviations refer to faults and selected folds in structural Zone 2. Faults: AF = Amphitheatre Fault; BF = Buckwaroon Fault; BIF = Biddabirra Fault; BNF = Bundella Fault; BUF = Buckambool Fault; CF = Cobar Fault; CCF = Crowl Creek Fault; CTF = Cougar Tank Fault; DF = Dusty Tank Fault; EF = Elliston Fault; JF = Jackermaroo Fault; LF = Little Tank Fault; LUF = Lucknow Fault; MF = Myrt Fault; MOF = Mopone Fault; NF = Nymagee Fault; NOF = Norwood Fault; O = Oakden Fault; PTF = Plug Tank Fault; QF = Queen Bee Fault; RF = Rookery Fault; TF(L) = Thule Fault (Lineament); WF = Woorara Fault; YF = Yanda Creek Fault. Cross-section line for Fig. 11 also marked. Folds: m = Maryvale Anticline; w = Western Anticline; n = Nullawarra Anticline. For details of Zone 1, refer to Fig. 2.7

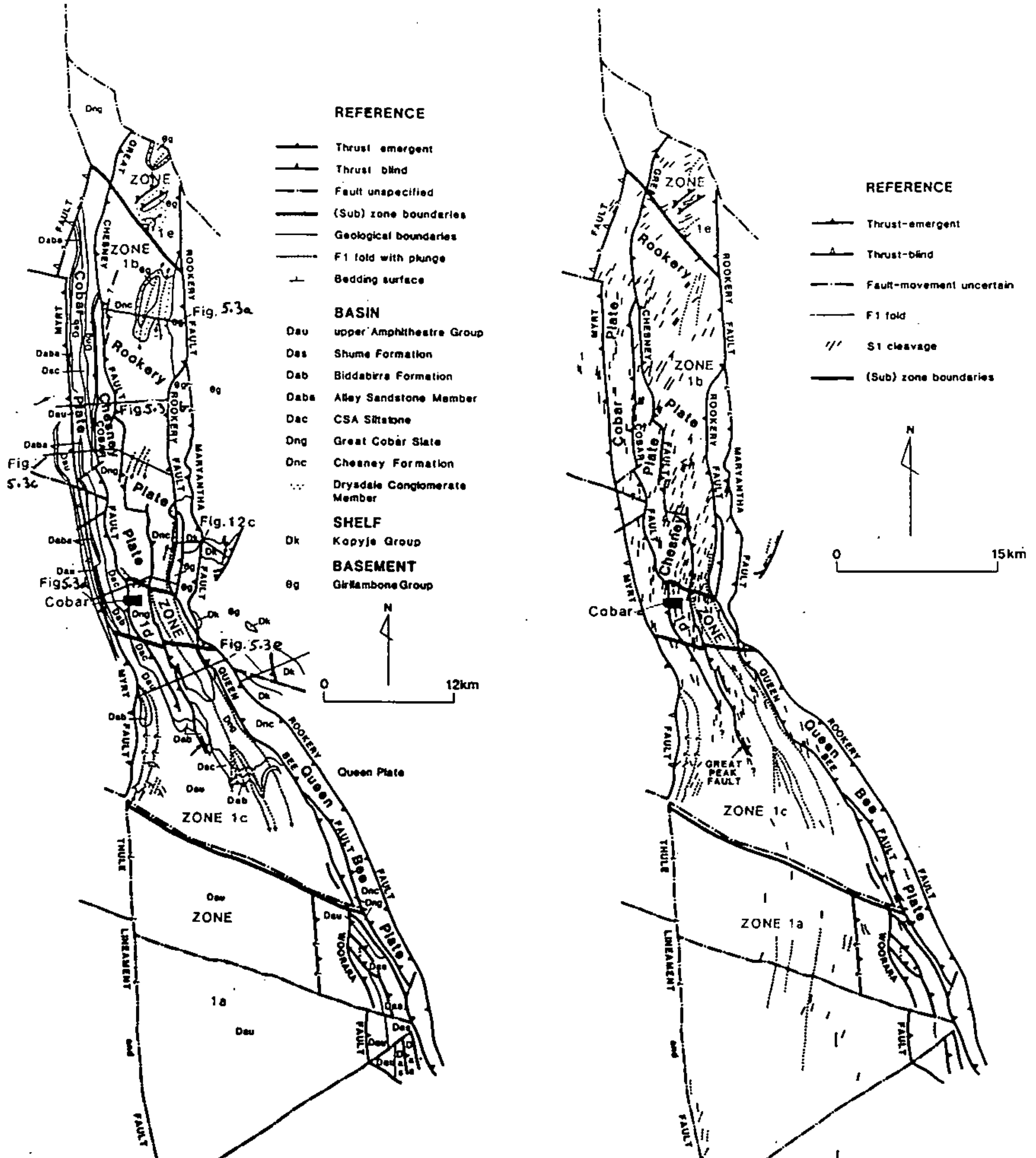

A

. Map of structural Zone 1 showing major F_1 folds and faults. See text for discussion. Cross-section lines refer to Fig. 5.3

B

Strike trajectories of S_1 cleavage and F_1 regional folds in Zone 1. See text for discussion.

FIGURE 2.7 ZONE 1 STRUCTURAL MAPS. FROM GLEN (1990)

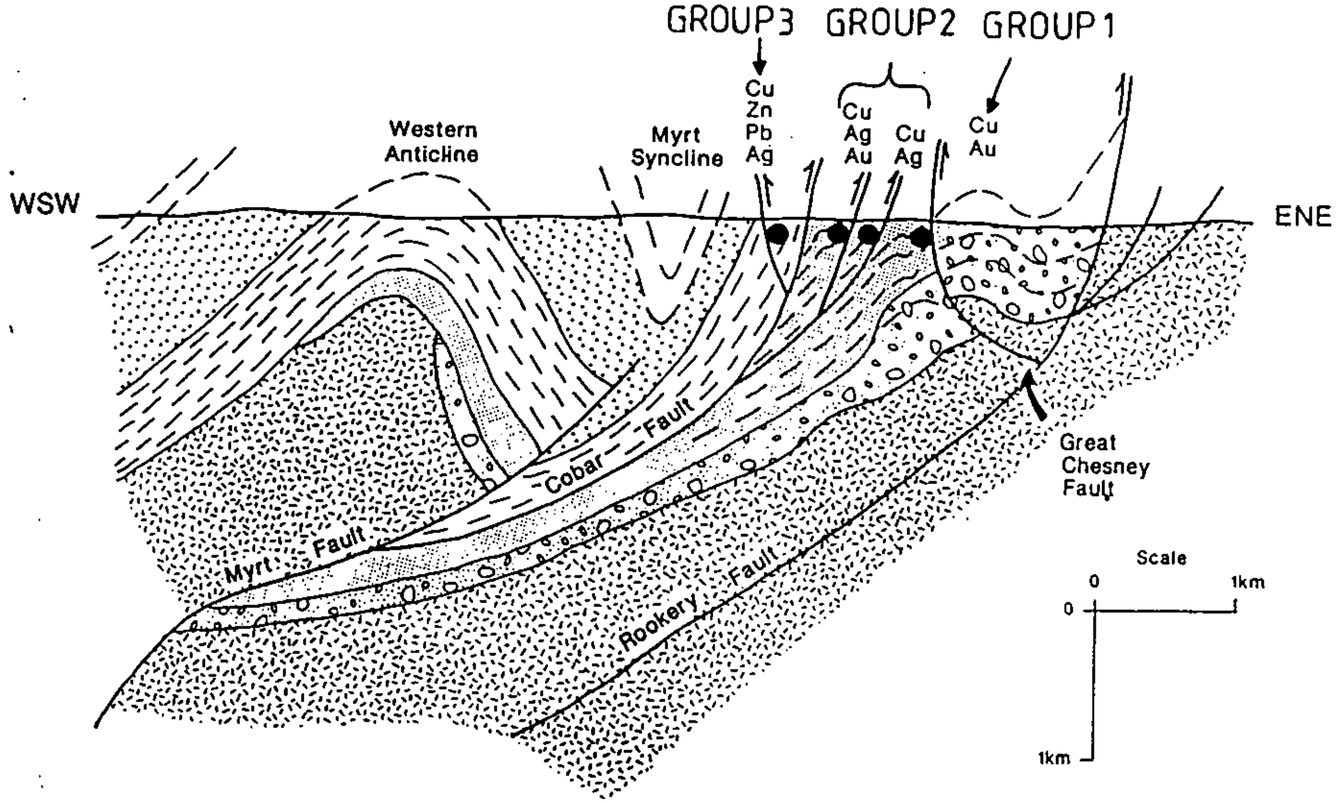

FIGURE 2.8 CROSS SECTION OF THE COBAR REGION WITH DEPOSIT GROUPS, INFERRED STRUCTURE AND SOURCE OF MINERALISATION. FROM GLEN (1988)

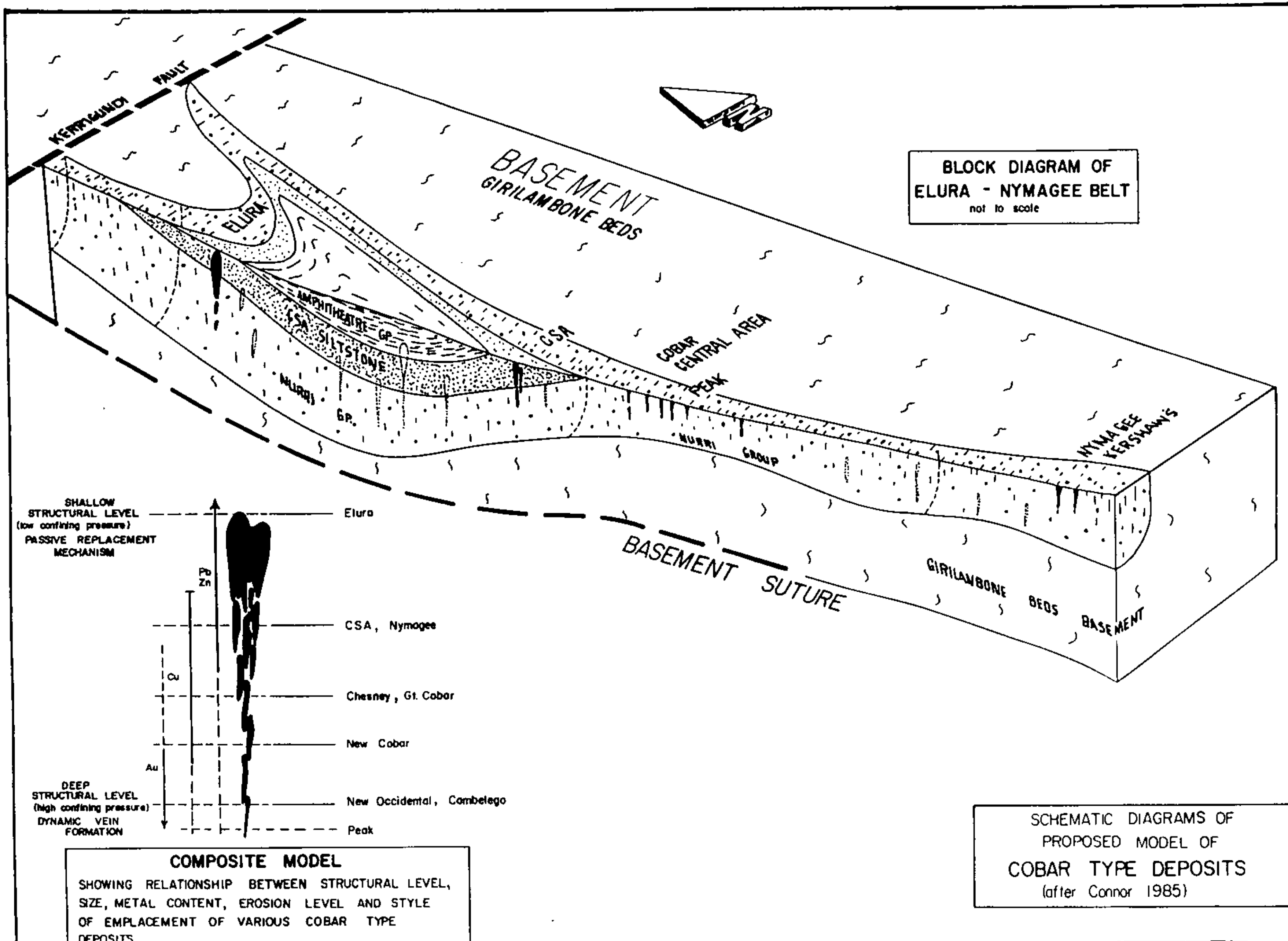

FIGURE 2.9 COBAR TYPE DEPOSITS FROM ELURA TO NYMAGEE. FROM CONNOR (1985)

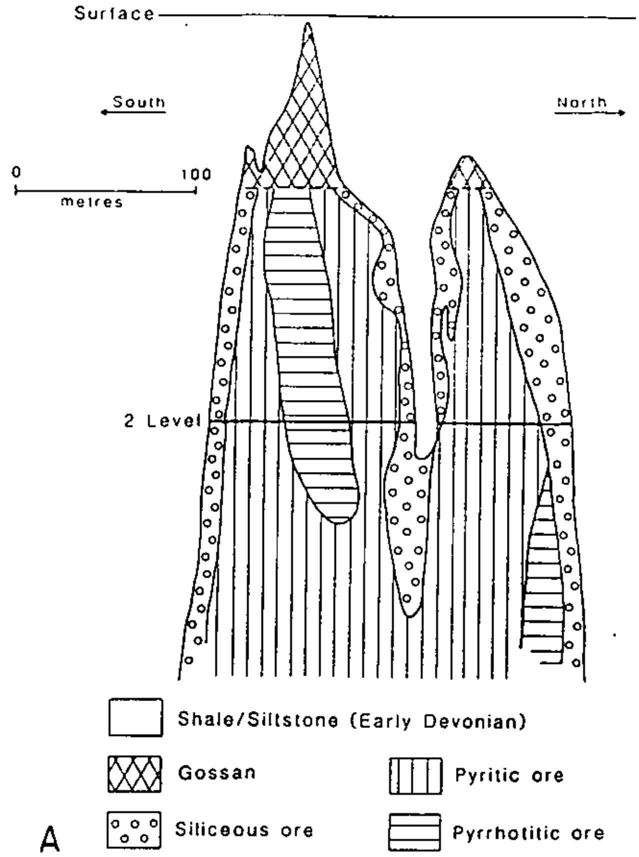

A

Longitudinal section through the Elura orebody, indicating the distribution of ore types and the position of number 2 mine level

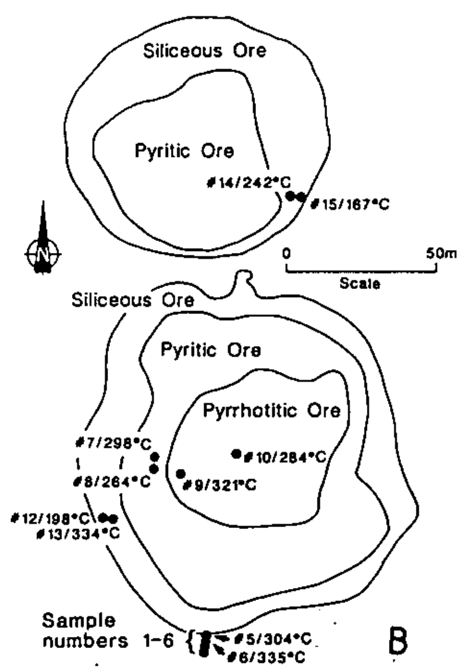

B

. Numbered sampling sites at the number 3 drill level (depth 240 m). Sulphur isotopic temperatures (°C) from sphalerite-galena pairs are reported for each sample site. Orebody outlines and ore types are given for the number 2 mine level (depth 230 m; see Fig. *A*)

FIGURE 2.10 METAL ZONATION OF THE ELURA DEPOSIT IN PLAN AND SECTION. FROM SECCOMBE (1990)

CHAPTER 3

GENERAL CSA MINE GEOLOGY

The CSA Mine is located approx 13 km north of Cobar (Fig 1.1). The host rock for the mineralisation is the CSA Siltstone, a unit of rhythmically banded siltstones (turbidites) containing minor fine to medium grained interbedded greywackes. Bedding strikes N/NW and dips steeply (75-80°) to the W/SW (250-270°). Facing is to the west, but west of the deposit it is variable. A pervasive cleavage strikes northerly and dips steeply (80-90°) to the east (Fig 3.1). This cleavage is strongly developed and quartz filled near mineralisation such that the bedding traces are obliterated.

Near the shafts (Map 1) is a monoclinal structure (the Plat Fold) which plunges to the S/SE at 70-80°. The fold is defined by a number of north trending narrow (10 cm wide) shears with subhorizontal slickensides that create a series of small blocks which rotates bedding in small increments. Movement on the shears is east block north.

Mapping of underground developments and drill core interpretation has identified two distinct packages of coarse and silicified greywackes. One of these packages links the QTS North, Central and South areas of the mine while the other occurs around the plat area and west of the Western System (Map 1). Correlating this information reveals that the greywackes trace monoclinal fold structures near mineralisation in the same sense as the Plat Fold (Map 1).

This interpretation identifies a structural control on mineralisation, ie the warping of the bedding in which cleavage is developed appears to act as a trap for mineralisation. (Similar structures are mapped and interpreted in the Cu/Au deposits south of Cobar (Glen 1987)). The mineralisation trapped in the CSA structures occurs as pipe like lenses (vein complexes or submassive to massive bodies) that have a strike length of 10-200m, a maximum width of 30m and a near vertical plunge of 300-500m (typical dimensions of all Cobar Ore Systems). The lenses pinch and swell in all three directions.

The lenses are surrounded by a narrow halo (5-20m) of pervasive green (Fe 2+) chlorite altered siltstone. Cleavage orientated quartz veining and pervasive silicification of the siltstone increase towards the core of mineralisation where black (Mg rich) chlorite and talc may be found. It can be argued that the change from green to black chlorite is a chemical transition however in places the black chlorite is associated with shears. Sulphide mineralisation is concentrated in and around these cores and becomes weaker away from them. The lenses occur in N/S trending shear zones that are collectively referred to as systems (Map 1) which are hundreds of meters long.

The Western System outcrops at surface and consists of a Cu rich ore (chalcopyrite, pyrrhotite and pyrite) and a banded Pb/Zn rich ore (sphalerite, galena, pyrite and disseminated chalcopyrite blebs). The Pb/Zn banding is parallel to the pervasive steep easterly dipping cleavage seen in the mine sequence. Above 9 Level the average lens grades are 0.5-1% Cu, 3% Pb, 6% Zn, but below 9 Level they are 3% Cu, and less than 1% combined Pb and Zn with the lenses having a narrow Pb/Zn halo. The approximate line of transition is shown in Fig. 3.2. The process of alteration has produced a grey-green to blue-green silicified and silica flooded unit referred to as elvan.

The Western Gossan Zone, located west of the Western System (Fig. 3.1) contains weak Cu/Pb/Zn mineralisation which was mined between 1908 and 1912. Gossans, ironstones, and altered rocks are exposed on surface but to date the mineralisation remains uneconomic. Surface and underground mapping combined with core orientation has shown that between the Western Gossan Zone and the Western System bedding dips steeply to the east. West of the Western Gossan Zone bedding dips steeply west (Fig. 3.1). From this it is inferred that there is a detachment structure located on the footwall of the Western System.

The Eastern system, not exposed at surface, consists of numerous chalcopyrite, pyrrhotite, quartz and pyrite veins. Economic lenses are defined by a sufficient concentration of veining containing above cut-off grades at widths greater than 4m. Pb/Zn is rare, with known intersections occuring near the top of the system.

Between the Eastern and Western Systems, and isolated from both by weakly altered siltstone, is the CZ System which has an average grade of 10% Zn, 3% Pb, and less than 1% Cu. The ore contains banded sphalerite and galena, and up to 60% massive pyrite with disseminated blebs of chalcopyrite. However, with depth the Cu content increases and Pb/Zn decreases. The host rock is strongly black chlorite altered and the ore is surrounded by a footwall and hanging wall black chlorite talc shear.

The QTS North System is a blind system composed of several lenses of copper mineralisation grading up to 4% Cu over widths of 5-20m. The lenses strike north-south and dip steeply east. Mineralisation is chalcopyrite, pyrrhotite, cubanite and bornite. The largest lens, M lens, is cut by a steep easterly dipping quartz filled structure (D Zone) which appears as a post mineralising structure due to sinistral displacement of the mineralisation.

QTS South is also a blind system composed of a series of subparallel lenses of chalcopyrite and pyrrhotite mineralisation. Isolated uneconomic pods of sphalerite and galena occur on the margins of the system while economic intersections occur at the top. Low angle faults defined from drilling and development mapping extend through the ore displacing cleavage and mineralisation by up to 2m. These faults can only be traced for 10-20m away from the ore zones before they are lost as kink bands in surrounding unaltered material. Between QTS North and QTS South is a weakly altered and mineralised area referred to as QTS Central.

Overall, the systems appear as a series of stacked en echelon lenses which increase in depth from surface towards the east (Fig 3.1). As this occurs copper mineralisation increases with depth and eastward migration, leaving the Pb/Zn mineralisation at the top and edges of the systems. Hence metal zonation is visible at the CSA.

Quartz veining at the CSA can be classified into 6 types based on those defined by Glen (1987) in the Cu/Au deposits south of Cobar (ie classified by orientation, type, and cross cutting relationships (Fig. 3.3). Set 1 veins are ptygmatic and are cross cut by all other types. It is suggested that this could be an early pervasive cleavage deformed by later events. However it can be argued that the veining formed due to one phase of injection based on fluid inclusion data (Chapter 6) and that Set 1 veins occupy an unusual fracture patten. Ptygmatic veins are confined to the mineralised systems and are not seen in the unaltered siltstone between systems. A more detailed interpretation of these quartz veins is given in Chapter 4.

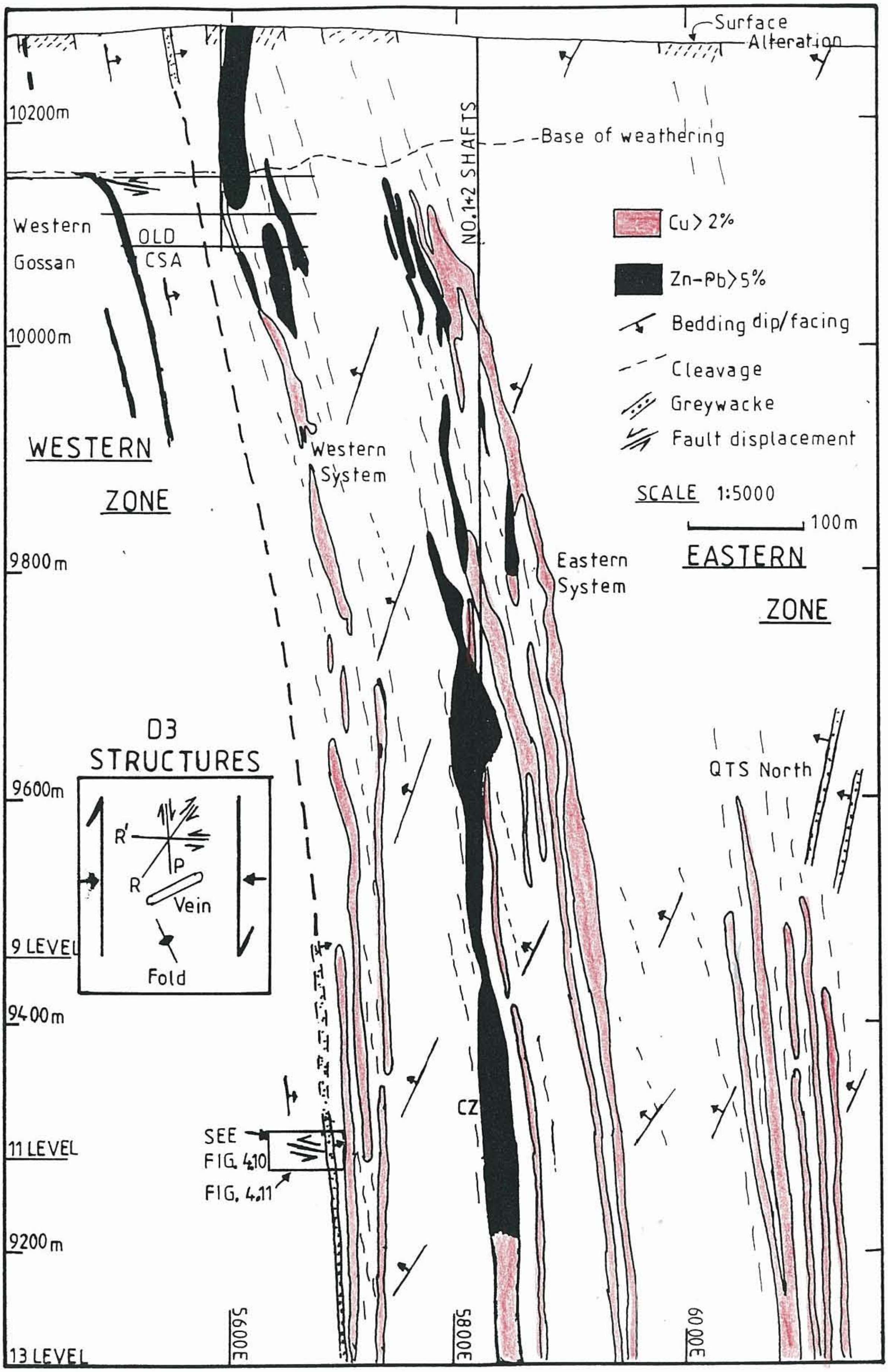

FIGURE 3.1 CSA DEPOSIT CROSS SECTION LOOKING NORTH

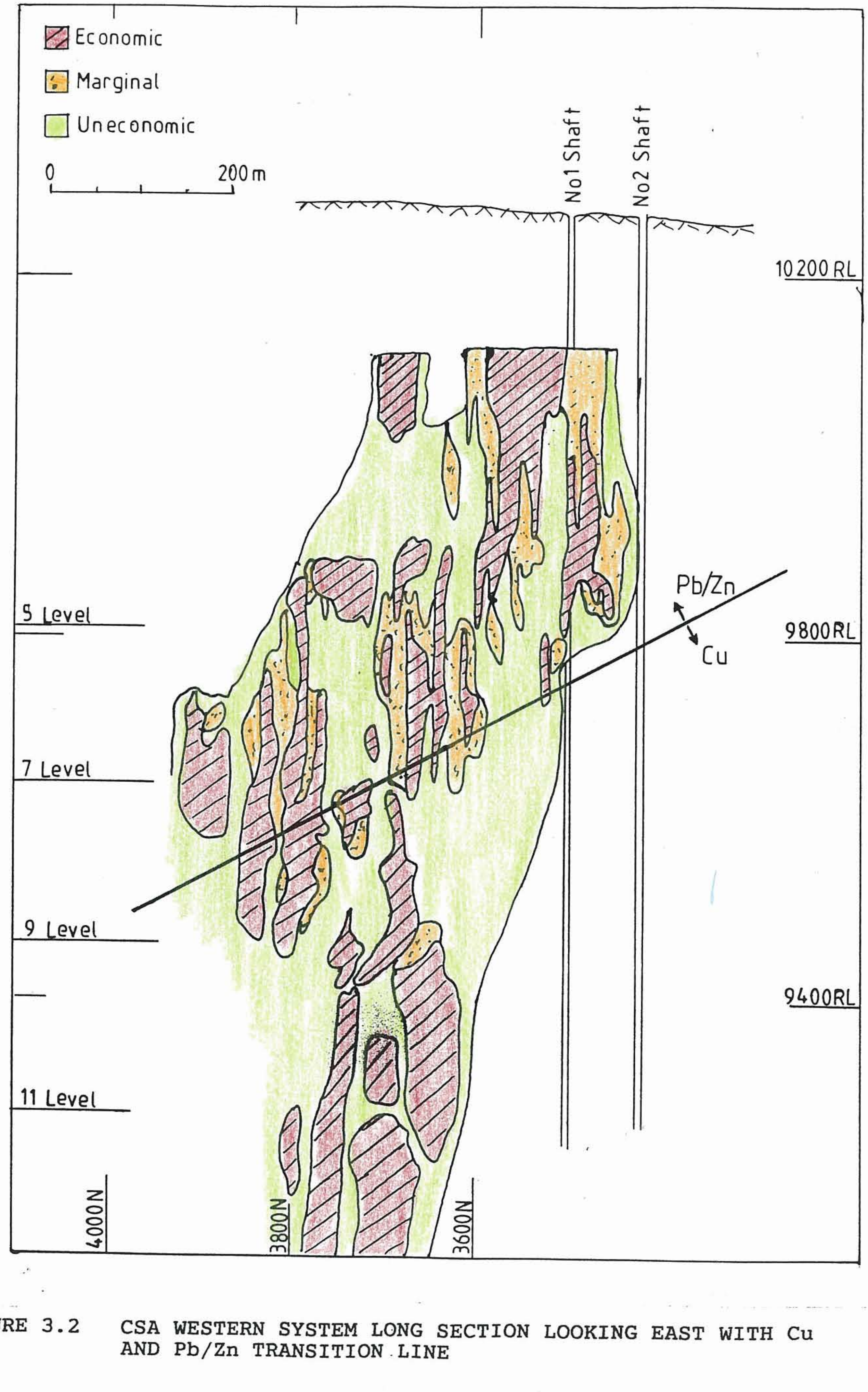

FIGURE 3.2 CSA WESTERN SYSTEM LONG SECTION LOOKING EAST WITH Cu AND Pb/Zn TRANSITION LINE

Set 1) Ptygmatic veins cut by S1 cleavage

" 2) Large compound to thin veins that parallel cleavage and which are commonly boudinaged

" 3) Subhorizontal, massive tension gashes that can be terminated by set 2 veins

" 4) Northwest striking, northeast dipping veins

" 5) Uncommon splays off set 2 striking 020°

" 6) Veins dipping 40°-60° east similar to set 2

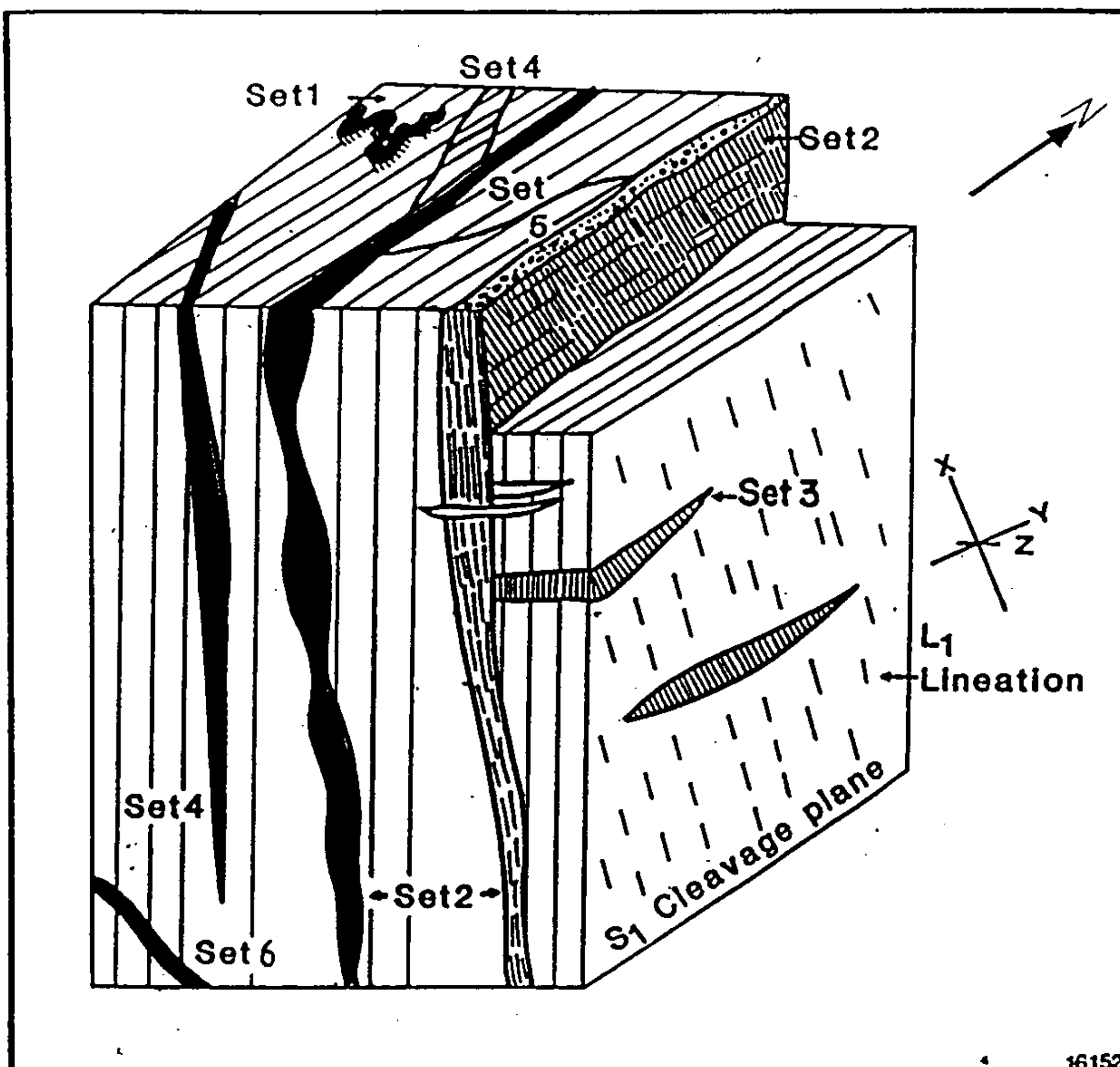

FIGURE 3.3 SUMMARY DIAGRAM OF QUARTZ VEIN RELATIONSHIPS AT THE Cu/Au DEPOSITS. FROM GLEN (1987)

CHAPTER 4

DETAILED CSA STRUCTURE

In relation to the structural interpretations placed upon the Cobar Basin by Glen (1985, 1990) (Section 2.2) the CSA deposit occurs within Zone 1b. Zone 1 is the high strain eastern portion of the basin (Figs. 2.6, 2.7) while subzone 1b (termed the Cobar Plate) is defined as having different fold and cleavage trends to the other subzones of Zone 1 (Glen 1990).

The structural analysis presented here results from detailed mapping and remapping of the deposit by the author and the interpretation of the data. Comparisons are made to the work of others in the basin to highlight the structural similarities of the Cobar deposits.

4.1 SURFACE GEOLOGY

The surface geology of the CSA is depicted in Map 2. It is compiled from a number of sources [Knight (1958), company geologists, De Mark (in prep)] given the cultural and physical changes which have occurred since the mine was discovered in 1871. From this map the mine area can be divided into two zones based on structural character.

4.1.1 WESTERN ZONE

This exists west of the Western System (Map 2) and includes the mineralisation of the Western Gossan. Compared to the Eastern Zone, the stratigraphy of the Western Zone contains more coarse siltstone and greywacke units which may correlate with the stratigraphy of the lower Biddibirra Formation or upper CSA Siltstone. Occurring within the sequence is an extremely fine grained siliceous unit with a conchoidal fracture containing blebs of iron staining after pyrite (?) (Fig. 4.1). It has been suggested that this unit is an ash fall " tuff " (B.L. Schmidt pers. comm.), but it may represent a highly altered sedimentary unit.

Mapping in the Western Zone shows that bedding dips steeply east and west which defines a subhorizontal fold axis trending NNW (Fig. 4.2a). Other small scale folds exist within the area which have long west dipping limbs and short east dipping limbs that are truncated by shearing (Fig. 4.3). These folds reorientate the bedding and create fold axis that plunge at approximately 70° to 180° (Fig. 4.2a). Facing directions for the stratigraphy are obtained from the fining up sequences and erosional bases of the coarser units. Bedding within the Western Zone is dissected by three cleavage traces. These dip at 80° to 090°, 80° to 060°, and 70° to 120° (Fig. 4.2b). The structural data is listed in Appendix 1. Movement directions are difficult to obtain given the patchy exposure.

Just inside the eastern boundary of the Western Zone exposed in a mullock pass (Map 2) is a series of steep east dipping and east facing greywacke units (Fig. 4.4). Also visible is a steep east dipping cleavage (80° to 090°) and a series of quartz filled cleavage planes dipping at between 30° and 50° to the east. This exposure typifies the discordant nature of the Western and Eastern Zones.

4.1.2 EASTERN ZONE

The Eastern Zone contains west dipping bedding planes at 70° to 265° (Fig. 4.5a). The most common lithology is fine siltstone with minor coarser siltstone and rare greywacke, which is typical of the CSA Siltstone.

Occurring within the Eastern Zone are the mineralised Western, Eastern, CZ, QTS North and QTS South Systems. Alteration in the form of silicified siltstone , quartz veining and cleaved brick red (chlorite altered) siltstone are observed above the Western and Eastern Systems. Weaker chlorite alteration and strong quartz veining are observed over QTS North where exposure is limited by soil cover. Exposure of QTS South is non existent. Four cleavage orientations are visible from surface exposures. The most dominant of which is the pervasive steep east dipping cleavage at 85° to 090° (Fig. 4.5b). Other cleavages dip at 85° to 116°, 89° to 140°, and 88° to 040° (Fig. 4.5b, 4.6, 4.7). The structural data is listed in Appendix 2.

In relation to the work of Glen (1987) on the Cu/Au deposits south of Cobar the cleavage dipping to 116° is equivalent to Set 5 (Fig 3.3), those dipping to 040° are equivalent to Set 4 and those dipping steeply to the east are equivalent to Set 2. Note that the low angle east dipping veins seen in the mullock pass of the Western Zone equate to Set 6. Glen (1987) did not report veins dipping to 140°. Where bedding planes can be traced in these cleavage zones it is possible to assign a sense of direction to the cleavages. Those cleavages dipping to 140° have a sense of motion where the southern block moves east (Fig. 4.5c, 4.6) while those dipping to 040° have a sense of motion such that the SW block moves north west. These directions are summarised on Fig 4.5c.

4.2 UNDERGROUND MAPPING AT CSA

From underground developments a three dimensional view of the deposit is gained. The data presented in Map 1 is a compilation of the geology mapped between 9 Level and 11 Level (810m and 990m below surface respectively). The data, listed in Appendix 3, is heavily biased towards the Eastern Zone as defined in Section 4.1.2 due to the presence of economic mineralisation. Some Western Zone data appears west of the Western System where development has exposed east dipping bedding and a greywacke sequence that can be correlated directly with those exposed at surface in the mullock pass. This is possible as drilling through the footwall lenses of the Western System has always located a greywacke package. This greywacke is faulted out of the drive on 11 level but drilling has identified its continuation behind the W2BN lens (Map 1).

Within the underground environment bedding dips predominantly at 80° to 258°, however there is some bedding that dips at 88° to 081° within QTS South and the Western Zone. Overall this creates a shallow south plunging F1 (?) fold axis (Fig. 4.8a). Within the monotonous units of siltstone are recognisable coarse greywacke units. As already mentioned (Chapter 3 and above) one of these is located in the Plat Fold and Western System while the majority are found from QTS North to QTS South (Map 1). Interpretations from drill core and development mapping indicate that some of these greywacke units are continuous over large areas while others have a short strike length and are considered to be lenticular. In general, these greywacke units are not recognised in the ore zones of QTS North or QTS South as bedding is obliterated due to the strong cleavage. However mapping does suggest that the greywacke units are warped near mineralisation and that movement is sinistral (east block north).

A similar relationship is seen approximately 4 km south of the CSA deposit at the Spotted Leopard anomalies. Here costeaning has revealed two quartz filled structures associated with chlorite alteration (brick red staining) and weak mineralisation. Bedding is warped around these structures and indications are that the east block has moved north (Map 3). Drilling has indicated that the structures are pipe like as per the CSA Systems. Overlaying Maps 1 and 3 reveals that the Spotted Leopard anomalies equate to QTS North and South structures, ie they have a strike separation of approximately 750m and an east-west offset of 180-200m. A similar anomaly is located 750m south of QTS South, 750m north of QTS North, and south of Cobar the separation of the New Cobar, Chesney, and Young Australia-Wood Duck deposits is of similar proportions. This repetition clearly points to a structural control on mineralisation.

Through the mine sequence there is a pervasively easterly dipping cleavage of 80° to 090° (Fig. 4.8b). Other measured cleavages have a dip of 85° to 110° and 87° to 080° (Fig. 4.8c). Examination of the faults and shears (Fig. 4.8d) produces three main orientations being 88° to 120°, 87° to 060° and 28° to 336°. The latter represents a series of flat dipping faults and joints seen through the mine sequence and in particular QTS South (Map 1). The other two orientations correlate with cleavage orientations seen on surface, underground, and the Set 4 and Set 5 veins of Glen (1987). These two orientations of shears have on their surfaces subhorizontal slickensides implying a near horizontal sense of motion. In plan view (Map 1) the economic mineralisation lies in N/S orientated lenses which have their beginnings at one of these cleavage orientations. This combined with the subhorizontal sinistral movements may explain why the lenses are pipe like.

The process of orientating drill core from down hole survey data has proven to be useful. The assumption made is that the pervasive easterly dipping cleavage always dips due east, which is defined from mapping. Consequently the intersection of this cleavage (85° to 090°) and the bedding planes defines the fold axis, termed L for lineation. As a result of this work the fold axis plunge steeply at $30-70^\circ$ to the south in areas devoid of mineralisation but are subhorizontal in mineralised areas (Map 1,

Fig. 4.8e). Between the Eastern System and the M Lens South area (Map 1) a steeply southerly plunging fold axis has been identified that is not dissimilar to that seen in the Western Zone on surface or the Plat Fold. Within 5m of D Zone the fold axis becomes subhorizontal and immediately east of D Zone the steep southerly plunge returns. It also appears as if the eastern limb of the fold is sheared out. This can be seen in the length of orientated drill core from the CSA deposit (Fig. 4.9). Note the west dipping bedding, east dipping cleavage with the fold structure indicating west block up, and the subhorizontal quartz vein equivalent to Set 3 of Glen (1987) (Fig. 3.3). Similar features are observed 4 km south of the CSA deposit at the Spotted Leopard anomalies.

Within the steep pervasive easterly dipping cleavage it is also possible to see a steep southerly plunging mineral or stretching lineation (Fig. 4.8f). This is seen on a larger scale with respect to the long section of the Western System (Fig. 3.2) where economic mineralisation is orientated parallel to the stretching lineation.

In cross section the structure of the deposit is quite different. On 11 Level (990 sub level) development to the west of the Western System has intersected east dipping bedding and quartz filled structures (Fig. 3.1, 4.10, Map 1). One of these quartz filled cleavages dips at 20° to the east similar to that seen in the mullock pass on surface and Set 6 of Glen (1987). The sense of motion on this cleavage is bottom block east which is the same as the displacement mapped for the Western Gossan mineralisation from the Old CSA 2 level (Fig. 3.1). It would also explain the rapid easterly displacement (1 to 5m) occasionally seen in Western System, CZ and QTS South mineralisation. The displacement in QTS South was first noted through a geostatistical study by Schofield (1990). In long section the mineralisation also shows displacements along the low angle faults of bottom block north by up to 5m (also mapped in the Western Gossan developments).

Also exposed in the same area on 11 Level is a series of subhorizontal tension gashes (Set 3 of Glen (1987)) displaced by a west dipping cleavage (Fig. 4.10, 4.11).

Through the deposit but rarely seen are east dipping sulfide veins that displace quartz veins but are parallel to Set 6 veins. These may represent late D3 sulfide remobilisation or another as yet ill defined event.

4.3 PREVIOUS STRUCTURAL MODELS

Previous structural models for the CSA Mine only deal with two deformational events for the basin. Kapelle (1970) along with Scott and Phillips (1990) have models where in cross section the east block is up thrown (Fig. 4.12). Rayner (1969) and Robertson (1974) identified solid state deformation of the mineralisation. As will be demonstrated, the latter observation is correct but the former is not.

4.4 STRUCTURAL HISTORY AND RELATIONSHIP TO THE BASIN

Having made numerous structural observations of the deposit it is possible to complete the structural history of the deposit. However in the past only two deformational events were thought possible in the basin when in fact there are three.

4.4.1 THE D1 EVENT

From the work of Glen (1985, 1987, 1990) and of Smith and Marshall (1992) there is no doubt that the Cobar Basin was closed (inverted ?) by dextral oblique (transpressional) tectonics. This produced the tight NNW trending folds seen in the Western Zone on surface and in part with the underground data.

It is not known if the D1 event produced a cleavage or fracture pattern and if it did the structures could have been reactivated by D2 and D3 thus showing D2 and D3 senses of motion. The D1 event may have produced the consistant basin wide due east dipping cleavage that is not quartz filled and which was later reactivated by D3 and filled with quartz. In addition the Set 1 ptygmatic quartz veins of Glen (1987) may reflect a D1 cleavage, but quartz vein data (Chapter 6) places this in doubt.

Clearly there is some difficulty in identifying D1 structures in what has become a multiply deformed sedimentary basin.

4.4.2 THE D2 EVENT

The regional work of Glen (1985, 1987, 1990) and of Smith and Marshall (1992) suggests that D2 was sinistral with the principle axis of stress orientated NW/SE. In Zone 2 (Glen 1990) D2 refolds

F1 limbs to form NE trending F2 folds and domes. In Zone 1 however the rocks are standing on end after D1 and are not easily refolded. Consequently they form a cleavage and shear pattern. The subhorizontal slickensides suggest that not only were the principle axis of maximum stress orientated NW/SE but were essentially subhorizontal. Hence the cleavage intersections were near vertical thus creating pipe like structures for the mineralising fluids to move through. The orientation of the principle axis of maximum stress also means that the mineralised lenses are orientated N/S. In this case the cleavages orientated to 140°become P shears, those orientated to 060° become R' shears while those orientated to 110°become R shears (Fig. 4.13). This implies that the Set 4 and Set 5 cleavage orientations of Glen (1987) are D2 in origin. Note that the P shears are not dilational (rather compressional) and do not host mineralisation while the R shears are dilational and contain mineralisation.

4.4.3 THE D3 EVENT

Although not previously described as a single event, a D3 event does exist and has been suggested in passing. Glen (1990) in the description of the Cobar Plate of Zone 1 suggested that the plate was internally imbricated by thrust faults one of which is the steep east dipping brittle footwall fault of the Western System (Kapelle 1970). It was suggested that this structure shows east block up movement by Scott and Phillips (1990, Fig. 4.12). However the evidence from 11 Level and surface mapping indicate that the motion is west block up in a transpressional regime (Fig. 4.14). The low angle east dipping cleavage that displaces mineralisation is an R' shear (dilational as quartz filled), the west dipping cleavage is an R shear and the pervasive east dipping cleavage a P shear as it contains brecciated fragments of host rock. From this it is concluded that:

1) the tight steep south plunging folds seen on surface in the Western Zone (Fig. 4.3), in core near M Lens South (Map 1), the Plat Fold, and other core examples (Fig. 4.9) are D3 in origin, ie. now L0/3 and not L0/2 of Hinman and Scott (1990), Fig. 4.15,
2) that the mineralisation is pre D3 as it is displaced by the D3 cleavages,
3) the fold axis mapped in the deposit are of different orientation in mineralised areas compared to unmineralised areas. It could be suggested that each orientation of quartz veining represents a single deformation event with the last event overprinting all before it, thus creating the illusion of one event, but based on structural evidence this is consided less likely.
4) the quartz veining is of one origin and one event (D3) based on fluid inclusion and isotope data (Chapter 6) and fills the cleavages and fractures produced in D1, D2 and D3,
5) the quartz veining is not always mineralised but in places has mechanically reorganised and partly remobilised

mineralisation. This explains the sulphide stretching lineation (now L2/3 and not L2/2 of Hinman and Scott (1990), Fig. 4.15) seen in the pervasive cleavage and the cleavage parallel banding in the Western System and CZ Pb/Zn lenses. This is consistent with the interpretations of Rayner(1969) and Robertson (1974) with regard solid state deformation of the ores.

6) the Set 2, Set 6, and Set 3 vein orientations of Glen (1987) are D3 in origin, and
7) in plan view the movement on D3 structures like D Zone that displaces mineralisation, and the Plat Fold faults, indicate a small degree of sinistral strike slip movement. Near mineralisation this produces talcose black chlorite shears and may reactivate D2 structures.

Table 4.1 provides a summary and comparison of the structural events of the basin as seen at the CSA Mine and other deposits in Cobar.

4.5 OTHER DEPOSITS

At the Elura deposit mapping by De Roo (1989) identified NE trending D1 folds and cleavages. These were overprinted by later D2 folds and cleavages in which the Elura mineralisation is located, ie mineralisation is D2 in origin.

Hinman and Scott (1990) have identified fold and cleavage trends at the Peak deposit (Fig. 4.15) similar to those listed above for the CSA deposit. However they have not recognised the

D3 event as seen at the CSA. In viewing core from this deposit the author has observed two phases of quartz injection into the same structures possibly indicating overpressuring of the area.

FIGURE 4.1 THE HIGHLY SILICIFIED ASHFALL TUFF (?) OR HIGHLY ALTERED SEDIMENTS WEST OF THE WESTERN SYSTEM, CSA DEPOSIT.

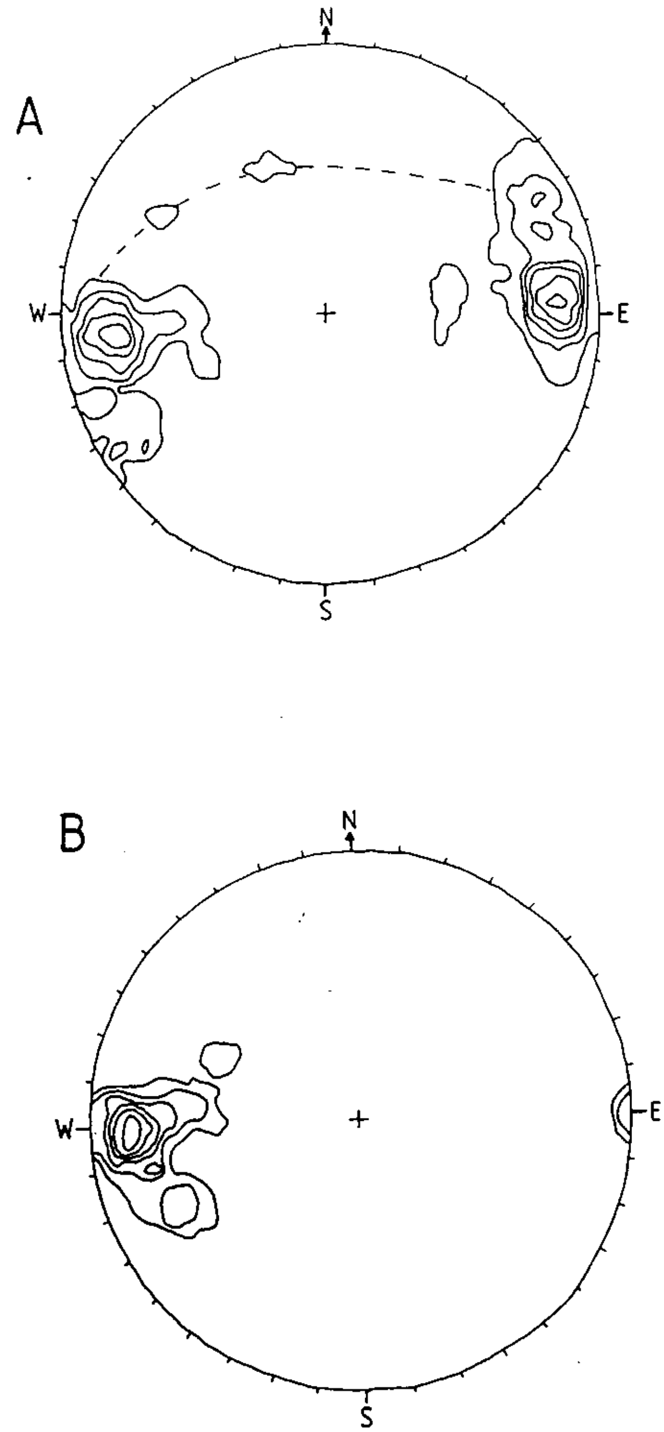

FIGURE 4.2 BEDDING AND CLEAVAGE STEREONETS FOR THE SURFACE WESTERN ZONE.

A) 110 BEDDING DATA AT 2.5, 5, 7.5, 10, 12.5, AND >15 % AREA. NOTE SMALL EFFECT OF REFOLDING BY D3 PLUNGING TO SOUTH.

B) 48 CLEAVAGE DATA AT 5.5, 11, 16.5, 22, 27.5, AND >33 % AREA. NOTE TRENDS TO 060°, 090° AND 120°.

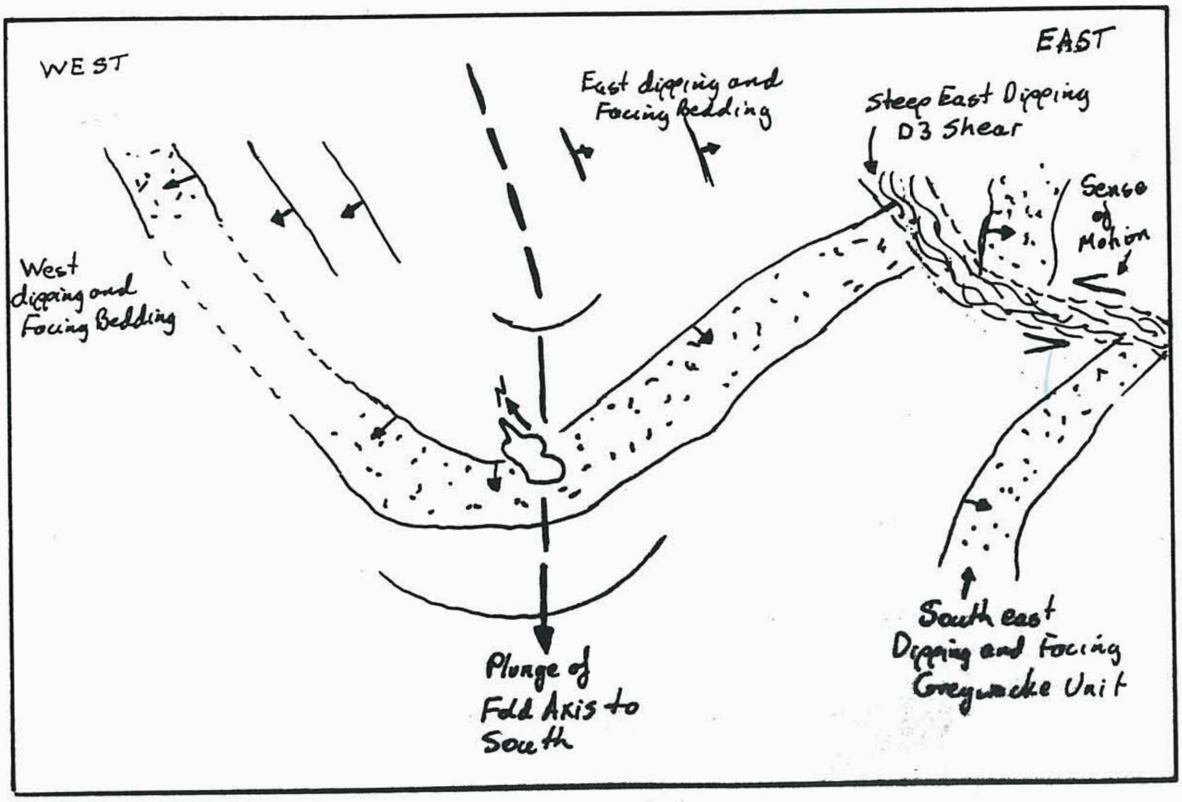

FIGURE 4.3 WESTERN GOSSAN FOLDS AND SHEARS

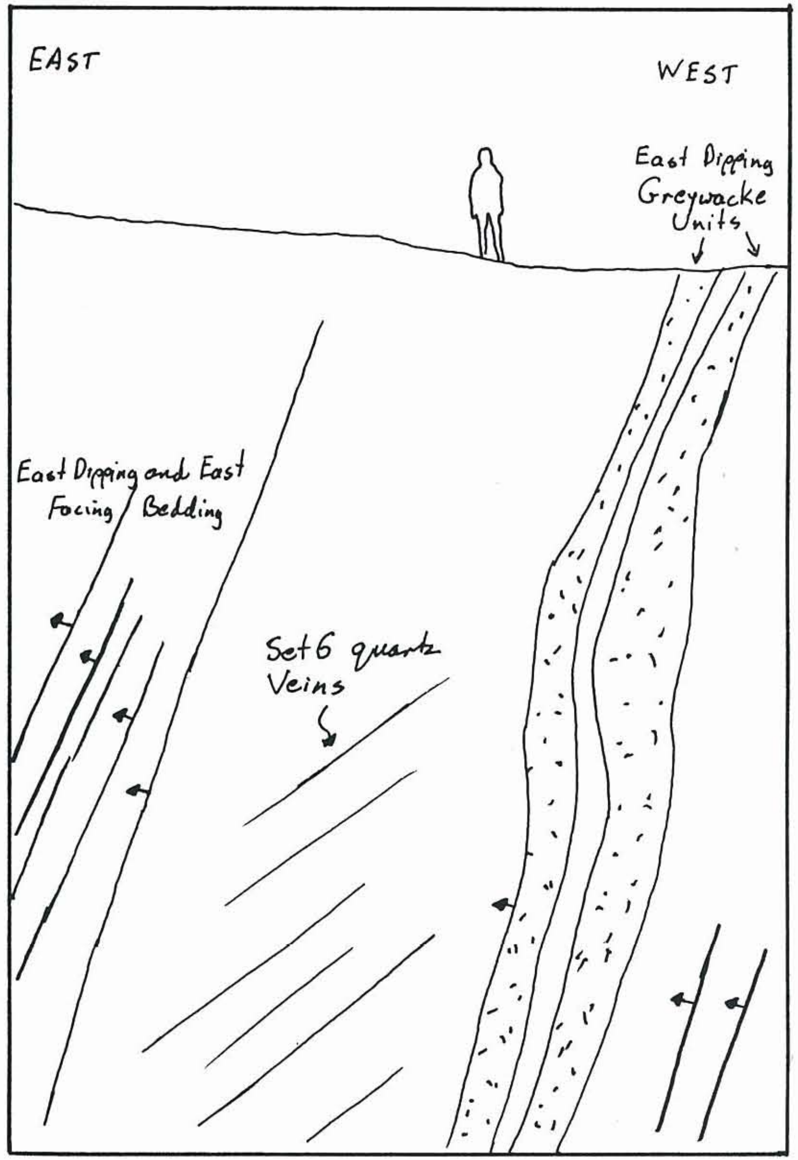

FIGURE 4.4 MULLOCK PASS GEOLOGY LOOKING SOUTH.

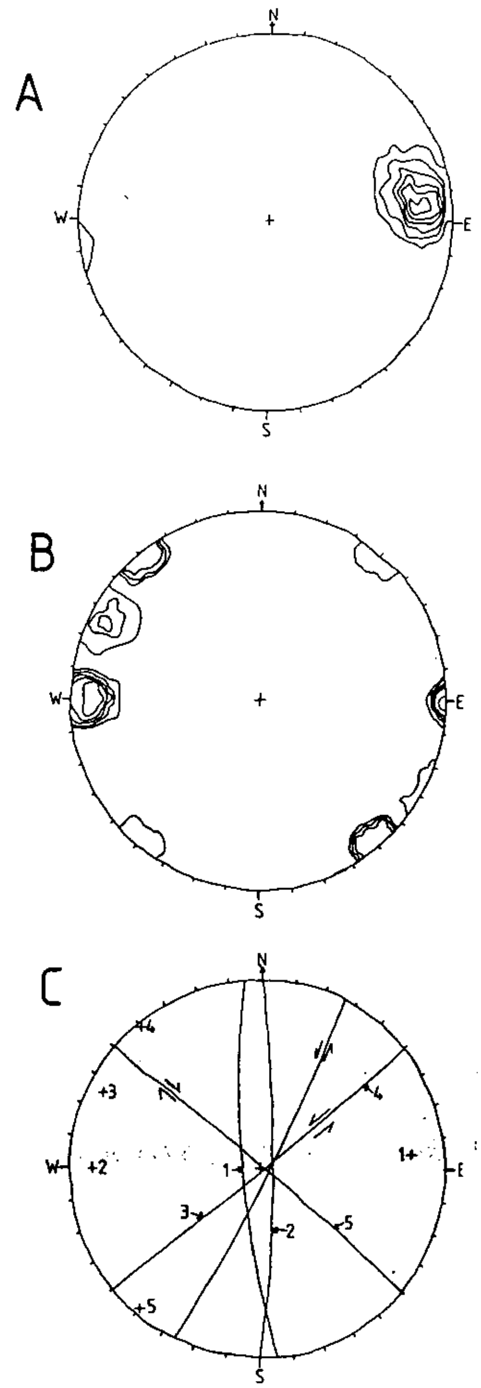

FIGURE 4.5 BEDDING AND CLEAVAGE STEREONETS FOR THE SURFACE EASTERN ZONE.

A) 53 BEDDING DATA AT 6.5, 13, 19.5, 26, 32.5, AND >39% AREA.

B) 46 CLEAVAGE DATA AT 6, 12, 18, 24, 30, AND >36% AREA.

C) GIRDLES AND POLES. BEDDING (1) AT 79° TO 265°, EAST DIPPING CLEAVAGE (2) AT 83° TO 090°, CLEAVAGES (3) AT 85° TO 116°, (4) AT 89° TO 140°, (5) AT 88° TO 040°. NOTE SENSE OF MOTION.

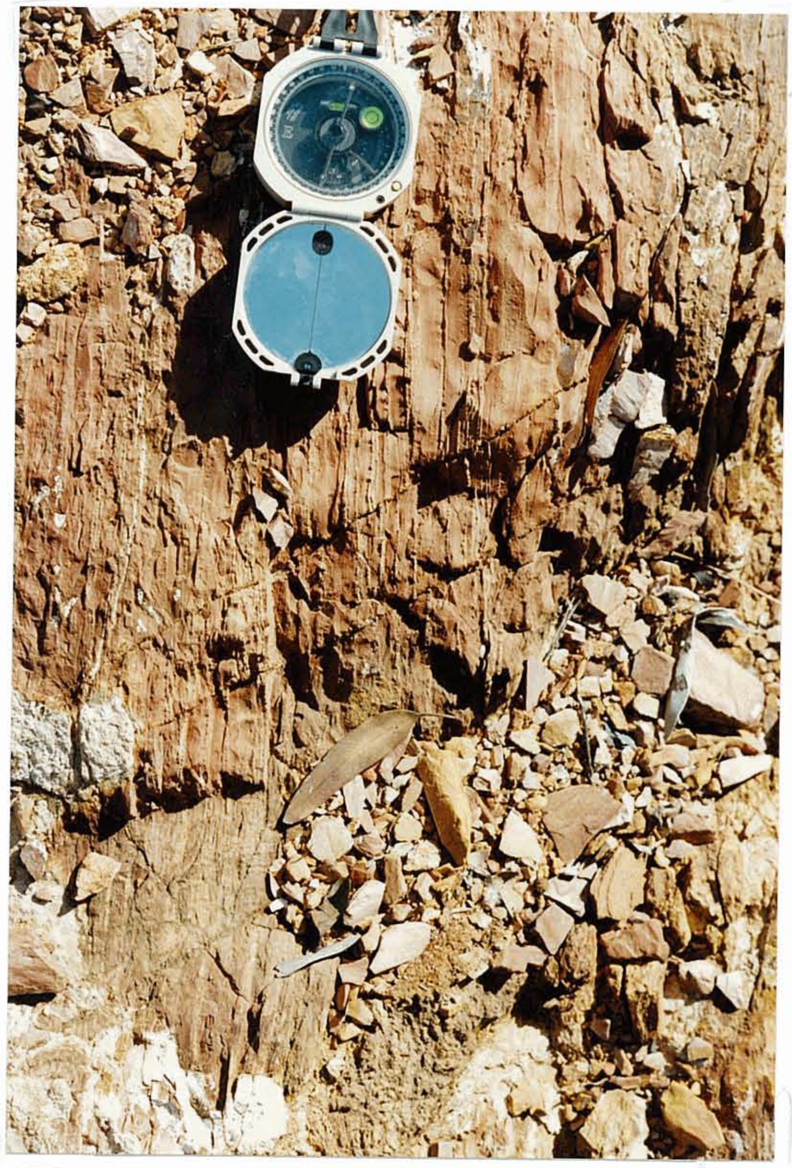

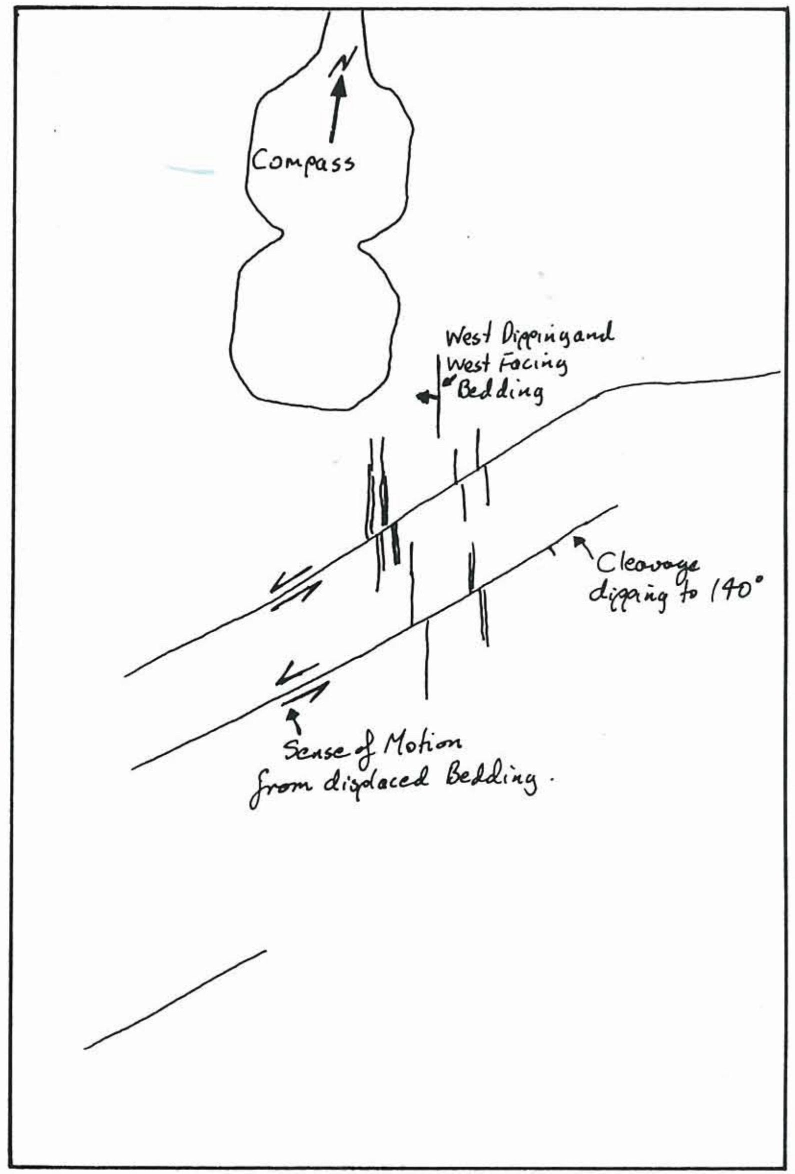

FIGURE 4.6 CLEAVAGE DIPPING TO 140° WITH DISPLACEMENT

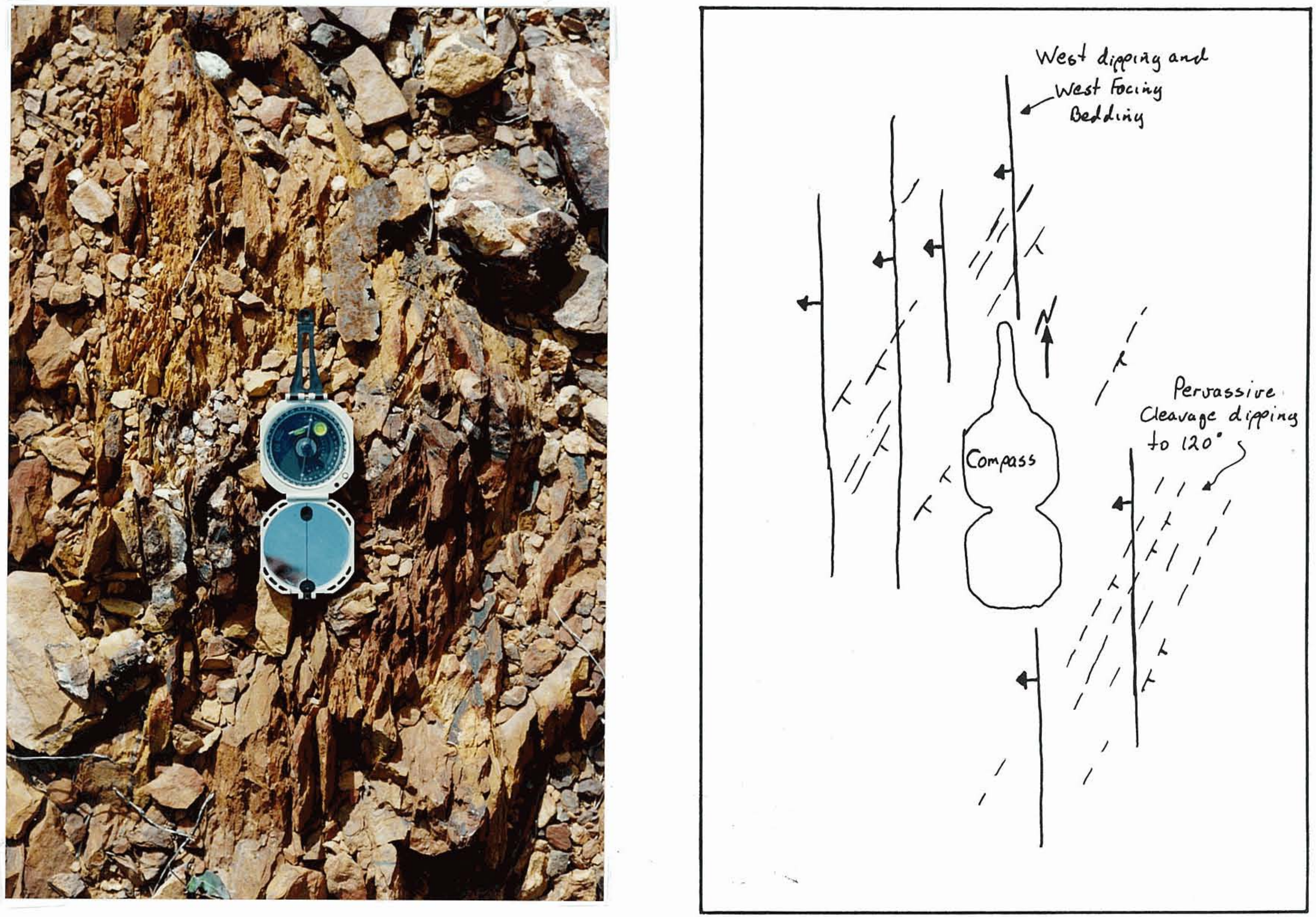

FIGURE 4.7 CLEAVAGE DIPPING TO 120° AND BEDDING

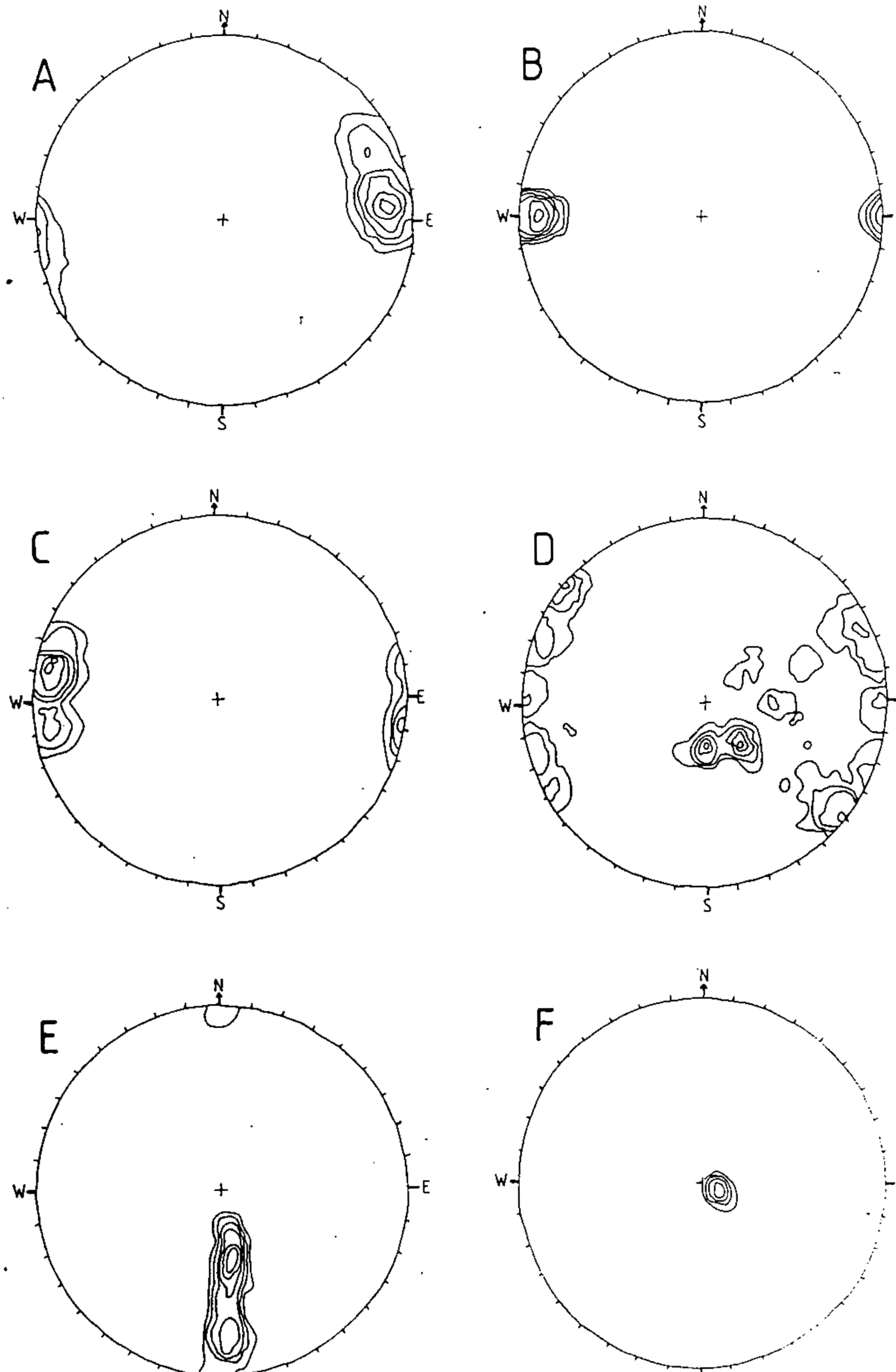

FIGURE 4.8 SEE OVER FOR TEXT

FIGURE 4.8 CSA DEPOSIT UNDERGROUND STEREONETS.

A) 811 BEDDING DATA AT 5, 10, 15, 20, 25, AND >30% AREA. NOTE FOLD ORIENTATION STRIKING NNW.

B) 228 DUE EAST DIPPING CLEAVAGE DATA AT 15, 30, 45, 60, 75, AND >90% AREA.

C) 256 OTHER CLEAVAGE DATA AT 7, 14, 21, 28, 35, AND >42% AREA. NOTE ORIENTATIONS TO 105° AND 080°.

D) 73 FAULT AND SHEAR DATA AT 2, 4, 6, 8, 10, AND >12% AREA. NOTE CONCENTRATIONS AT 110° TO 140°, 050° TO 080° AND THE LOW ANGLE FAULTS TO 340°.

E) 96 FOLD AXIS (L0/3) PLUNGE DATA AT 4, 8, 12, 16, 20, AND >24% AREA.

F) 31 STRETCHING LINEATION (L2/3) DATA AT 15, 30, 45, 60, 75, AND >90% AREA.

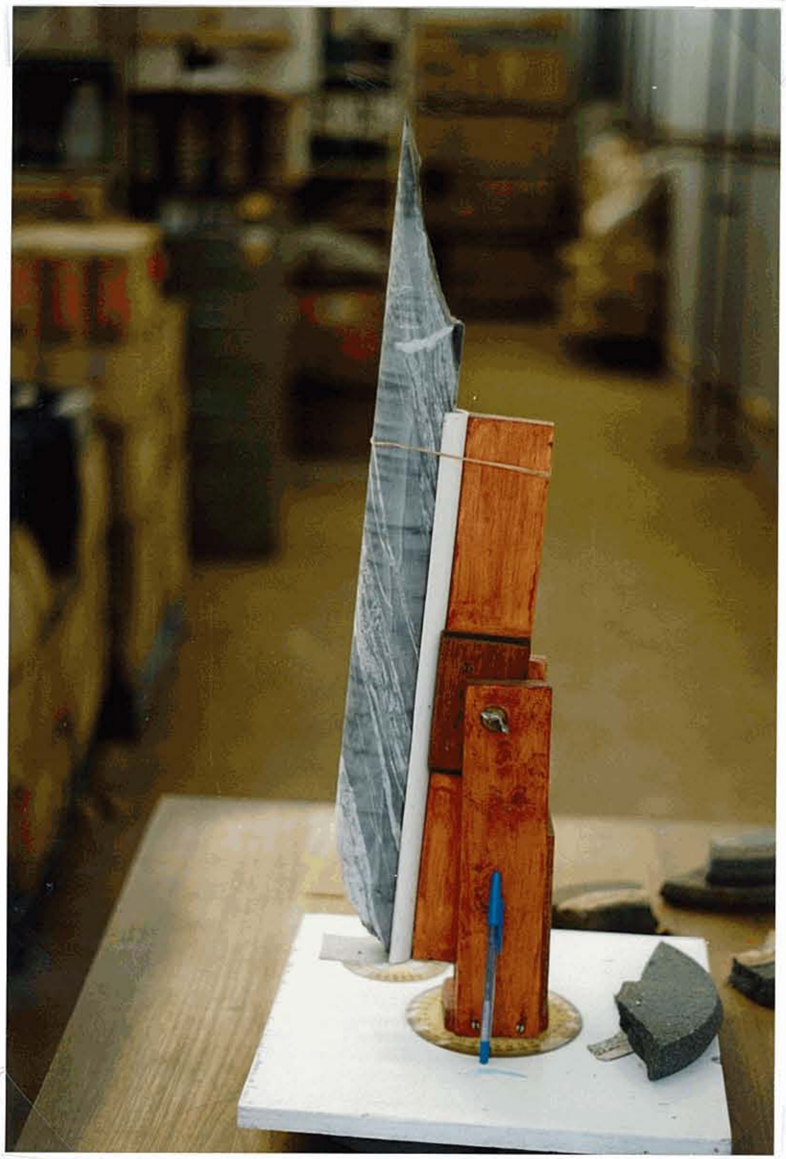

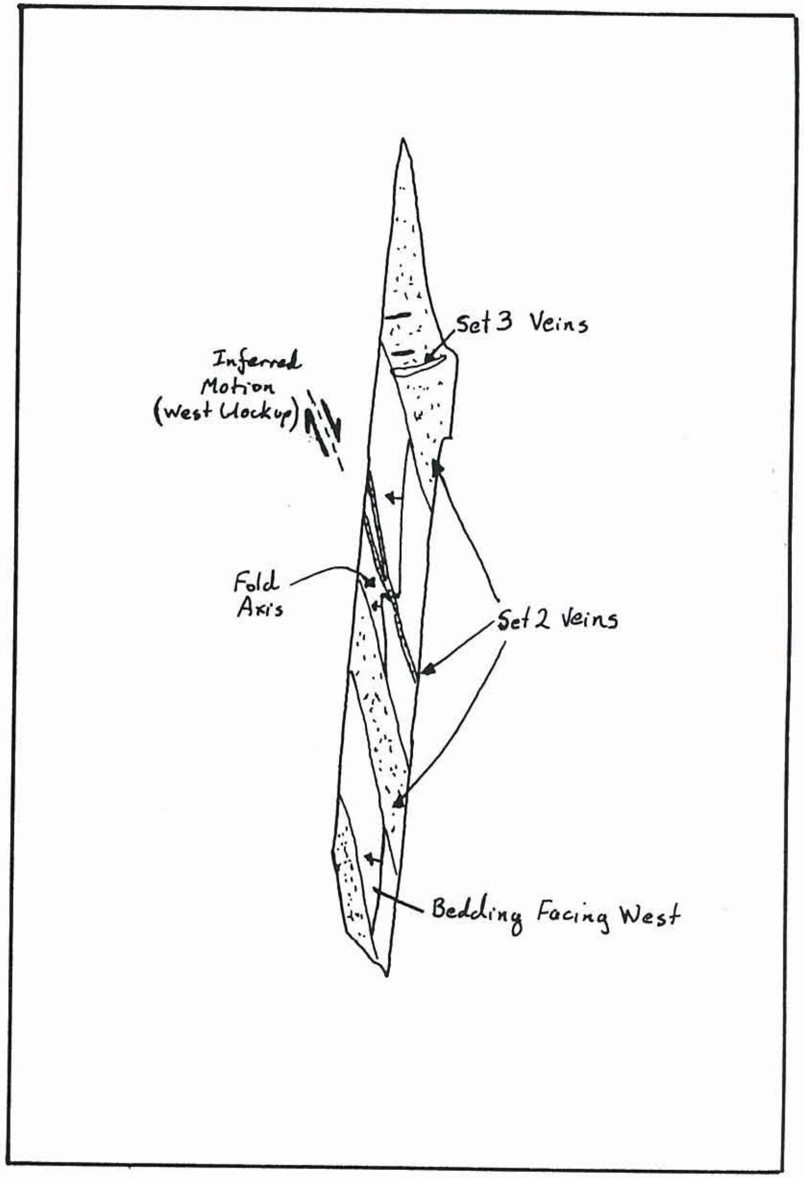

FIGURE 4.9 ORIENTATED DRILL CORE FROM HOLE DDHCM46 SHOWING QUARTZ FILLED CLEAVAGE AND ASSOCIATED FOLD STRUCTURES, LOOKING NORTH.

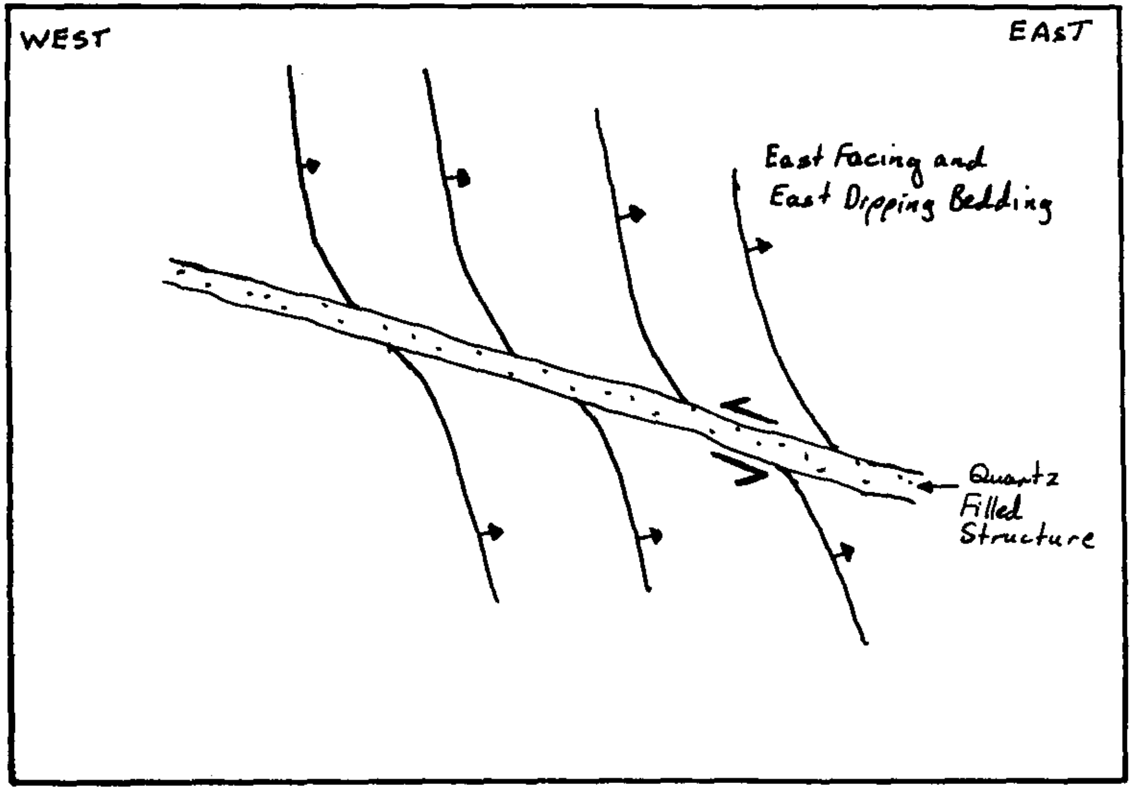

FIGURE 4.10 SET 6 ORIENTATED VEINS WITH SENSE OF MOTION EQUIVALENT TO R' SHEARS (SEE FIG. 4.11, 4.14). FIELD OF VIEW ABOUT 1 METRE LOOKING NORTH. NOTE EAST DIPPING BEDDING. LOCATED NEAR WESTERN SYSTEM ON MAP 1

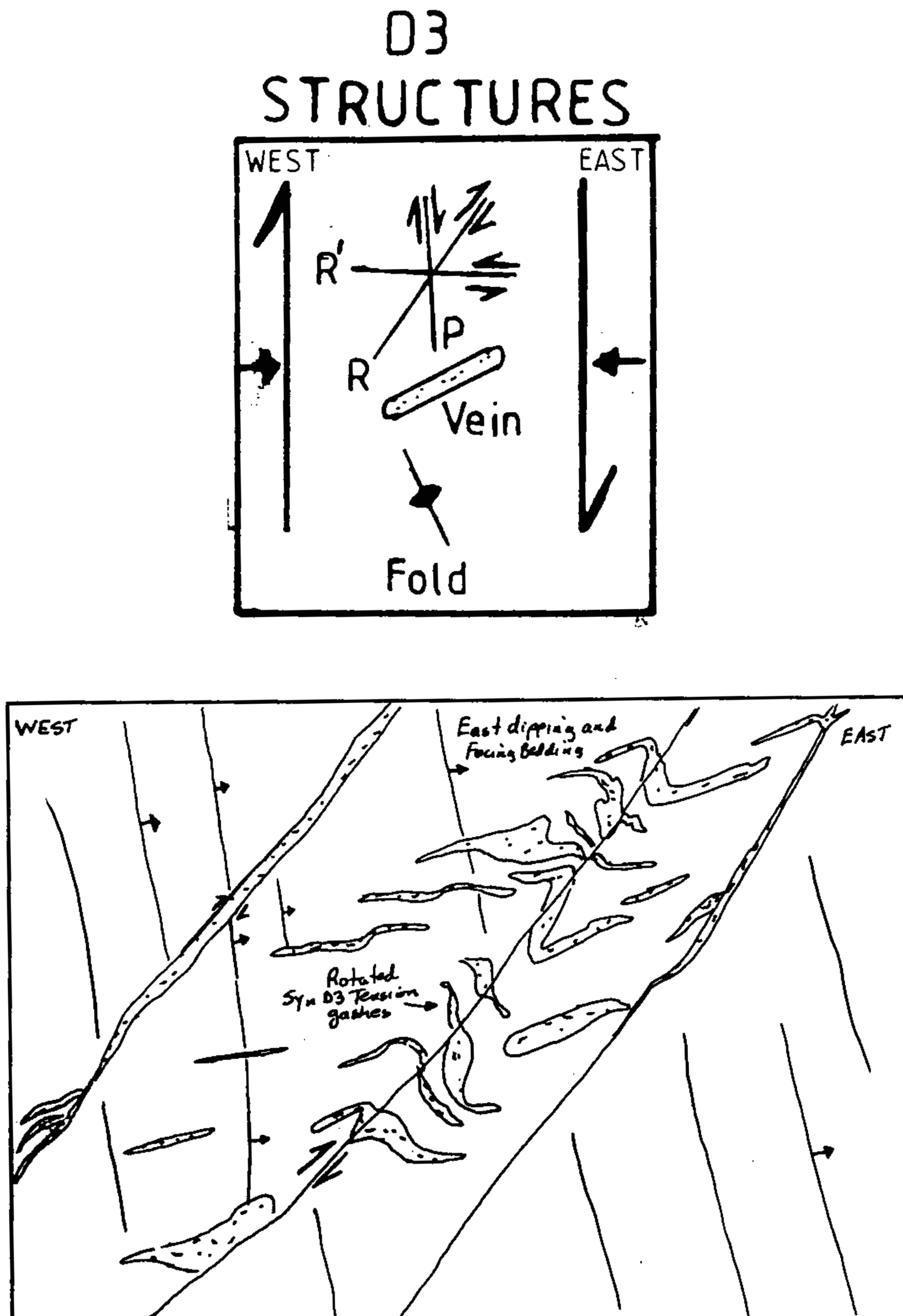

FIGURE 4.11 EAST DIPPING BEDDING, TENSION GASHES AND FAULTS EXPOSED NEAR THE WESTERN SYSTEM ON 11 LEVEL (SEE MAP 1). NOTE THE RELATIONSHIP TO THE D3 STRUCTURES. FIELD OF VIEW ABOUT 3 METERS.

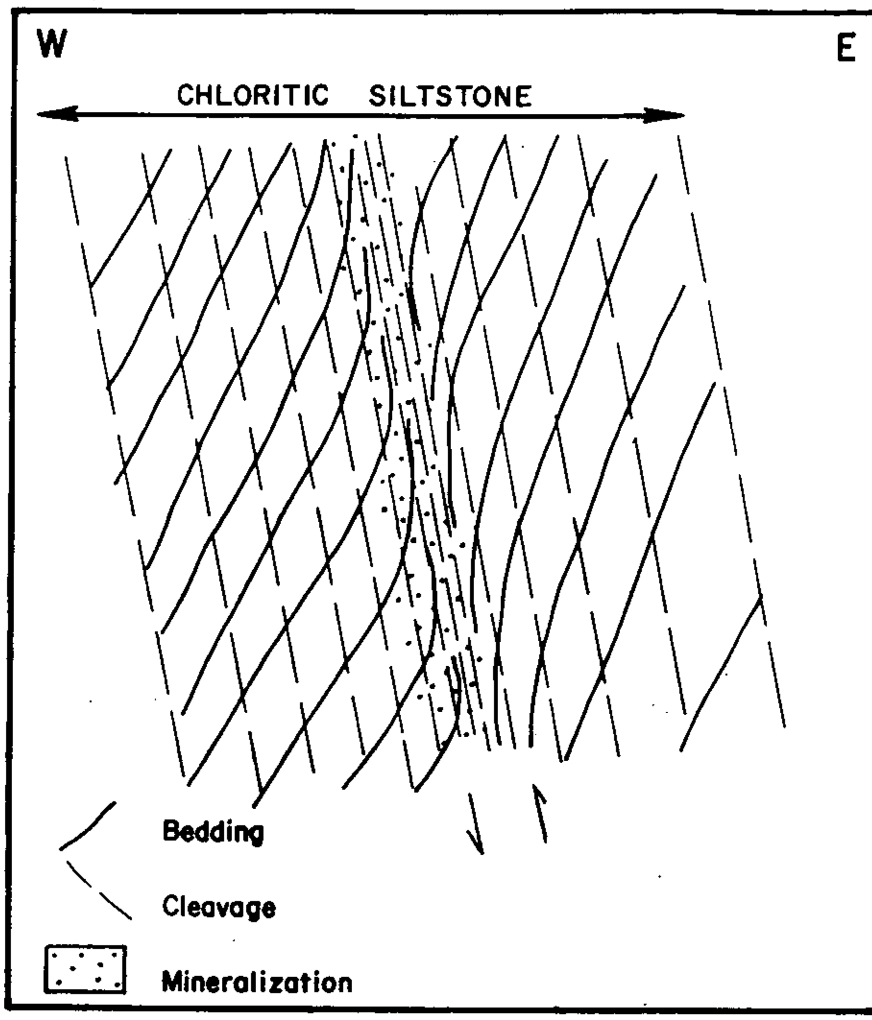

FIGURE 4.12 IDEALISED STRUCTURAL MODEL (CROSS SECTION) SHOWING ROTATION OF BEDDING INTO INTENSELY CLEAVED ZONES WITH MINERALISATION. FROM SCOTT AND PHILLIPS (1990).

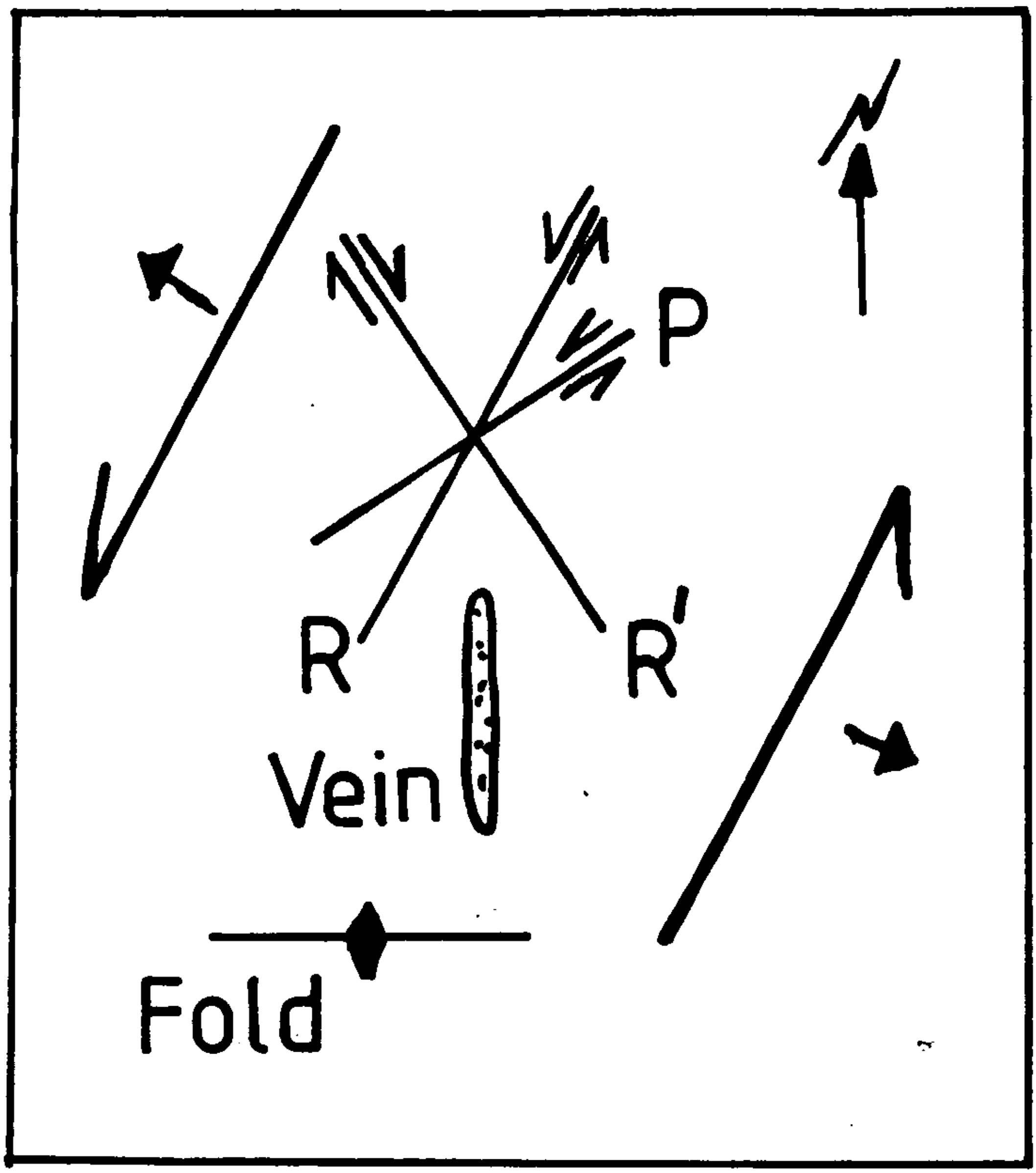

FIGURE 4.13 D2 STRUCTURAL FEATURES IN PLAN. ALSO REFER TO MAP 1.

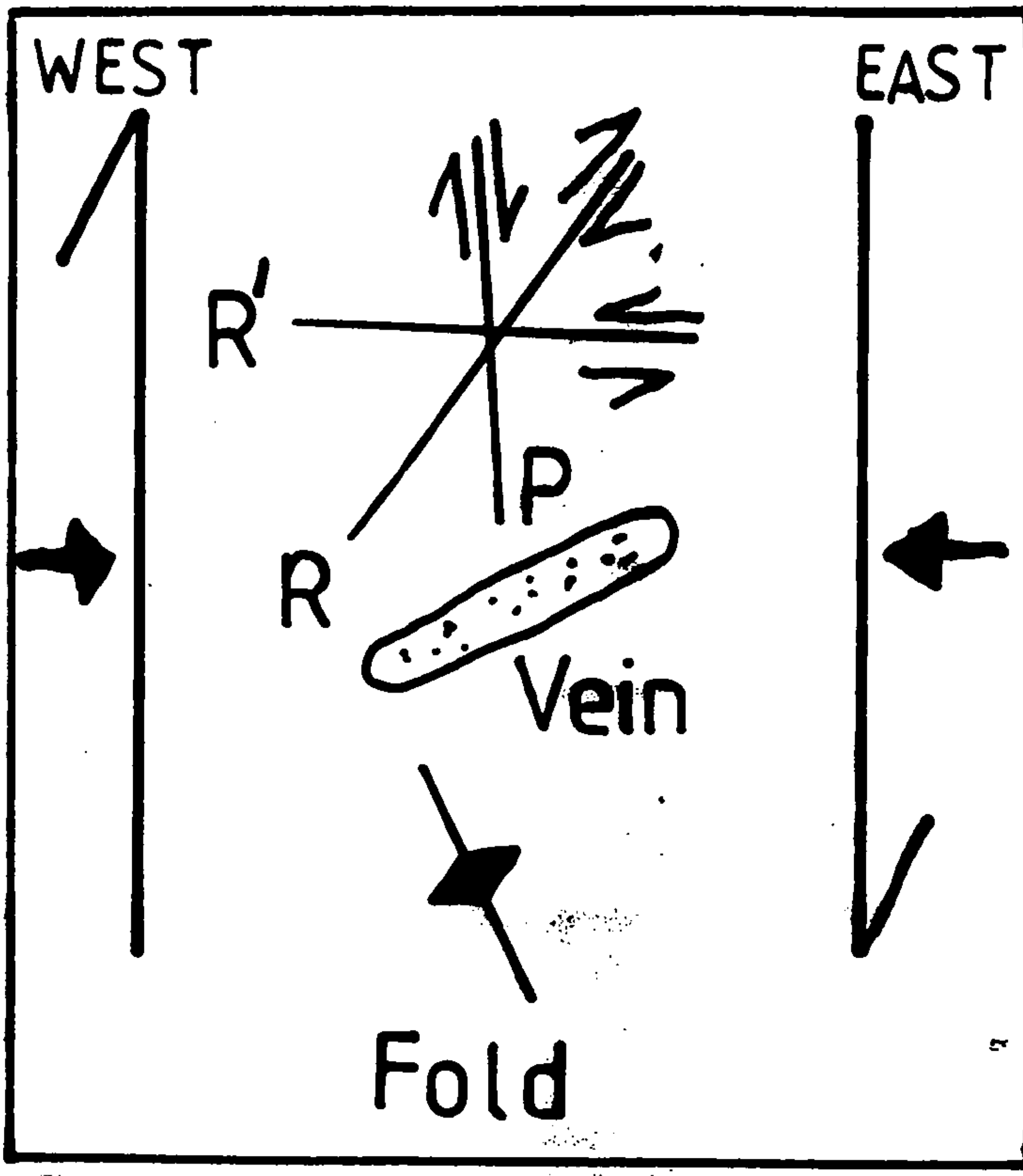

FIGURE 4.14 D3 STRUCTURAL FEATURES IN CROSS SECTION LOOKING NORTH.

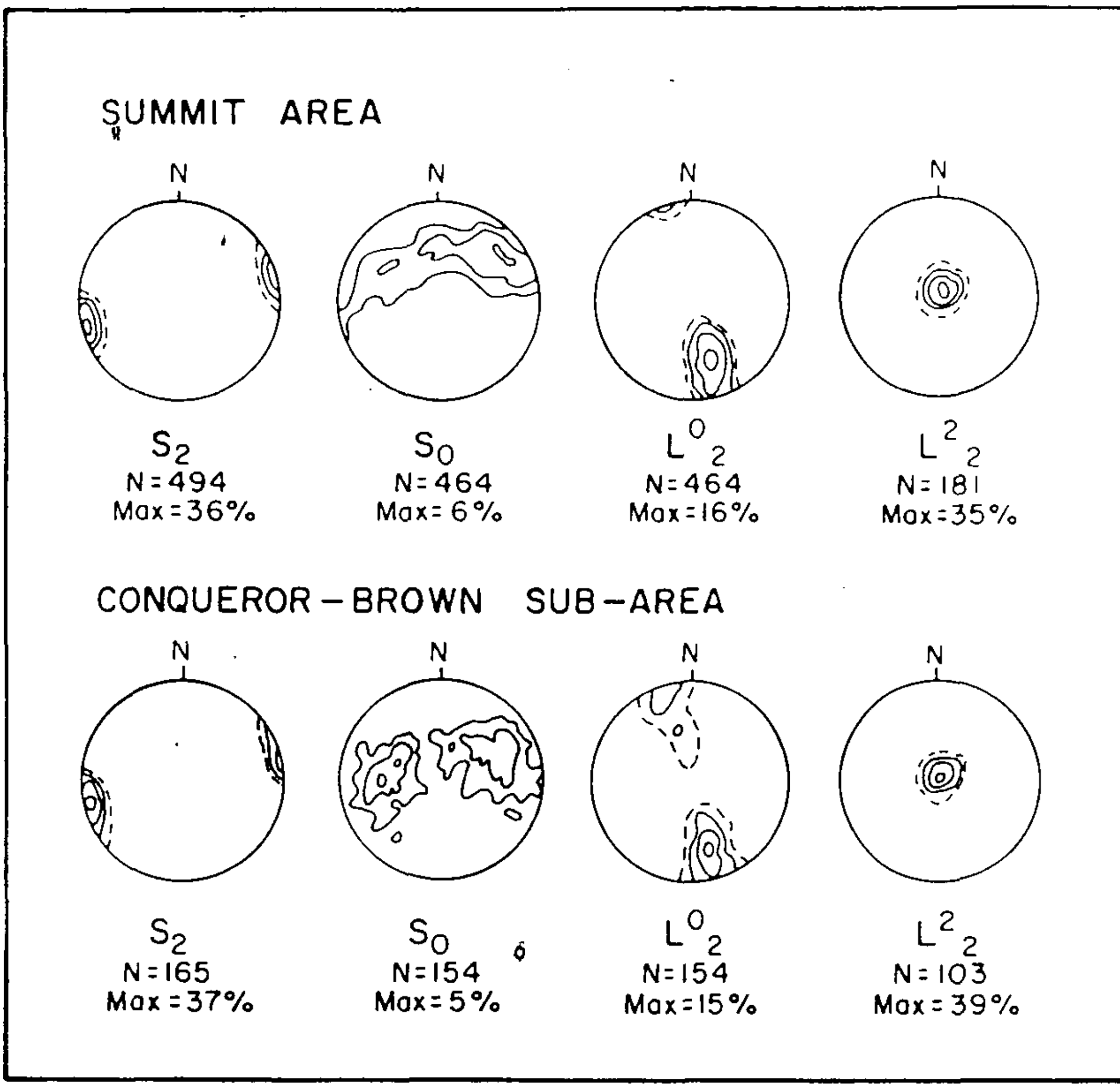

Surface structural data from The Peak summit and Conqueror-Brown sub-areas. Number of data points (N) and the maximum data density (Max) are shown for poles to S_2 and S_0 and for L^0_2 and L^2_2. Contours at 92.5%, 46.25%, 23.1% and 11.55% of the maximum.

FIGURE 4.15 SURFACE STRUCTURAL DATA FROM THE PEAK SUMMIT AND CONQUEROR-BROWN SUB AREAS. FROM HINMAN AND SCOTT (1990).

TABLE 4.1 SUMMARY OF STRUCTURAL HISTORY

EVENT	PREVIOUS MODEL	PROPOSED MODEL
D1	PRODUCED NNW TRENDING TIGHT FOLDS AND DUE EAST DIPPING CLEAVAGE POSSIBLE PTYGMATIC VEINS (SET 1)	ONLY PRODUCED NNW TRENDING FOLDS (DUE EAST CLEAVAGE FORMATION BUT NO QUARTZ ??)
D2	CLEAVAGE FORMATION (SET 2 TO 6) SINISTRAL MOVEMENT MINERALISATION L0/2 FOLD AXIS AND L2/2 STRETCHING LINEATION FORMED QUARTZ VEINING IRON CHLORITES AND BLACK CHLORITE SHEARS PRODUCED	SUB HORIZONTAL SINISTRAL DEFORMATION FROM SE/NW CLEAVAGES OF SET 4, SET 5 AND THOSE TO 140° DEVELOPED MINERALISATION IRON RICH CHLORITES ACCOMPANY MINERALS
D3	NOT RECOGNISED	WEST BLOCK UP SINISTRAL STRIKE SLIP DEFORMATION SET 2, SET 3, SET 6 AND SHALLOW WEST DIPPING FAULTS CREATED QUARTZ INJECTION SULFIDE REMOBALISATION AND DISPLACEMENT BY SET 6 ORIENTATED FAULTS L0/3 FOLD AXIS AND L2/3 MINERAL STRETCHING LINEATION FORMED LATE STAGE BLACK CHLORITE Mg RICH SHEARS DEVELOPE

CHAPTER 5

GEOPHYSICAL INTERPRETATIONS

5.1 SEISMIC DATA

In 1989 a seismic survey was conducted over the Cobar Basin by the Bureau of Mineral Resources (BMR) and the NSW Department of Mineral Resources (Glen 1992). Three lines of data were collected (Fig. 5.1) with the most relevant line to the CSA Area (Line 2) being shown in Fig. 5.2.

From this data Glen (1992) suggests that at its deepest point the basin (Zones 1 & 2) is about 5 km thick and that there are a series of horizontal "detachment" structures within the basin. This is quite contradictory to the earlier work of Glen (1990) who after producing balanced sections of the basin (Fig. 5.3 and 2.7) could only predict the basin in Zone 1 to 2.5 km and Zone 2 to 8 km. Based on current exploration data and the gravity data of Section 5.2 the author agrees with Glen's (1990) interpretation.

5.2 GRAVITY DATA

5.2.1 THE ORIGINAL COBAR GRAVITY SURVEY

A regional gravity survey was conducted by Cobar Mines Pty Ltd (CMPL) between 1970 and 1974 which extended from north of the CSA deposit to the Chesney deposit in the south and almost for the width of the basin (Zone 1 of Glen (1987), Fig. 5.4). The interest in gravity surveys followed a previous Department of Mines gravity survey over the CSA deposit (Pegum 1962) which identified a "positive" gravity trend over the deposit using a density of 1.7gm/cc.

Stations for the CMPL Survey were initially set out over areas of interest at intervals of 30 m (100 ft) on lines 152 m (500 ft) apart and later on lines 305 m (1000 ft) apart in areas of lower priority. Within the CSA/Spotted Leopard Area an Ultimate Base Station (UBS) was set up and along each line of the survey was a Base Station (BS). Each BS was tied to the UBS. Corrections for latitude, instrument drift and elevation were applied to the data, however topographic corrections were not applied given the flat Cobar landscape and trials that produced corrections of only 0.05mgals (Harvey and Clarke (1972)).

The Bouguer Anomaly values for the CSA/Spotted Leopard Area were then calculated using a density of 1.7 gm/cc based on density measurements from near surface diamond drill core. Values calculated for the areas south of Cobar used densities of 2.1 and 2.2 gm/cc. Surveys completed by other companies in the area were calculated using multiple density values, one of which was 2.2 gm/cc and regional BMR gravity maps held at CMPL were also known to be calculated using 2.2 gm/cc. So it was decided that the CMPL data calculated at 1.7 gm/cc would be reprocessed and the data for Cobar standardised to 2.2 gm/cc.

5.2.2 REPROCESSING THE DATA

Unfortunately only about 5% of the original data recording sheets were available for the original CMPL Survey. Fortunately a complete set of plans, profiles, and topographic maps existed allowing northing, easting, elevation and Bouguer Anomaly values at 1.7 gm/cc to be obtained either directly (in the case of calculated gravity value) or by scaling (in terms of elevation data) and entered into Lotus 1,2,3 spreadsheets. Latitudes of the stations were also recalculated and theoretical gravity (gTheo) determined.

In order to recalculate the Bouguer Anomaly at 2.2 gm/cc, a back calculation had to be done to determine the observed gravity reading (gObs). The equation used by Harvey and Clarke (1972) to calculate the Bouguer Value for a station (GS) when simplified is:

$$GS = gObs + (es - eb)(0.09406 - p \times 0.01276) + gb \quad ...(1)$$

or

$$GS = gObs + FA - BC + gb \quad ...(2)$$

where gb is the base station gravity value, es is the station elevation, eb the base station elevation, FA is the Free Air Correction, and BC is the Bouguer Correction. As gObs was not available due to the lack of original data sheets a constant was created. At the UBS the gravity at a density of 1.7 gm/cc was calculated from (1) as 0.0, and as es = eb and gb = 0 then is assumed that gObs UBS equals gTheo UBS. This means that for the survey the estimated gObs is:

$$gObs = GS - (FA - BC + gb) + 982642.41 \quad ...(3)$$

where 982642.41 is the gTheo UBS value.

So, substituting the density of 2.2 gm/cc for 1.7 gm/cc it is possible to recalculate the Bouguer anomaly values using equation 4, which does not take into account the terrain correction as less than 1% of the data is affected by gradients greater than 5 from station to station:

GS = (gObs + FA - BC) - GTheo ...(4)

The values produced by equation 4 at a density of 2.2 gm/cc were unusually high (50 to 60 mgal), compared to the BMR survey values of -8 to - 20 mgal. Fortunately there is one station of the BMR regional survey which overlaps with the CMPL survey, ie station A4708 with a BMR value of -11.4 mgal. The corresponding CMPL station has a value of +50.3 mgal, giving a difference of 61.7 mgal between the two surveys. This constant of 61.7 mgal is then subtracted from all values generated by equation 4 to reduce the CMPL survey to the BMR level. In doing this the earlier assumption of gObs UBS equals gTheo UBS is accounted for.

Although the new gravity data at 2.2 gm/cc is an improvement on the old data set, it is planned to use the correction techniques described above to reprocess the CMPL and other surveys at a density of 2.67 gm/cc to standardise the surveys with current BMR maps. This can now be done with relative ease as for the first time since 1974 the data is compiled and digitally recorded. It is expected that this will further highlight basin structures which have been seen to occur in the change from 1.7 gm/cc to 2.2 gm/cc.

5.2.3 DENSITY DETERMINATIONS

In order to assist in interpretation of the gravity data, the densities of various rock types within the Cobar area were determined. This was done by weighing the sample dry, suspending the sample in water and re-weighing the sample (thus determining the volume using the approximation of 1 ml of water equals 1 gm), and dividing the former by the latter to produce a density. Approximately 100 samples of each rock type listed in Table 5.1 were recorded and when samples were not available density values were assumed. All density calculations are listed in Appendix 4. It should also be noted that regards the altered rock types, density does alter with the amount of quartz in the sample.

In the model discussed in Section 5.4 the density of the ore systems is calculated by proportioning the area of mineralisation and alteration to produce an overall density. Densities of the Ballast Beds, Zone 1 and Zone 2 are assumed as a constant 2.75 gm/cc given they are composed of sedimentary material while granite/basement density is assumed as 2.55 gm/cc for the model as basement rocks are unknown. The author acknowledges that the basement density could vary substantially from the assumed value and thus alter the model or its validity accordingly (see discussion below).

5.3 REGIONAL GRAVITY DATA

The regional BMR gravity data was collected on a grid approx. 14 km x 14 km (Map 4). The high strain Zone 1 of Glen (1987) which defines the eastern position of the Cobar basin and where much of the economic mineralisation is found is only approximately 8 to 10 km wide. Hence very little of the regional BMR data is representative of Zone 1, particularly when the recalculated CMPL data over the CSA deposit is -5.16 mgal and the BMR map suggests -12 mgal. Despite the wide spacing of the BMR stations, the trends of the contours do respond to the less dense granites found to the north and north east of the regional geological map (Map 4 and Map 5).

However, by using the value of -5.16 mgal at the CSA deposit and the geophysical modeling programme of Roach (1992) it is possible to construct a regional cross section of the geology and gravity based on current geological ideas (Fig. 5.5). The programme of Roach (1992) uses the difference (contrast) in the densities listed in Table 5.1 and a standard density of 2.67 gm/cc in order to calculate a profile.

From the profile in Fig. 5.5 and the information taken from Maps 4 and 5 it can be seen that the major control on the gravity profile is the depth to granite/basement assuming that Zone 1, Zone 2 and the Ballast beds are composed of sediments of similar density. This is primarily due to the negative effect basement has on the calculations and partly due to the fact that no samples of basement material exist, thus making it necessary to assume a density of 2.55 gm/cc. To the west the granite is at some considerable depth, but to the east it is relatively shallow beneath the Ballast Beds.

In creating the regional model (the only model created is the one shown in this text) variations were tried whereby the granite/basement density was varied by 0.1 gm/cc at a time. This resulted in the depth to basement being reduced by about 500m on each occasion until exposed on surface which is geoogically impossible unless

1) basement does have the same density as the sedimentary rocks and cannot be distinguished by gravity and/or
2) the model is geologically incorrect and/or
3) the original data and later reprocessing is invalid.

Clearly there needs to be much more work conducted on understanding the geology on a regional setting in relation to the gravity data as other geological models could give the same result.

The parameters of this regional model, similar to the early interpretations of the basin by Glen (1987, 1990), control the mine detailed local model discussed in Section 5.4. The physical parameters of the regional model (Fig. 5.5) are listed in Appendix 5.

5.4 BASIN WIDE MODEL

From the recalculated Bouguer anomaly values and the new contour maps of the CMPL survey (Map 6) plus the regional model presented in Section 5.3 it is possible to construct a basin wide model (Fig. 5.6). The gravity data used in Fig. 5.6 is derived from the line across Map 6 which includes the CSA Deposits in the west and a series of small highs in the east.

When the observed gravity data is plotted on the profile of Fig. 5.6 the features visible are:

1) the data becomes more negative to the east,

2) small highs exist on the negative easterly trend,

3) a high exists over the CSA Deposit.

The negative easterly trend is due to the granite/basement contact shallowing to the east. Initial models used a density for the granite/basement of 2.50 gm/cc which implied the contact had a depth of approximately 2.6 km. The model shown in Fig. 5.6 uses a granite/basement density of 2.55 gm/cc which produces a depth to the contact of approximately 2 km. This is in keeping with the balanced sections of Glen (1990) (Fig. 5.3). It has also been noted that a granite/basement density of 2.6 gm/cc could place the contact at a depth between 1.5 km and 2.0 km. The deepest drilling at the CSA deposit is now at 1.35 km below surface and there has been no changes in rock types so it is possible that the contact is between 1.5 and 2 km below surface.

As for the slight highs that occur on the negative easterly trend, these equate to known shears within the basin. The shears are partly quartz filled and weakly mineralised (as identified during a regional surface geochemical survey, Fig. 5.7) and the gravity highs over these are partly explained by the density contrast in fresh rock and partly by the contrast in weathered material. In some cases modeling of the shears inadequately explains the highs and may indicate the presence of other rock types not yet recognised in the basin.

Using the granite/basement contact information and what is known of the CSA mineralisation, it is possible to extend the ore systems to basement (ie to 2 km). As already stated above, the depth to basement depends on the density chosen and it is more likely that mineralisation extends to a depth between 1.5 km and 2 km below surface.

Other assumptions made in generating the model are:

1) the rocks in Zone 1, Zone 2 and the Ballast Beds being sedimentary are of the same density, and
2) with the exception of the near mine environment where the depth of weathering is 120m in the other areas it is 80m based on drill information.

The last remaining feature of Map 6 to be noted is on the western edge of the survey where a strong negative NNW trend exists. To date there is no acceptable explanation of this trend other than it may represent the highly silicified ashfall tuff of Schmidt (pers. comm) referred to in Section 4.1.1. However the gravity low does correspond to a magnetic ridge as discussed in Section 5.5.

As with the regional model only one basin wide model was created (the one shown and referred to in this text). Varyiny the basement density by 0.1 gm/cc in the basin wide model produced similar results to that documented in Section 5.3 above for the regional model. This implies that there is something fundamentaly wrong with the model selected and clearly more work is required in understanding the basin on a regional and local scale.

The parameters used to create the basin wide model are listed in Appendix 6. In producing both models the author realises that the solution presented is not unique and other geological could give a similar result, however a better understanding of the basin has been gained.

5.5 MAGNETIC DATA

Using the modeling programme of Roach (1992) it is also possible to model the cause of the magnetic anomalies seen in the Cobar area. However still not enough is known of the relationship of the anomalies to mineralisation. The facts and observations about the magnetic anomalies are:

1) of the 15 or so deposits only three (Elura, Dapville, and the Western and Eastern Systems at the CSA) lie in the centre of a 'bulls eye' magnetic anomaly,
2) the remaining deposits occur adjacent to or offset from magnetic anomalies, the source of which is usually cleavage orientated pyrrhotite or magnetite,
3) some magnetic anomalies occur as ridges indicating a relationship to structure (Fig. 5.7). One of these ridges corresponds to the NNW trending gravity low referred to in Section 5.4 above. All the Cu/Au deposits south of Cobar occur on magnetic ridges induced by structure,
4) some magnetic anomalies appear to be stratigraphically controlled. The best example is the Mopone Magnetic anomaly to the east of the CSA deposit and near the eastern edge of the basin which indicated a folded stratigraphic unit plunging to the SW (Fig. 5.8). The

position and trend of this fold is to be expected given the dome like structures that occur to the north at Mt Drysdale (Map 5), and

5) the remainder of the anomalies are due to maghemite concentrations associated with drainage patterns.

Clearly the anomalies are of interest to exploration but attempting to discern information from them other than that listed above is temporarily impractical.

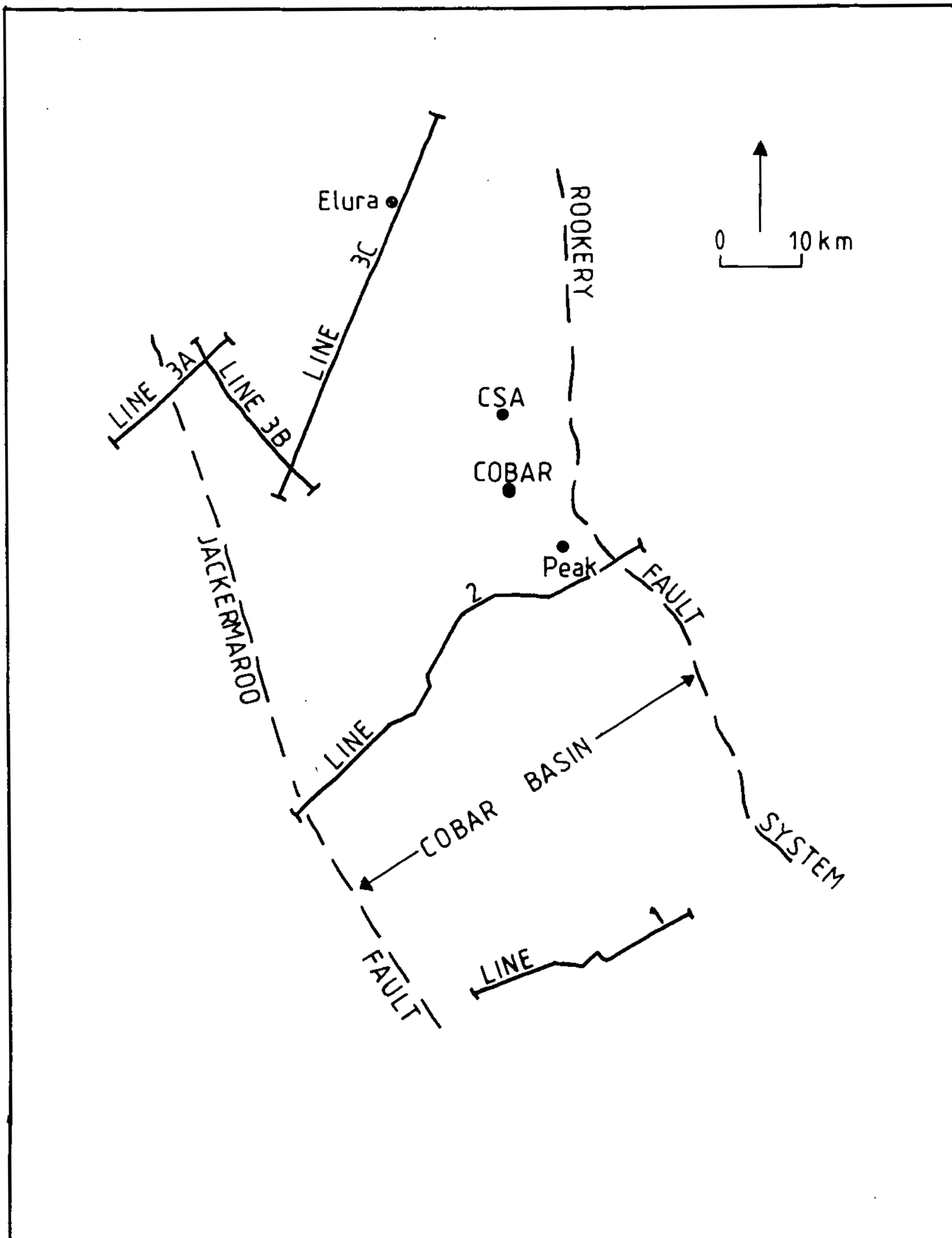

FIGURE 5.1 COBAR BASIN, STRUCTURAL FEATURES AND ACORP SEISMIC SURVEY LINES. FROM GLEN (1992).

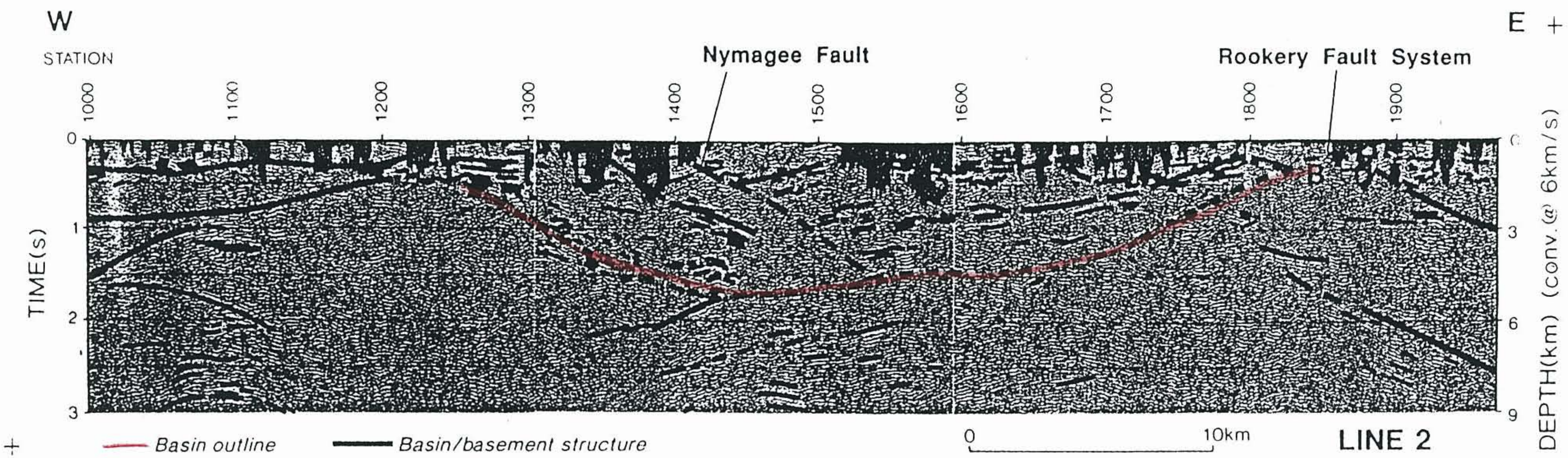

FIGURE 5.2 COBAR BASIN, CROSS SECTION ALONG ACORP SEISMIC SURVEY LINE 2. FROM GLEN (1992).

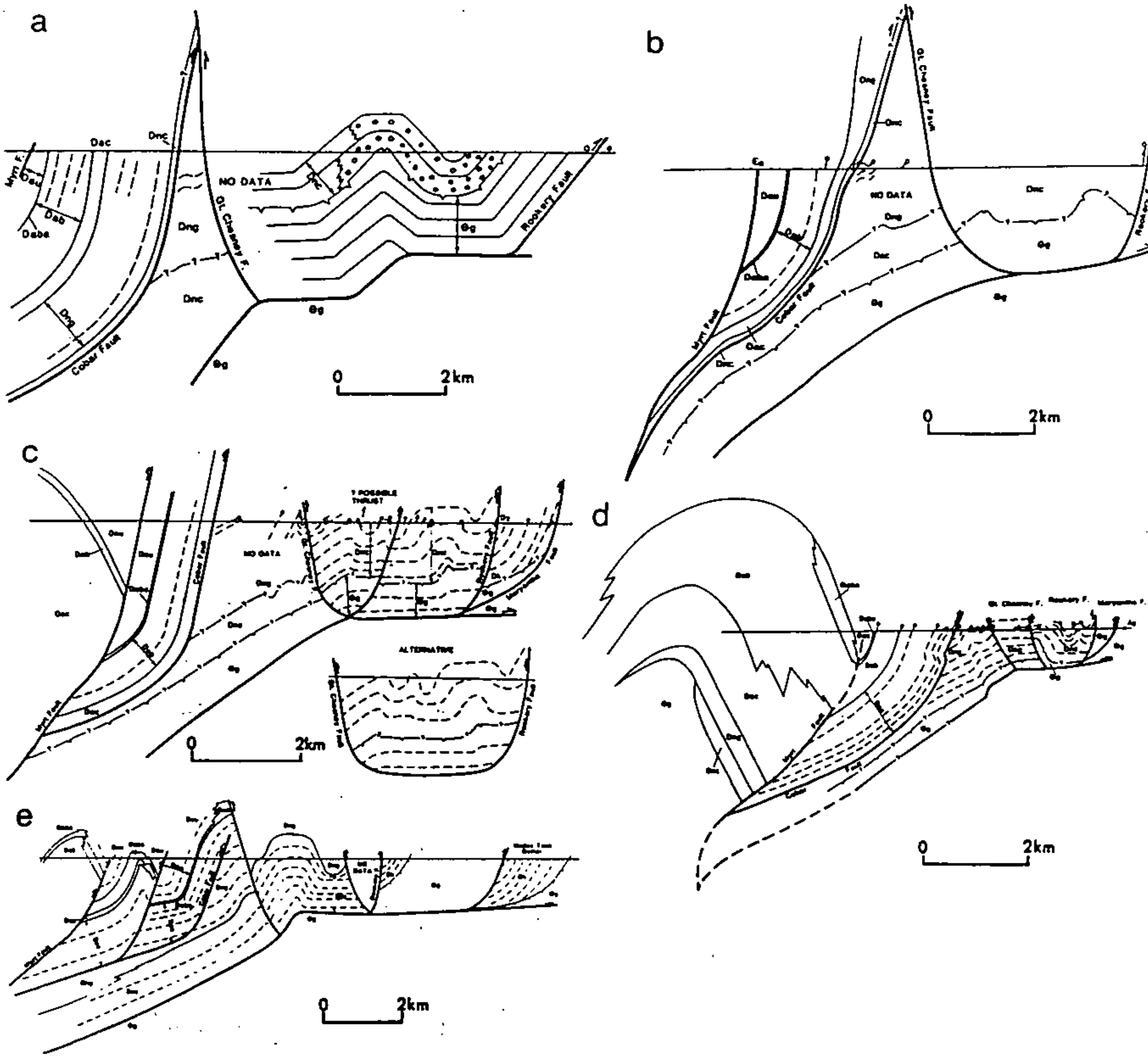

North to south series of cross-sections through structural Zone 1 and in part extending east of the zone. For discussion see text. Sections were drawn using kink-type constructions of Suppe (1983) which were then modified by rounding hinges and by taking into account limited drill data which suggests faults remain steep down to 1 km or so. Sections are line balanced, but have not removed unquantifiable cleavage strain. They do not take strike-slip movements into account. Sections are not unique, given lack of relief, and absence of subsurface data. Presence of other units at depth (e.g. volcanics) would cause significant changes to the sections. Note that the CSA Siltstone and Great Cobar Slate are, in part, laterally coeval, representing deposition from different fan systems. As a result, Dac in (b) passes up into Dng, and Dac in the Cobar Plate is equivalent to Dng in the Chesney Plate. This means that the Cobar Fault puts Dac on top of Dac equivalent plus older rocks. For abbreviations see Fig. 2.7

FIGURE 5.3 NORTH TO SOUTH SERIES OF CROSS SECTION THROUGH STRUCTURAL ZONE 1. FROM GLEN (1990).

TABLE 5.1 COBAR AREA ROCK DENSITIES

ROCK TYPE		AVERAGE DENSITY (gm/cc)	CONTRAST TO 2.67 gm/cc
WEATHERED UNALTERED SEDIMENTARY [WUNALT]		2.33	-0.34
WEATHERED ALTERED SEDIMENTARY [WALT]		2.59	-0.08
GOSSAN/IRONSTONE		2.45	-0.22
FRESH UNALTERED SEDIMENTARY [FUNALT]		2.75	+0.08
FRESH ALTERED SEDIMENTARY [FALT]		2.80	+0.13
FRESH PORPHYRY (QUEEN BEE)		2.64	-0.03
VOLCANIC BRECCIA (PEAK)		2.67	0.00
RHYOLITE (PEAK)		2.68	+0.01
*GRANITE/BASEMENT		2.55	-0.12
*BALLAST BEDS, ZONE 1 & 2		2.75	+0.08
**CSA ORE SYSTEMS	- Pb/Zn	3.70	
	- Cu		
	QTS NORTH	3.10	
	QTS SOUTH	3.00	
	WEST SYS.	3.25	
	EAST SYS.	3.10	

* ASSUMED
** PROPORTIONED BY AREA WITH ALTERED MATERIAL TO GIVE VALUES IN CSA MODEL.
[] ABBREVIATIONS USED IN NAMING BLOCKS FOR THE MODELS.

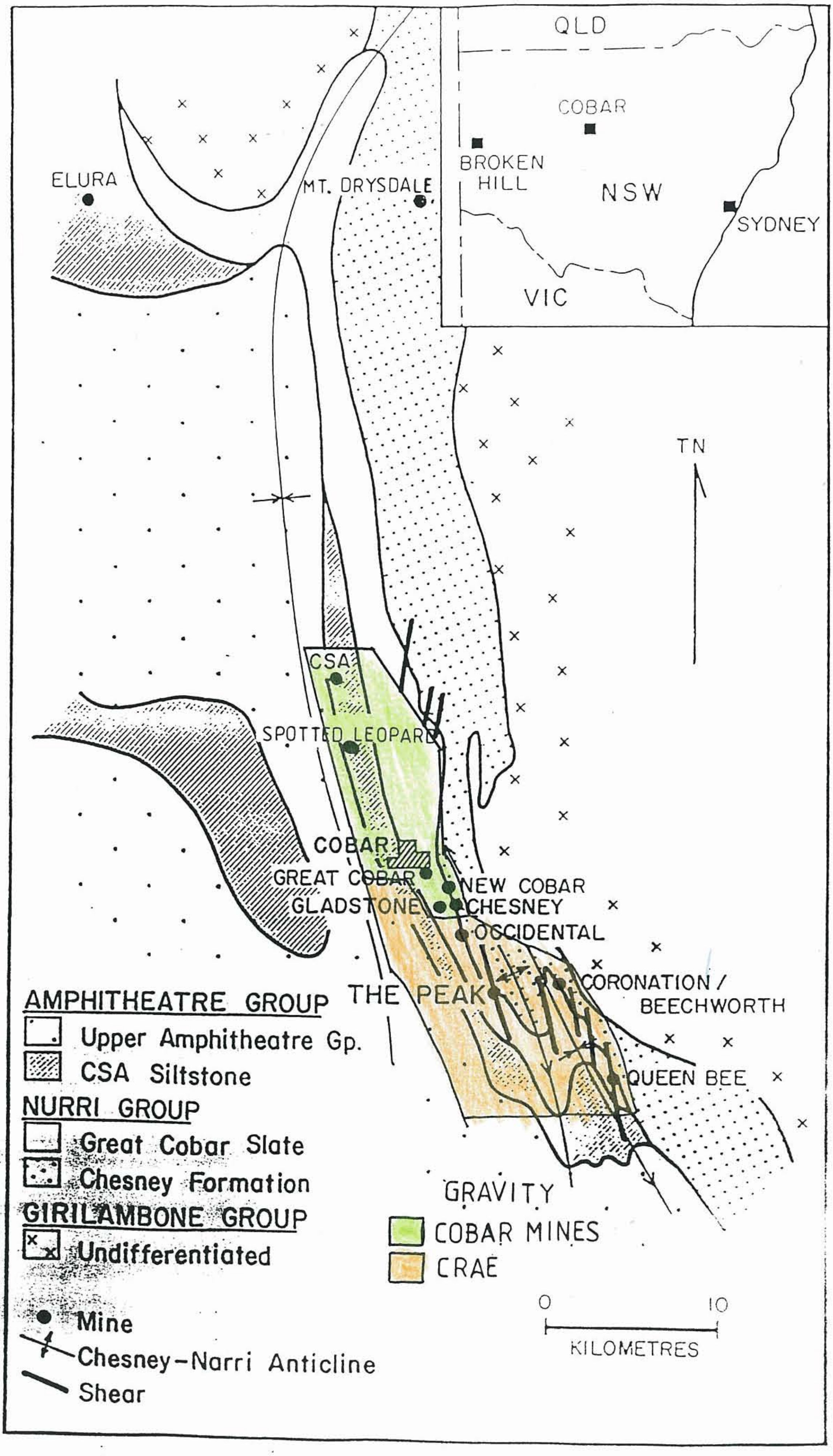

FIGURE 5.4 COBAR REGIONAL GRAVITY SURVEYS.

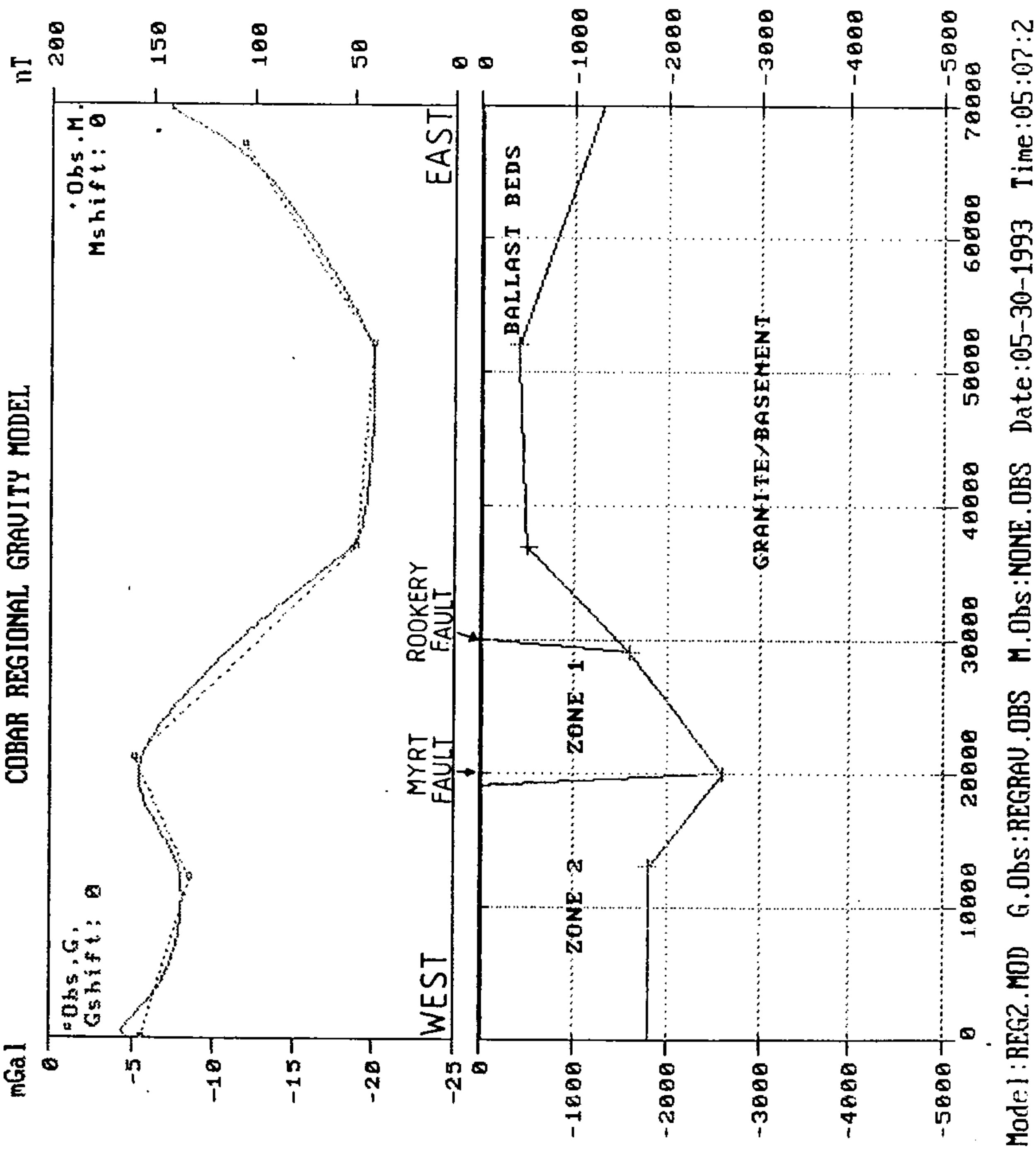

FIGURE 5.5 COBAR REGIONAL GRAVITY MODEL.

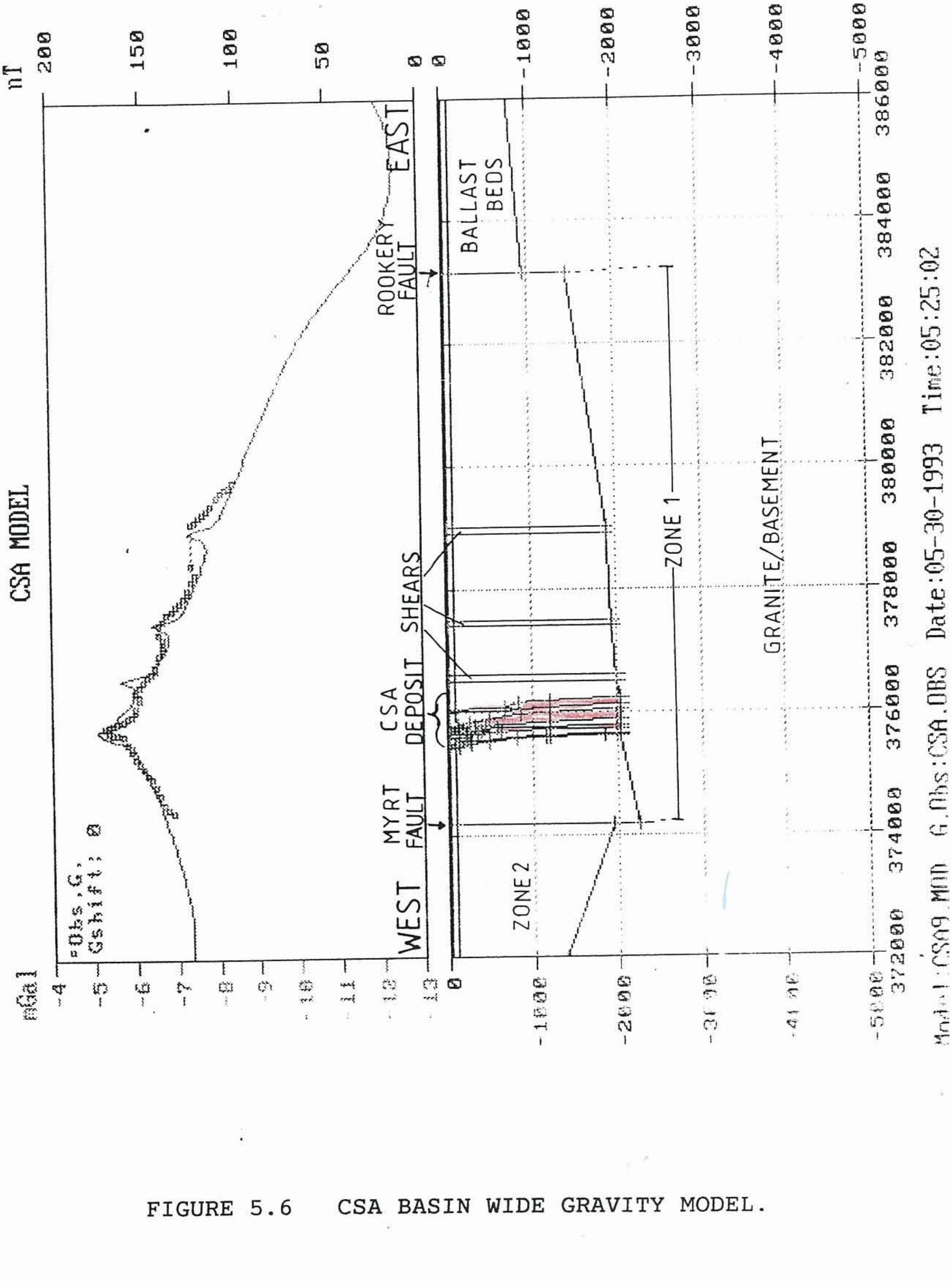

FIGURE 5.6 CSA BASIN WIDE GRAVITY MODEL.

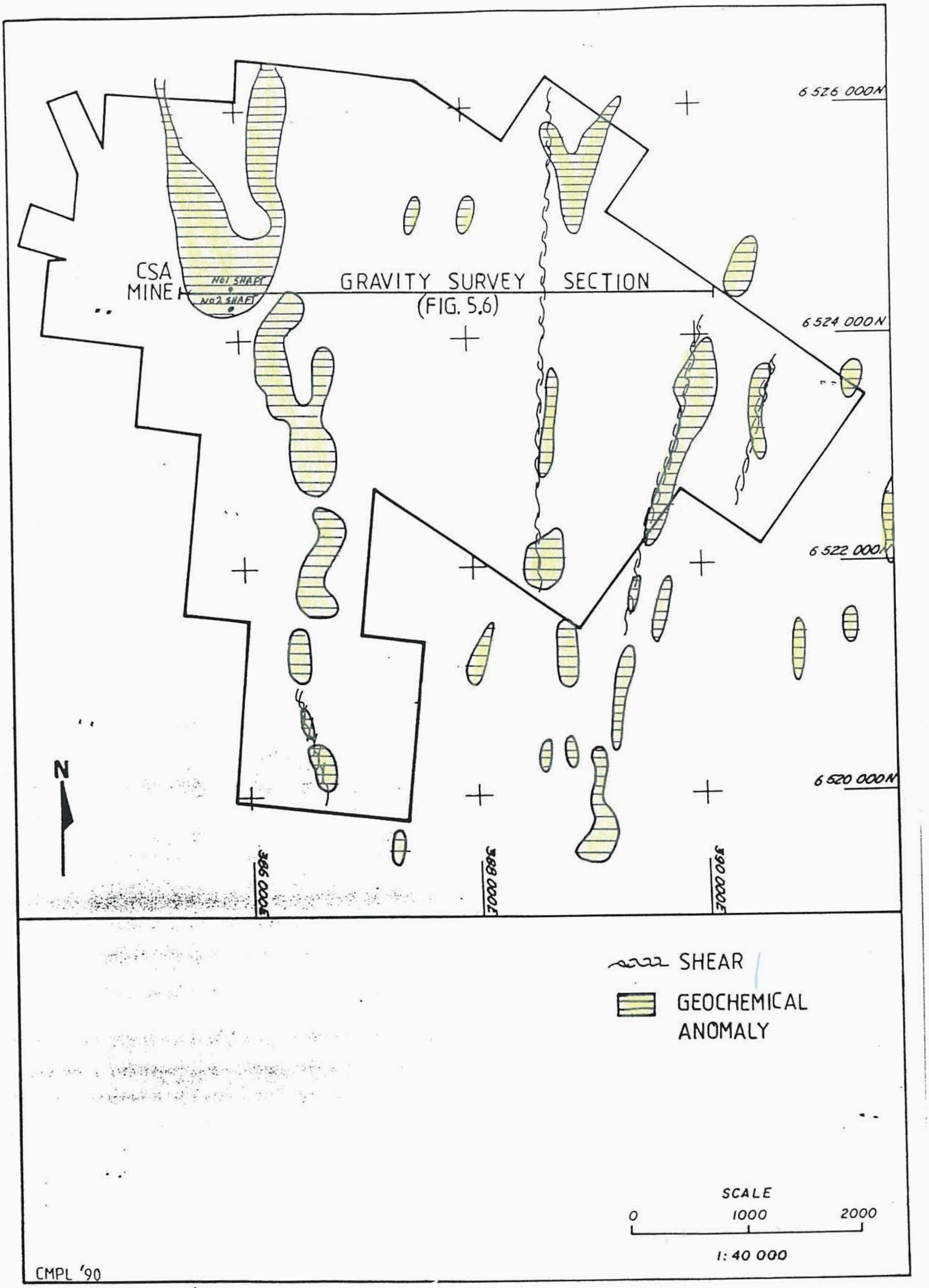

FIGURE 5.7 SURFACE GEOCHEMICAL ANOMALIES RELATED TO SHEARING.

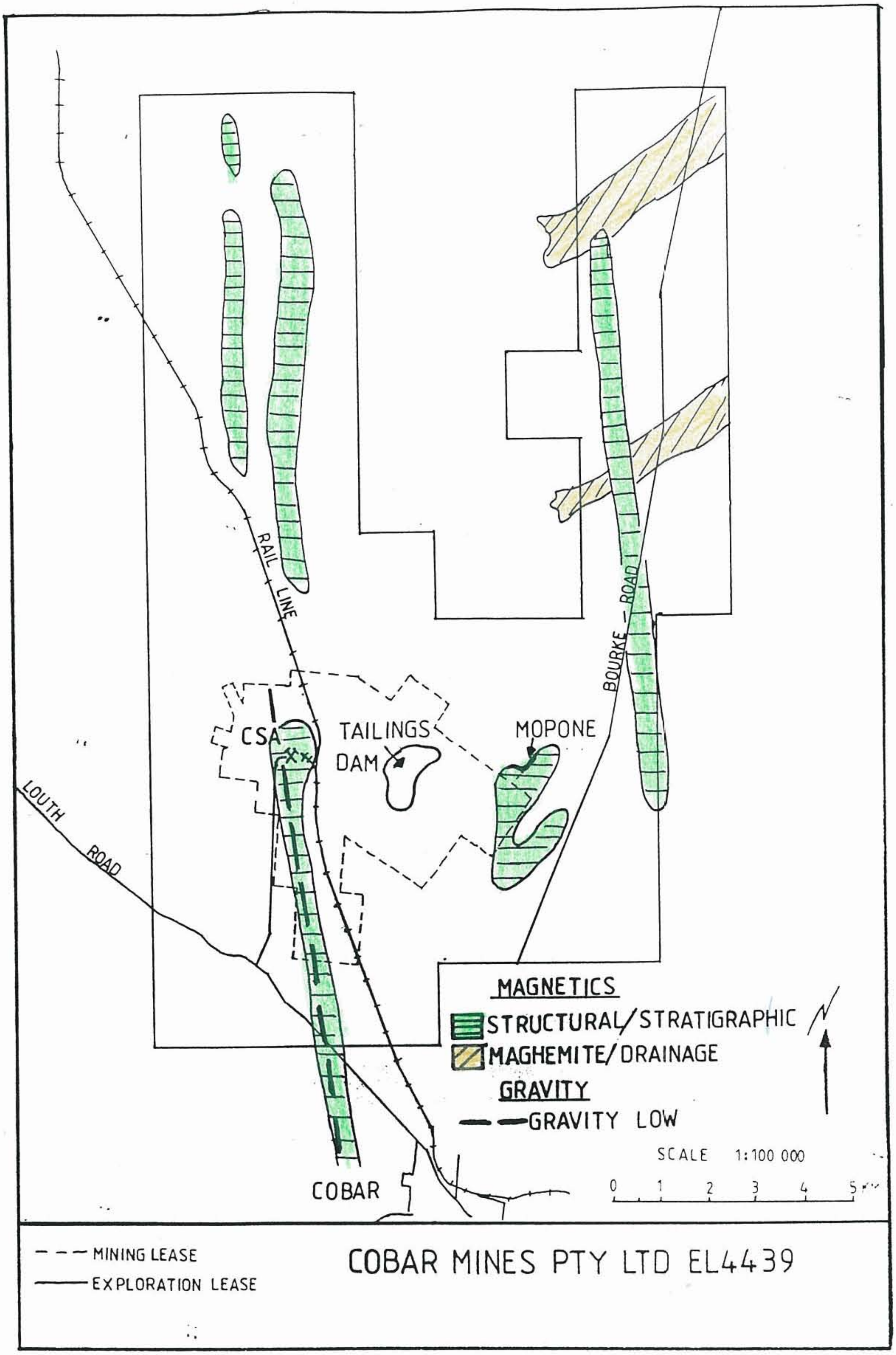

FIGURE 5.8 SURFACE MAGNETIC AND GRAVITY TRENDS.

CHAPTER 6

ISOTOPE, FLUID INCLUSION AND CHLORITE DATA

Although much time and effort has been applied to obtaining isotope, fluid inclusion and chlorite data for the Cobar deposits and suggesting the source of mineralisation, little time has been applied to comparing the results from the deposits. As will be demonstrated, there are clear similarities between the deposits and hence some interesting genetic implications. The data referred to in this chapter was not collected by the author. Rather, the author has added to the interpretations placed on the data in order to show that there is more than one explanation and that these explanations can account for the genetic and structural model pursued through this text.

6.1 ISOTOPIC DATA

6.1.1 $\delta S34$ DATA

6.1.1.A THE CSA DEPOSIT

Brill, Seccombe and Chivas (unpub.) noted that the $\delta S34$ range for the CSA deposit was 4.5 to 9.8‰ with a mean of 7.5‰ (Fig. 6.1). The samples used to derive this were taken from a number of lenses and levels within the mine. From the study it was noted that: 1) galena has slightly lower values than other sulfides,

2) there is no variation in the $\delta S34$ isotopic composition between the Cu and Pb/Zn rich ore types, different mineralised lenses or levels within the mine, and
3) the results were consistent with those of Marshall (1981)

and Sun (1983).

Temperature estimates range from 240°C (pyrite-pyrrhotite) to >1000°C (pyrite-chalcopyrite, pyrite-sphalerite). It is suggested by Brill, Seccombe and Chivas (unpub) that a complex paragenesis with several generations of pyrite and chalcopyrite are responsible for this isotopic disequilibrium. Sphalerite-galena pairs gave the expected order of isotopic enrichment (pyrite>pyrrhotite = sphalerite> chalcopyrite> galena) with temperatures of 407° to 857°C. Fluid inclusion, chlorite compositional and mineralogical data from Brill and Seccombe (unpub) suggest the temperature of formation to be 300° to 350°C. From the difference between the isotopic temperatures and those from the chlorite and fluid inclusions Brill, Seccombe and Chivas (unpub) suggested that isotopic equilibrium was approached or subsequently disturbed.

6.1.1.B THE Cu/Au DEPOSITS

δS34 isotope data was obtained for the Cu/Au deposits south of Cobar by Seccombe (unpub). The data is listed in Appendix 7 and displayed in Fig. 6.2. The deposits have a δS34 range of 3.8 to 11.2‰ with a δS34 average of 7.9‰. With the exception of the New Cobar deposit (mean 5.5‰) all other deposits have a similar isotopic distribution. Other features noted from the data by Seccombe (unpub) are:

1) where magnetite is associated with mineralisation (Occidental and Great Cobar deposits) the isotopic

composition is similar to those with no magnetite but pyrite and pyrrhotite as the major iron sulfides, and

2) of 21 sulfide pairs (either pyrite-pyrrhotite or pyrrhotite-chalcopyrite) 13 showed the expected order of isotopic enrichment (pyrite>pyrrhotite> chalcopyrite) and gave temperatures <100°C to >1000°C. Only one sample gave a temperature (318°C) consistent with fluid inclusion data. Again isotopic disequilibrium was sited as being responsible for this difference.

6.1.1.C THE ELURA Pb/Zn DEPOSIT

δS34 data for the Elura deposit comes from two sources. Sun (1983) reported a δS34 range of 8 to 12‰ from pyrite samples adjacent to and from within the deposit. Seccombe (1990) conducted a sulfur isotope study to gain information on the composition of the ore minerals and geothermometric data to compliment a fluid inclusion study. For 30 analysis the δS34 mean for ore sulfides was 8.1‰ with a range of 4.7 to 12.6‰ and stratabound sulfide bands in wallrock of 7.6 to 11.3‰ (Fig 6.3).

From this Seccombe (1990) deduced that the order of sulfur enrichment was pyrite > sphalerite = pyrrhotite > galena which was to be expected for deposition under equilibrium (or near equilibrium) conditions. Temperature estimates were made using sphalerite - galena pairs and range from 167°C to 335°C (mean 275°C). The temperatures are consistent with the fluid inclusion data and indicate near equilibrium conditions of deposition.

These are plotted on Fig. 2.10 relative to the orebody outlines.

6.1.2 SOURCE OF SULFUR

Brill and Seccombe (unpub), Brill and Seccombe and Chivas (unpub) and Seccombe (1990) using a combination of chlorite, inclusion and isotope data have suggested that the sulfides are of sedimentary origin and were transported by metamorphic fluids. Figure 6.4 shows the variation of sulphur isotopes in various rock types. From the above data the deposits have an overall δS34 average of approximately 8‰ implying that the sulfur could be of sedimentary or igneous origin, or even a combination of both (Fig. 6.4). However, from the sulfur:selenium data presented in Chapter 7 it could be clearly argued that the sulfur is igneous or hydrothermal in origin.

From the structural interpretations of Chapter 4 the quartz is post mineralisation. The injection of the quartz into mineralised areas combined with the mechanical relocation of some sulfides would explain the disequilibrium effects seen in the CSA and Cu/Au deposits. As this disequilibrium is not seen at the Elura deposit it suggests that the Myrt Fault partly shielded the deposit from the regional D3 event of Zone 1.

6.1.3 OXYGEN, CARBON AND HYDROGEN ISOTOPIC DATA

Data is only available for the CSA deposit (Brill, Seccombe and Chivas (unpub)). Samples from mineralised quartz veins have a δO18 range of 10.4 to 12.4‰ (Fig. 6.5). Quartz from barren veins have a $\delta O18$ range of 11.2 to 13.3‰ and those from greywacke tension gashes have an average $\delta O18$ of 12.1 ‰. Therefore quartz in the mineralised zone is depleted by 1 to 2‰ relative to unmineralised quartz (Fig. 6.5).

A similar trend is seen in the whole rock data. Unaltered whole rock has a $\delta O18$ of 8.9 to 9.7‰ while altered material has a range of 6.8 to 7.6‰ (Fig. 6.5). This means that altered rock is depleted relative to unaltered rock by 1 to 2‰.

Oxygen and carbon isotope data were also obtained from calcite material. In the mineralised zones this has a $\delta O18$ range of 9.5 to 9.6‰ and a $\delta C13$ range of -8.4 to -8.7‰. Barren calcite outside the mineralised and altered areas has $\delta O18$ range of 11.3 to 12.4‰ and a $\delta C13$ range of -6.5 to-8.8‰ (Fig. 6.5).

In general, Brill, Seccombe and Chivas (unpub) concluded that minerals and rocks from the alteration and ore zones show a lower $\delta O18$ and $\delta C13$ signature (by 2‰) than minerals and rocks from outside the alteration zones.

Similar trends are observed in the hydrogen isotope data. Altered whole rocks where chlorite is the major OH bearing phase have δD values of - 51 to - 61‰. Unaltered whole rock in which muscovite is the major OH bearing phase have a δD range of -43 to-50‰. δD values for two fluid inclusions from mineralised quartz were -42‰ and -44‰ (Fig. 6.6).

6.1.4 SOURCE OF O, C AND H

Based on the above results, Brill, Seccombe and Chivas (unpub) concluded that the source of the O, C and H isotopes (and hence the quartz and calcite veins) were metamorphic in origin. The composition of this fluid was calculated to have a δO18 of 5.1 to 6.8‰, δC13 of -4.4 to-6.7‰ and δD of -33 to-38‰. However, from the results presented it can be seen that some mixing or contamination may have occurred as samples from the altered and mineralised zones are clearly different from the unmineralised zones. If this is the case then the samples from unaltered host rocks best represent the source rocks as they are not contaminated, so there is some doubt on the validity of the above calculated fluid chemistry. The δO18 and δC13 ranges are plotted on Fig. 6.7 and clearly show that a number of sources are possible for the fluids that created the quartz and calcite veins, however there is little doubt from the δD data that the fluid is of metamorphic origin.

From the structural evidence presented in Chapter 4 the quartz and calcite veins appear late in the structural sequence (D3) and not syn-mineralisation (D2). The isotopic differences between veins located in altered and unaltered material due to contamination as described above would tend to support the idea that the quartz and calcite veins are of one event late in the structural history of the area.

6.1.5 ISOTOPIC DATING

A whole rock isotopic dating program was undertaken by Glen, Dallmeyer and Black (1986, 1992) to document Rb-Sr, K-Ar and

Ar40/Ar39 dating of low grade metamorphosed sedimentary rocks to determine the age of inversion of the Cobar basin. Results of the program are:-

1) Rb-Sr dates from Zone 1 samples indicate an age of 442 Ma, which is older than the base of the Devonian taken to be 408 Ma by Harland etal (1989). These results were consistent with earlier results of 442 Ma, 440 Ma, and 423 Ma (Glen and Black (1983)),
2) Three K-Ar dates from Zone 1 of 402 Ma, 402 Ma and 405 ma indicate that cleavage formation is of Early Devonian age.
3) Ar40/Ar39 dates in Zone 1 average from 389 to 404 Ma while in Zone 2 ages range from 401 to 423 Ma.

It is interpreted that the low-grade metamorphic cleavage forming event took place at 395-400 Ma. The Zone 1 K-Ar data suggest almost complete rejuvenation of the detrital phase during this event. The Rb-Sr ages and Ar40/Ar39 ages in Zone 2 reflect basement provenance ages preserved in non or partly rejuvenated detail micas and felspars in areas of low deformation strain.

6.2 FLUID INCLUSION DATA

6.2.1. THE CSA DEPOSIT

Brill and Seccombe (unpub) studied the quartz and calcite fluid inclusions of the CSA deposit. From this, three types of inclusion were identified:

1) Type A: two phase (H20(l) + CH4(g)) inclusions (l/g ratio 2:1 to 1:2) up to 15um in size. These are ragged shaped

inclusions considered primary (see discussion below) as they show no planar alignment or association with a particular vein orientation.

2) Type B: two phase $[H_2O(l) + (CO_2(g) + CH_4(g))]$ inclusions < 15um in size. These have no association with a particular vein orientation but occur as non planar primary and planar secondary inclusions.

3) Type C: One phase (liquid) and two phase (liquid and gas) inclusions < 5um in size that are present in all vein orientations.

Brill and Seccombe (unpub) defined the Type A inclusions as primary based on the observation of Kreulen (1980) that in metamorphic rocks primary inclusions are difficult to relate to any growth phenomena and the absence of planar arrangements is the only criteria by which they can be recognised as being primary. Consequently there are Type B and C inclusions which are also primary based on the definition of Kreulen (1980) but differ from Type A inclusions in size only. In addition, some Type B and C inclusions are classified as secondary as they occur on subgrain boundaries, deformation bands and planar features, and show signs of leakage. The Brill and Seccombe (unpub) definition of secondary inclusions is based on the observations of Wilkins and Barkas (1978) who worked on syntectonically recrystallised quartz from the Lachlan Fold Belt.

The homogenisation temperatures (Th) for 585 inclusions range from 199^{o} to 389^{o} C (average 305^{o} C for quartz and 273^{o} C for calcite) (Fig. 6.8). Low Th values (159° to 291° C, average 247° C) were recorded for one sample of vuggy quartz. Melting temperatures (Tm) of ice in Type A inclusions were between -1.2° C and -1.0° C, yielding low salinities of 1.8 to 2.2 wt% NaCl.

Points of interest drawn from the study include:

1) Th and Tm of fluid inclusions in barren quartz (in and away from mineralisation) are identical to those associated with mineralisation. This strongly implies that the quartz in barren and mineralised host rock could be of one source and deformation event.
2) Cu and Pb/Zn mineralised areas have identical Th and Tm values.
3) Th and Tm were consistent for all vein orientations sampled indicating one event of fluid injection.
4) Although 10-30 mole% CH_4 and 70-90 mole% CO_2 were recorded in inclusions, no N_2 or H_2S was detected.

Given that primary and secondary inclusions of Type A, B and C are found in all quartz vein orientations in both altered and unaltered host rock then it is likely that the quartz is of one structural event. As shown in Chapter 4, the quartz occupies D2 and D3 structures, and therefore is D3 in origin. The presence of secondary inclusions suggests some minor deformation after emplacement, which may also explain the rarely seen shallow east dipping sulfide veins that cut cleavage (Section 4.2). The fact that there is evidence for sulfide remobilisation by the quartz (Chapter 7) strongly suggests that the D3 quartz rich metamorphic fluids are not related to the mineralising event but post mineralisation.

Despite these conclusions and in the light of the structural reinterpretation, the author believes that more work could be done on fluid inclusions in an attempt to clarify their source and timing relationship to mineralisation and deformation.

6.2.2 THE Cu/Au DEPOSITS

Seccombe (unpub) conducted a fluid inclusion study of these deposits. Inclusions were classified as either Type 1 (up to 15 um in size and a gas/liquid ration 0.1 to 0.3 by volume) or Type 2 (<10um in size with a g/l ratio of 0.05 to 0.15 by volume). Samples were collected from all vein orientations and the data was determined for 422 primary two phase inclusions. This data is plotted by deposit in Fig. 6.9 and collectively in Fig. 6.10. Overall the Th range is 150° to 370° C (as per the CSA) but can be divided into Type 1 (250° C to 370° C) and Type 2 (150° C to 230° C) inclusions.

Freezing point depressions from both types of inclusions were rare, but ranged from -1.2° C to 2.3° C, averaging -1.7° C. This equates to a NaCl content of 2.1 to 3.9 wt %.

6.2.3 THE ELURA Pb/Zn DEPOSIT

Quartz samples from eleven sites in and around the deposit (Fig. 2.9) were analysed by Seccombe (1990). The primary inclusions are two phase with gas/liquid ratios from 0.1 to 0.4 by volume. Th data is listed in Table 6.1 and plotted in Fig. 6.11, and produces two distinct populations which range from 150.2° to 230.5° C (mean 188° C) and 298.2° to 353.5° C (mean 320° C). Seccombe (1990) noted that the low Th inclusions were of low gas/liquid ratios while the high Th inclusions contained higher and variable gas/liquid ratios.

Other inclusion data included:

1) a salinity range of 3 to 6 wt% NaCl,
2) 64 to 88 mole% CO_2 and 12 to 36 mole% CH_4 in inclusions, and
3) no N_2, H_2S, or daughter products being detected in the inclusions.

6.3 ALTERATION CHLORITES

Brill and Seccombe (unpub) used electron microprobe analysis of samples from the CSA deposit to identify seven chlorite types as shown in Fig. 6.12. The study discriminated between the early paragenetic Fe rich chlorite and the later more Mg rich chlorite associated with black chlorite shears. The calculated temperature for chlorite formation is between 243° C and 365° C (average 297° C) which has a positive correlation with oxygen fugacity (Fig. 6.12). Samples that gave temperatures > 330° C were excluded as it was thought they would give artificially high oxygen fugacities, and included the late stage Mg rich chlorites confined to late stage shears.

Collection of the chlorite compositional data was done using a JEOL 840 electron microscope at 15kV connected to a TRACOR NORTHERN 5500 computer using the TRACOR NORTHERN PRZ correction program. Calculation of temperature and redox conditions of the fluid in equilibrium with the chlorite was done using the thermodynamic six component chlorite solid solution model of Walshe (1986).

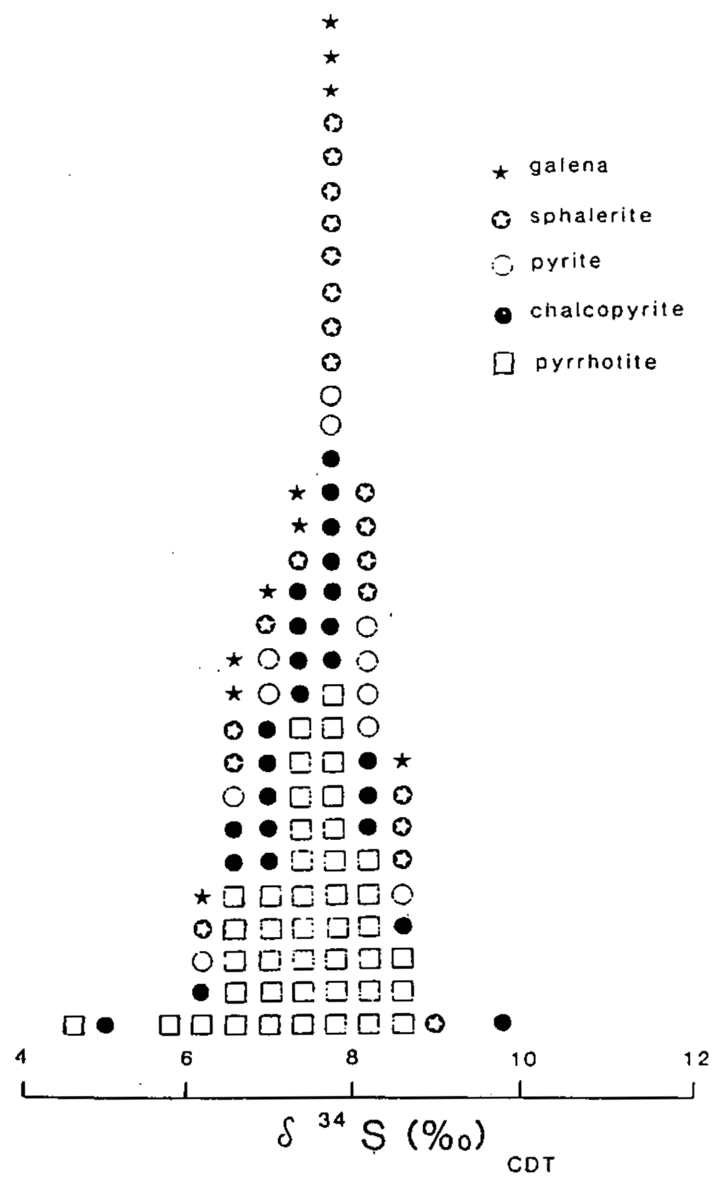

FIGURE 6.1 CSA DEPOSIT δS34 ISOTOPE DATA. FROM BRILL, SECCOMBE AND CHIVAS (UNPUB).

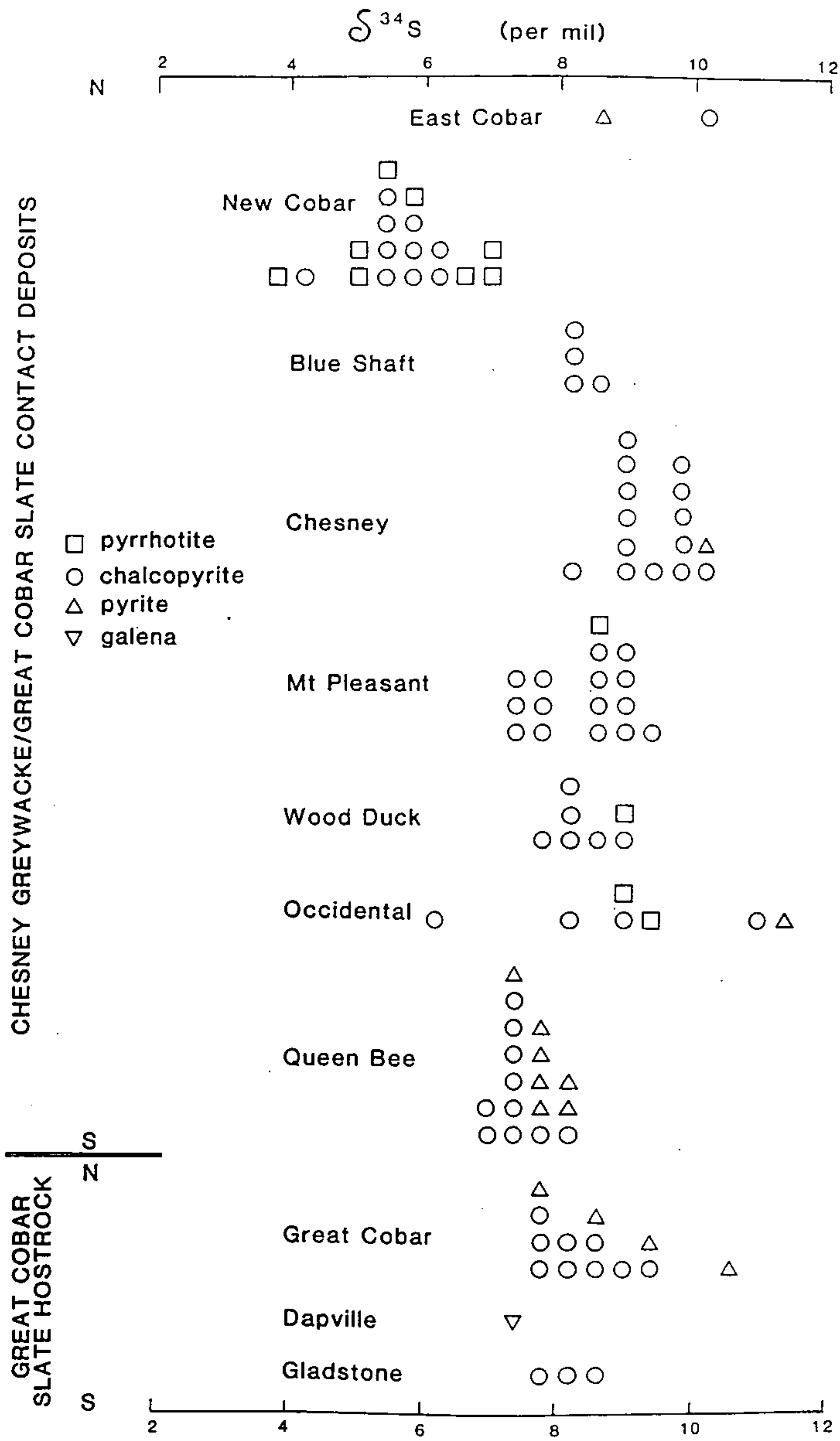

FIGURE 6.2 Cu/Au DEPOSIT δS34 DATA. FROM SECCOMBE (UNPUB).

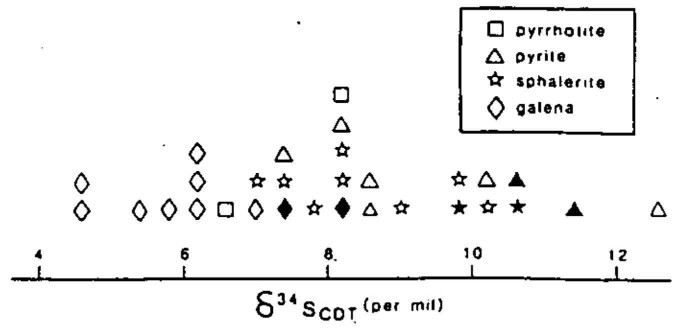

Sulphur isotopic distribution for sulphide minerals separated from ore (open symbols) and stratabound sulphide layers in wallrock (closed symbols)

FIGURE 6.3 ELURA DEPOSIT δS34 DATA. FROM SECCOMBE (1990).

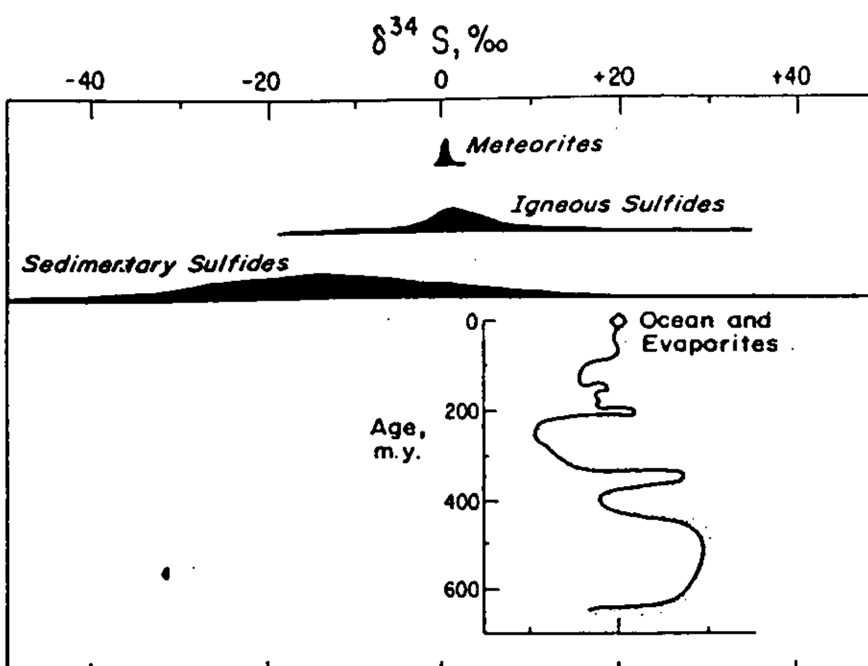

FIGURE 6.4 SULFUR ISOTOPE VARIATIONS IN DIFFERENT ROCK TYPES. FROM OHMOTO AND RYE (1979)

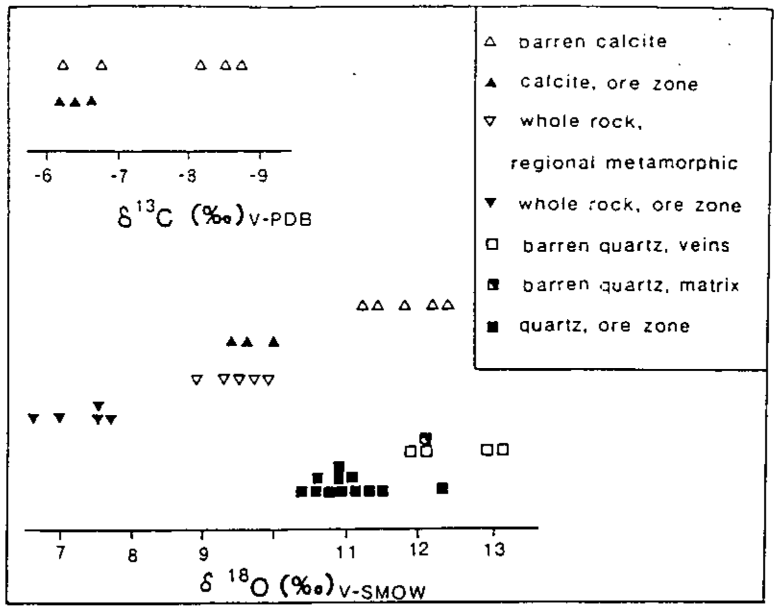

FIGURE 6.5 CSA DEPOSIT OXYGEN AND CARBON ISOTOPE DATA. FROM BRILL, SECCOMBE AND CHIVAS (UNPUB).

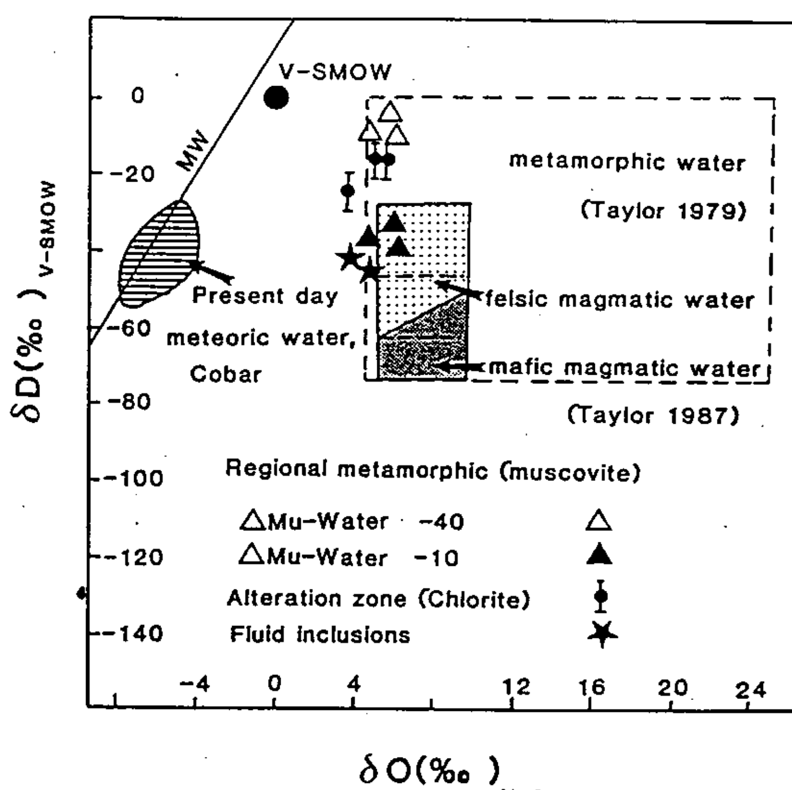

FIGURE 6.6 CSA DEPOSIT HYDROGEN ISOTOPE DATA. FROM BRILL SECCOMBE AND CHIVAS (UNPUB).

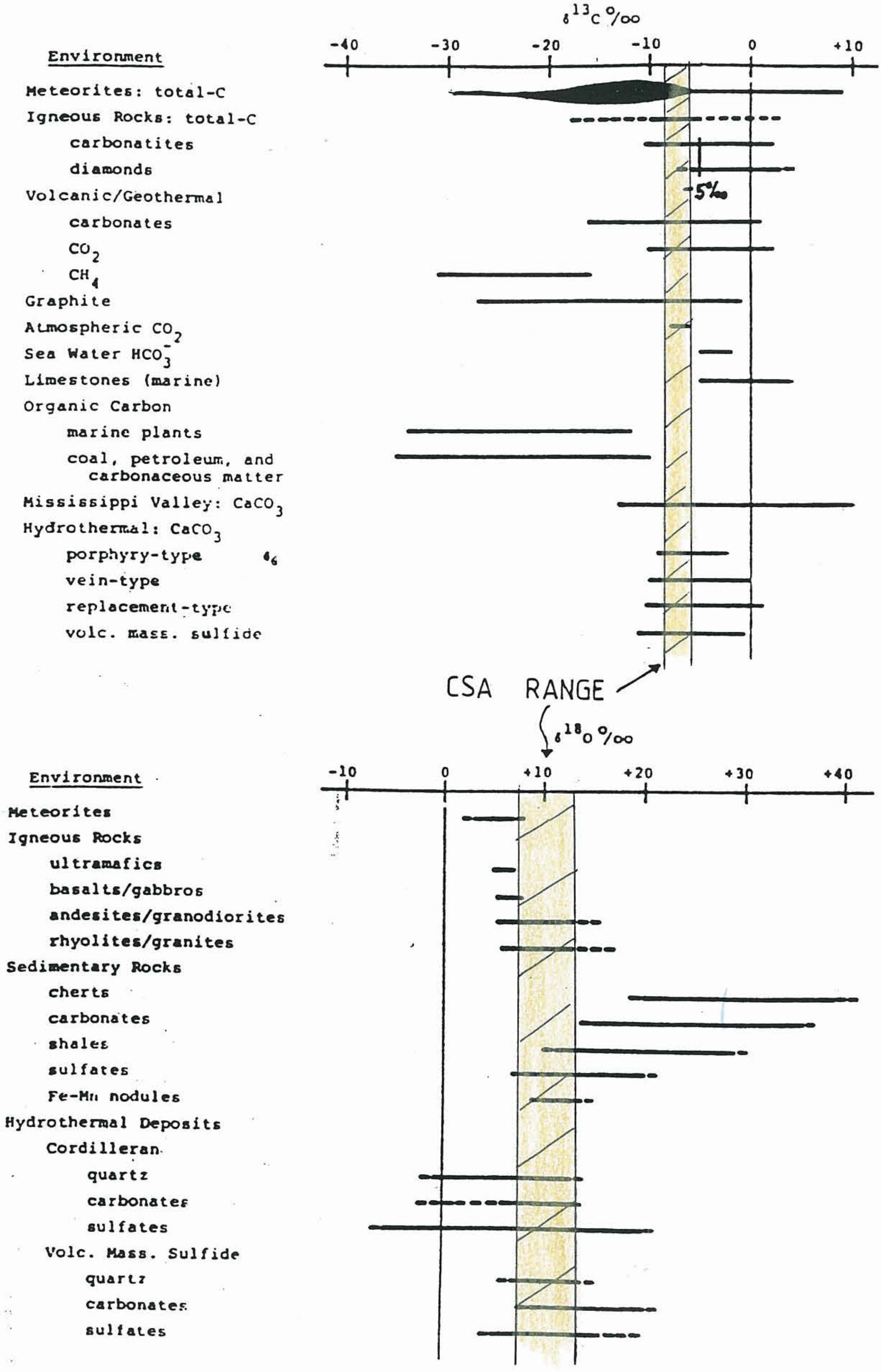

FIGURE 6.7 OXYGEN AND CARBON ISOTOPE VARIATIONS IN DIFFERENT ROCK TYPES. FROM FRITZ (1976).

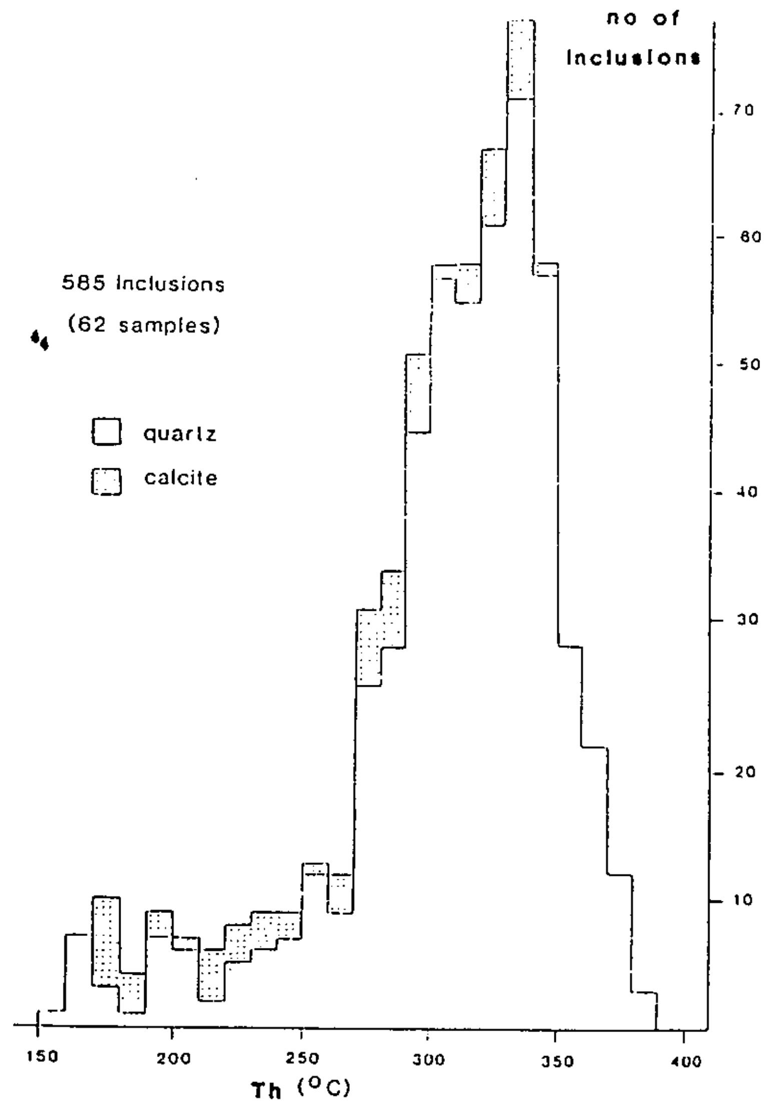

FIGURE 6.8 CSA DEPOSIT FLUID INCLUSION DATA. FROM BRILL AND SECCOMBE (UNPUB).

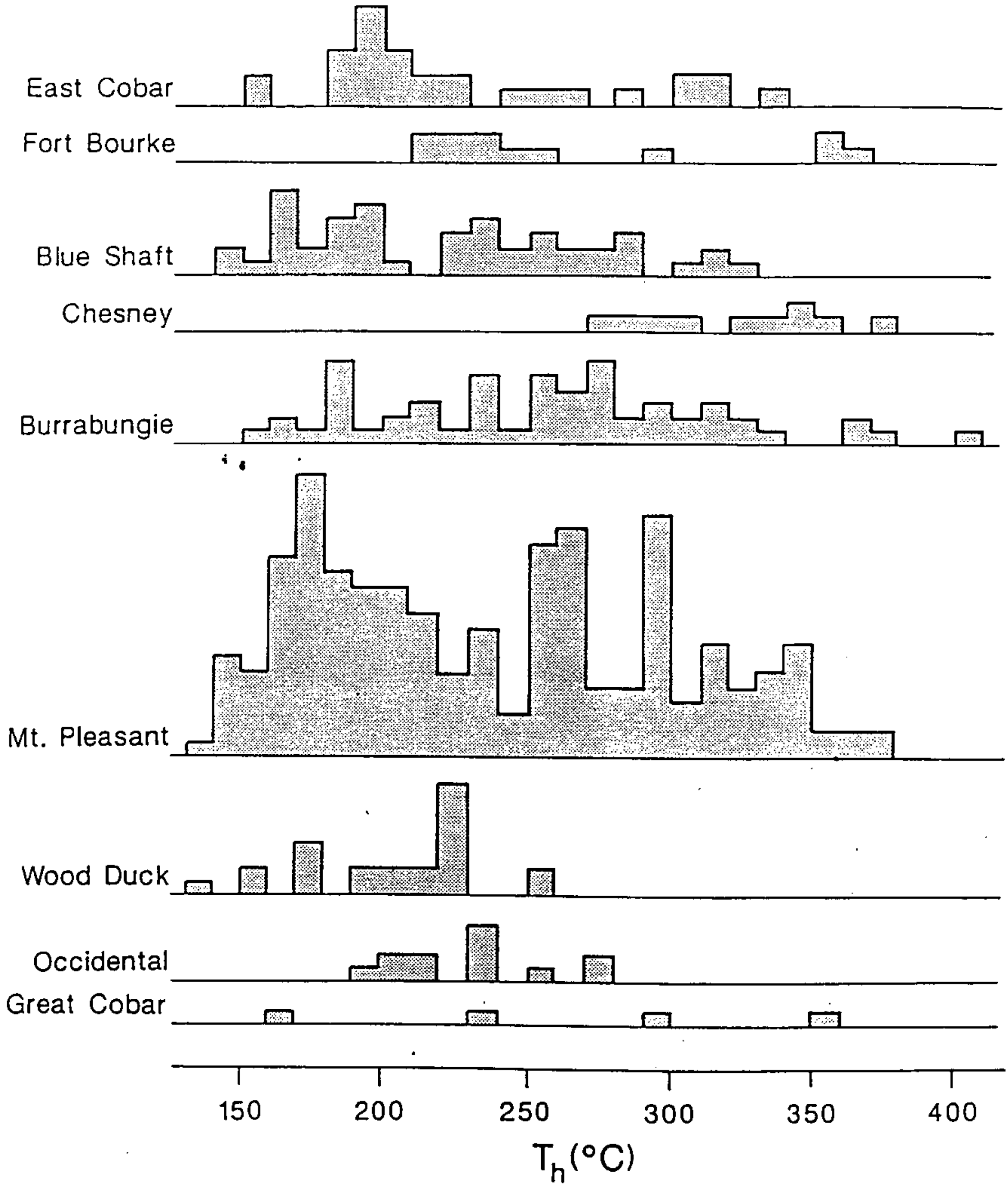

FIGURE 6.9 Cu/Au DEPOSIT FLUID INCLUSION DATA BY DEPOSIT. FROM SECCOMBE (UNPUB).

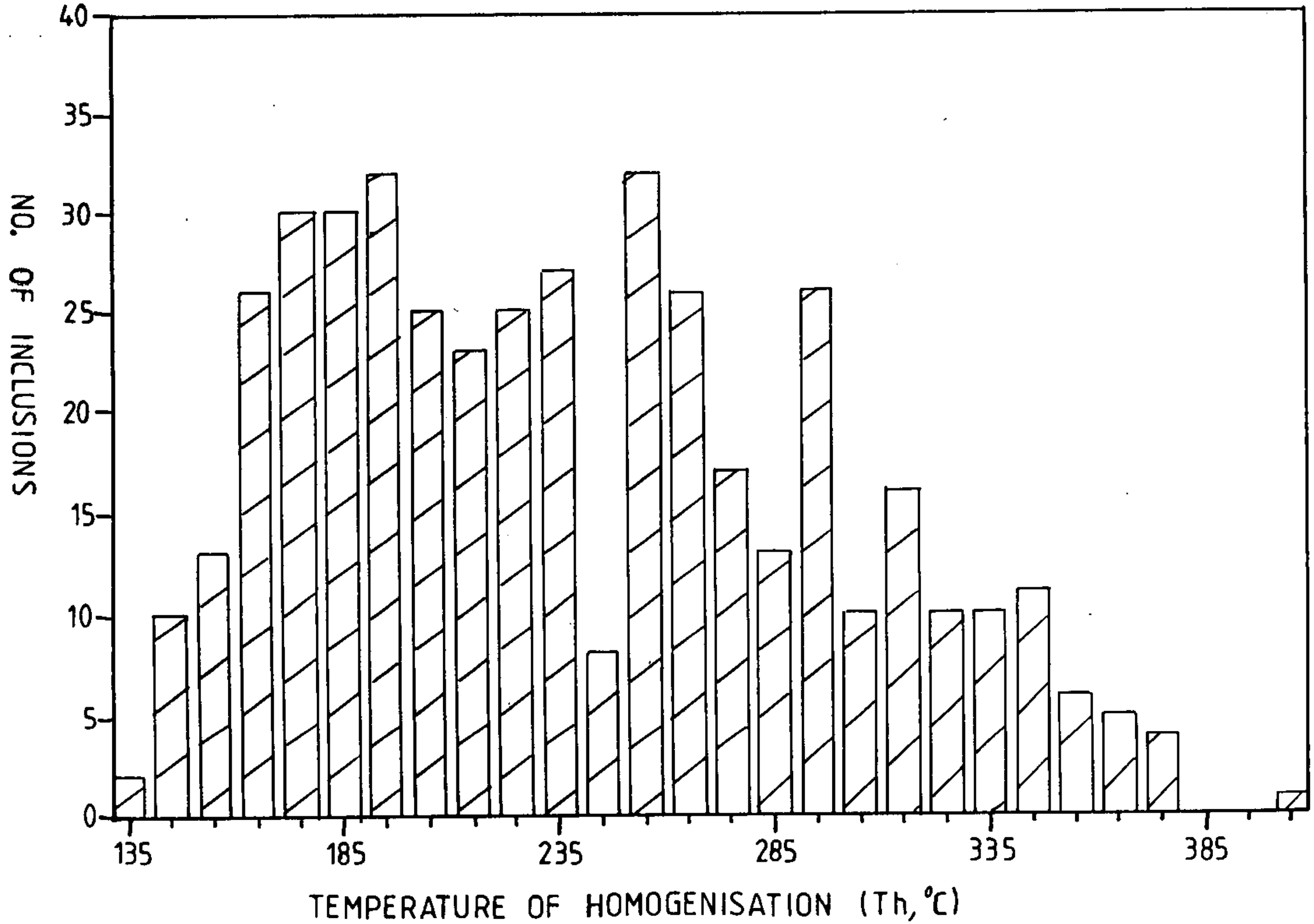

FIGURE 6.10 Cu/Au DEPOSIT COMBINED FLUID INCLUSION DATA. DATA FROM SECCOMBE (UNPUB).

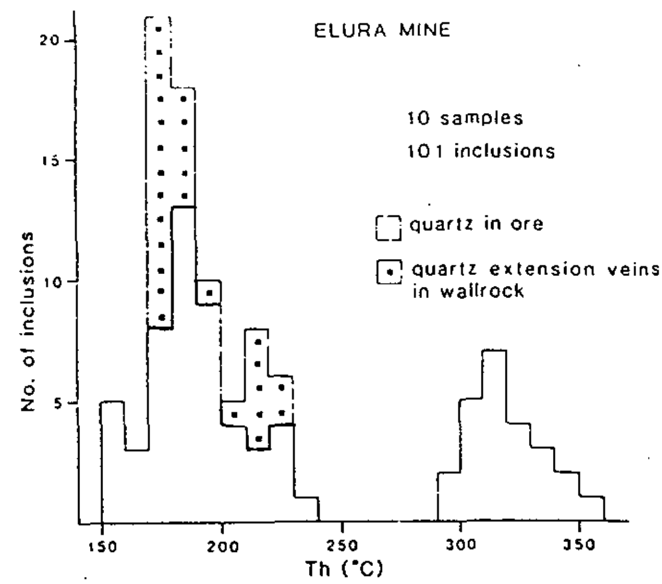

FIGURE 6.11 ELURA DEPOSIT FLUID INCLUSION DATA. FROM SECCOMBE (1990).

TABLE 6.1 ELURA DEPOSIT FLUID INCLUSION DATA. FROM SECCOMBE (1990)

Sample number	T_h (°C) range	T_h (°C) mean	std dev
Quartz veins in wallrock			
2	170–188	178 (14)[a]	5
3	185–225	210 (8)	16
4	173–213	193 (5)	17
Quartz in ore			
7A	177–229	201 (11)	17
7B	185–200	193 (2)	11
	308–343	329 (5)	15
7C	150–181	170 (8)	11
	298–354	329 (5)	25
7D	183–225	193 (13)	11
8	196–225	211 (3)	15
	333	– (1)	–
11	154–194	170 (11)	14
	302–328	317 (3)	13
13	224–231	227 (4)	4
	298–329	312 (10)	10
Overall means			
Low T_h	150–231	189 (77)	20
High T_h	298–354	320 (24)	16

[a] Number in parentheses indicates number of determinations for each data set.
Note: Sample descriptions and details of sampling sites may be obtained from the author

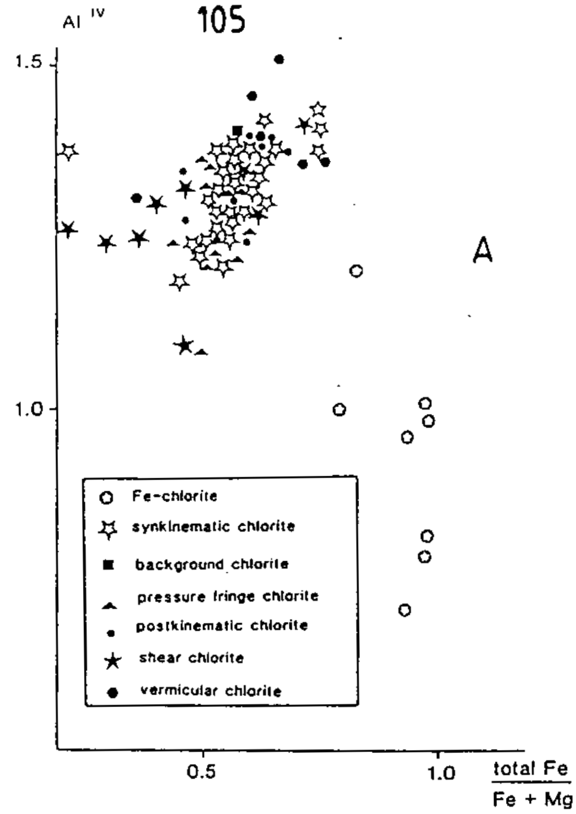

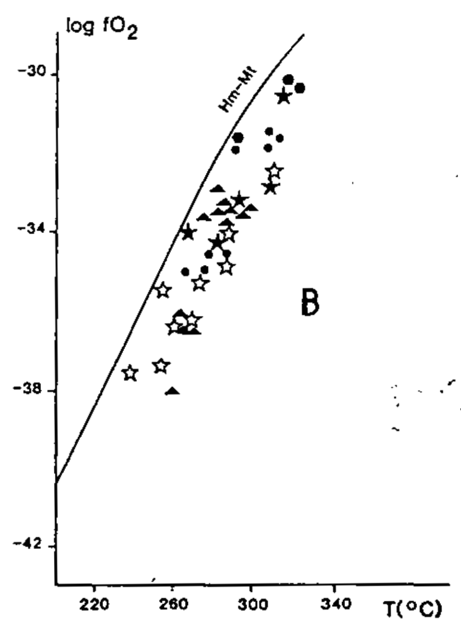

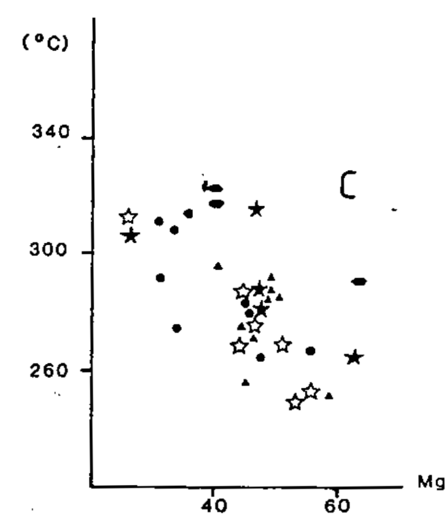

Figure A Scatterplot of tetrahedrally coordinated Al *vs.* total Fe/Fe + Mg, illustrating variations in chlorite composition for the several CSA chlorite types.

Figure B Calculated log fO_2-temperature conditions of chlorite formation at the CSA mine, relative to the hematite-magnetite buffer.

Figure C Plot of calculated temperature *vs.* Mg number for CSA chlorite types.

FIGURE 6.12 CSA DEPOSIT CHLORITE TYPES. FROM BRILL AND SECCOMBE (UNPUB).

CHAPTER 7

FRESH ROCK GEOCHEMISTRY

In a series of reports, Robertson (1982a, 1982b, 1983, 1984) studied the geochemical halo produced in fresh bedrock around the mineralisation in an attempt to quantify a "near miss" situation given the steep pitch and plunge of Cobar deposits. The studies used core from successful and unsuccessful holes drilled in the Cobar basin to obtain data on background and mineralised/altered material.

Given that all Cobar mineralised systems show signs of silica flooding (ie elvans, silicified siltstones and quartz veining) it was expected that some elements were added, diluted or removed from the systems. Trends identified from the work, most of which was done on the CSA deposit include:

1) The alkali and alkaline earth elements are represented by negative anomalies and depletion haloes. Lithium has the widest depletion halo covering the whole CSA deposit (Fig. 7.1) and stopping sharply on the footwall contact of the Western System (which is now seen as a structural contact following the work of Chapter 4). Sodium, barium and strontium have substantial depletion halos while those of potassium and rubidium occur close to mineralisation. These trends could not be followed in the weathered zone.
2) CO2 was also found to be depleted in mineralised areas and pursued in the weathering zone by Robertson (1985) who identified anomalies in methane, ethylene and ethane

marked an area around the CSA deposit.

3) depletion of base metals adjacent to quartz veining was linked to the CO_2 depletion.

4) enrichment halos for Fe, Mn, Se, Hg, and Co were found to occur with the base metal mineralisation while Al, Ti, P, Ni, and Th appear to be diluted during the process of silicification.

As a D3 event was not recognised by Robertson (1982a, 1982b, 1983, 1984, 1985) these trends were taken to represent the signature of the mineralisation because the quartz veining was thought to be syn-mineralisation. In light of the structural interpretations in Chapter 4 the CO_2 and base metal depletions adjacent to mineralisation indicate stripping by the later D3 quartz veins. This also coincides with the mechanical mobilisation of sulfides noted by Robertson (1974). As for the alkali and alkaline earth element depletions, these represent a change in rock type and not a signature of the mineralisation. The only true signature of the mineralisation is the trends seen in Fe, Mn, Se, Hg, Co, and base metals relative to the surrounding host rock.

Robertson (1982a, 1982b, 1983, 1984) also noted mineralogical changes with proximity to quartz veining. These changes accompanied the geochemical changes and included a decrease in plagioclase, sericite and muscovite which explained the decrease in alkali and alkaline elements near mineralisation.

Although not conclusive in determining the source of the sulfur it is possible to use a sulfur:selenium (S:Se) ratio to distinguish between sulfur of a sedimentary or igneous/hydrothermal origin. Stanton (1972) notes that a S:Se < 20,000 could indicate an igneous/hydrothermal origin for the sulfur and a S:Se > 100,000 could indicate a sedimentary origin, while a S:Se between 20,000 and 100,000 could indicate either or mixing. From data collected to date the CSA (Appendix 8) mineralisation has a S:Se of 191 to 14,000 which would indicate an igneous/hydrothermal origin for the mineralisation.

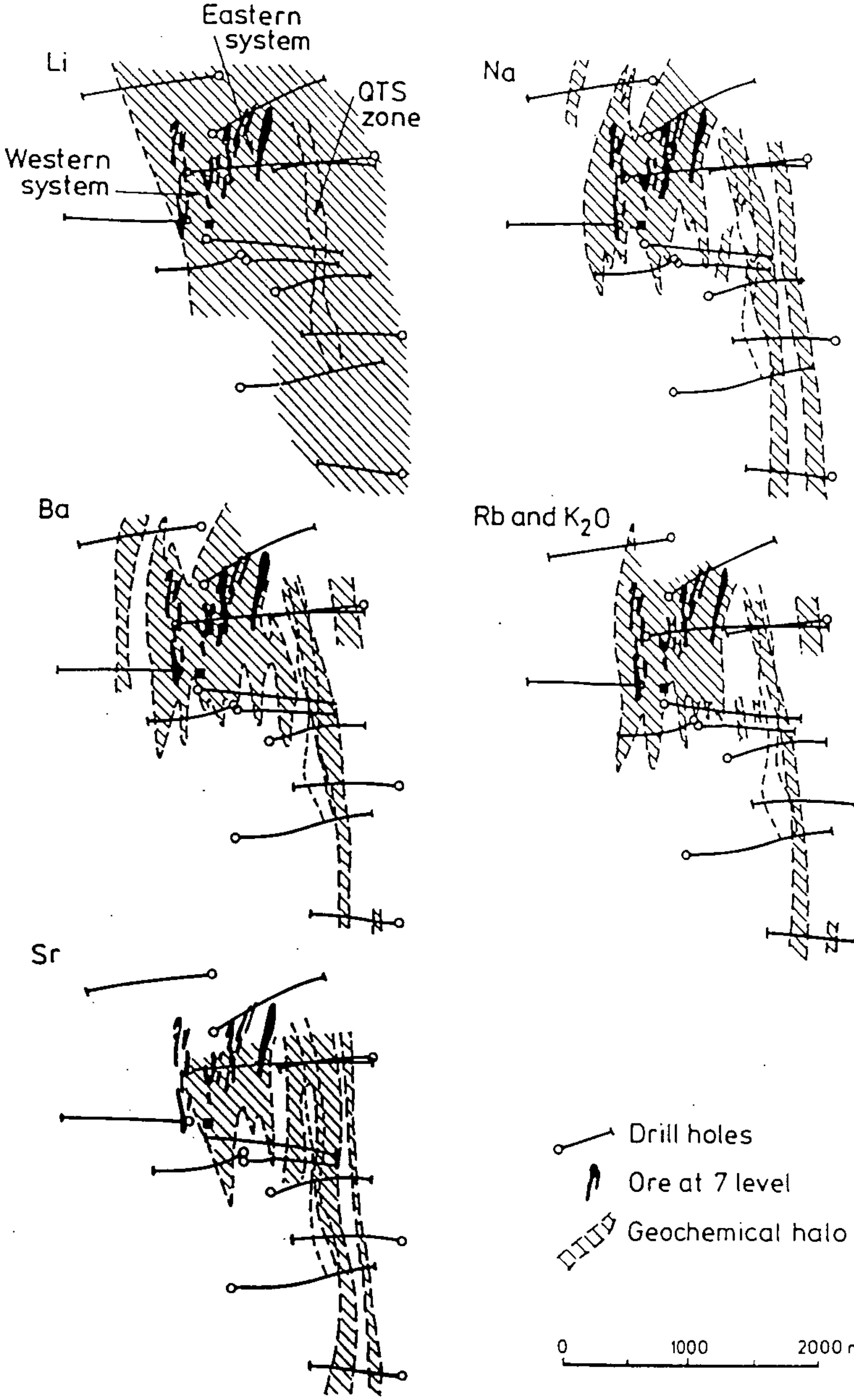

FIGURE 7.1 CSA DEPOSIT DEPLETION HALOES FOR THE ALKALI AND ALKALINE EARTH ELEMENTS. FROM ROBERTSON (1983).

CHAPTER 8

ORE GENESIS

8.1 PREVIOUS MODELS

Numerous models for the Cobar deposits have been suggested since their discovery last century. These models have changed with world wide trends and though not all are mentioned here, they can broadly be divided into three categories; epigenetic, syngenetic, and structurally controlled.

The first and most correct statement about the Cobar deposits was made by Andrews (1913) in noting that the mineralisation occurs within faults or fissure zones that cross cut sedimentary layering, thus implying an epigenetic model. The development of right lateral en echelon shear zones localised by competency contrasts between shales and greywackes was suggested by Mulholland and Rayner (1958) as creating the structural zones into which was injected ore bearing fluids from deep igneous activity. Sullivan (1950) and Rayner (1969) also used the idea of deep granites to explain the source of mineralisation. Sullivan (1951) suggested that mineralisation was localised by zones of intersecting cross fractures which resulted in north plunging pipe like bodies of highly fractured rock through which hydrothermal fluids moved.

Syngenetic models have been proposed by Robertson (1974) and Brooke (1975) who considered the mineralisation was formed or deposited close to its present position and later remobilised into structures. This partly explained Robertson's (1974) observations of mechanically remobilised sulfides. Gilligan and Suppel (1978) suggested the mineralisation is of the stratabound exhalative type with the parallel orientation to cleavage explained by strain during deformation. Adams and Schmidt (1980) and Schmidt (1983) suggested two models for the Elura deposit. The first suggests mineralisation was originally stratiform and remobilised into a favourable structural site during deformation (modified syngenetic) while the second model used overpressured metal bearing brines being trapped in a ruptured early anticline (modified epigenetic).

More recent models by Glen (1990, 1988, 1987) have focused the discussion on structural models of ore emplacement and basin deformation. Brill and Seccombe (unpub.); Brill, Seccombe and Chivas (unpub), and Seccombe (1990) have focused on the fluids generated by metamorphic and deformation processes.

8.2 NEW PROPOSED MODEL

From the data presented in previous chapters it is possible to propose a new genetic model for the CSA mineralisation, and hence the basin. It is a model which the author hopes takes into account all of the features seen in the basin to date and attempts to put them in a logical order of events.

Basin deformation due to closure, D1, appears to have produced little or no shearing. The development of tight subhorizontal folds can be attributed to this event.

The sinistral D2 event with the near horizontal stress field produced near vertical fracture zones through which a hot metal bearing fluid moved. Deposition of copper sulfides occurred in the lower portions of these fracture zones while the more volatile lead and zinc sulfides were deposited near the tops and at the edges of the fracture zones, hence the vertical zonation. Deposition of the metals from solution was induced by temperature change, wall rock interaction or the interaction with other fluids. The source of the metals is either sedimentary or igneous based on the S34 data, but the fluid contained Fe-chlorites that produce the alteration halo around and through the mineralisation.

The final deformation, D3, took place at about 404Ma based on the work of Glen, Dallmeyer and Black (1992, 1986). This metamorphic event reset the Rb-Sr systems by devolatilisation, the process whereby chlorite-calcite-albite-quartz assemblages (either mafic or sedimentary) are metamorphosed to produce large volumes of low salinity (0-3 wt % NaCl) H2O-CO2 fluids. This fluid then proceeded to infiltrate cleavages of D1, D2 and D3 events partly remobilising sulfides in the process. Coeval with D3 is the 'west block up' imbrication that displaces mineralisation at the CSA deposit.

As the quartz veins in the Cu-Au deposits south of Cobar are similar in orientation, salinity and low gas/liquid ratios to those at the CSA it implies that the D3 event and quartz injection is a basin wide event. The implications of this event are enormous as these low salinity metamorphic fluids are perfect for gold transport and common to 90% of all gold deposits (Phillips and Powell, 1992).

Given this, the gold mineralisation at the Peak deposit could be D3 in origin but the sulfides of D2. The same can be said with respect to the remaining Cu-Au deposits as Phillips and Powell (1992) suggest that the gold only comes out of solution when the solution interacts with iron or chlorite rich sediments, temperature changes, or sulfur content variations. As these features are seen at the Cu-Au deposits then the gold mineralisation is likely to be D3 in origin. Hence the gold mineralisation at the Peak deposit was probably sourced from the volcanics by the metamorphic fluids and deposited shortly after due to rapid chemical changes.

The author like Hinman and Scott (1990) believes that the volcanics could constitute near basement like material and if so gold mineralisation will be found near by. As basement below the CSA deposit is modelled geophysically to be at 2km then the chances of locating gold mineralisation are enhanced with proximity to source.

A summary of this model is presented in Table 8.1.

TABLE 8.1 SUMMARY OF THE NEW PROPOSED STRUCTURAL MODEL FOR THE CSA DEPOSIT AND HENCE THE COBAR BASIN.

EVENT	DESCRIPTION
D1	DEXTRAL (?) BASIN CLOSURE WITH MINIMAL SHEARING OR CLEAVAGE FORMATION THAT PRODUCED TIGHT NNW TRENDING FOLDS.
D2	SINISTRAL DEFORMATION WITH SUB HORIZONTAL STRESS FIELD. THIS PRODUCED VERTICAL FRACTURE ZONES ALLOWING METAL BEARING FLUIDS TO MOVE THROUGH THE ROCK CREATING PIPE LIKE BODIES. FRACTURE ZONES RESULT FROM A COMPETANCY CONTRAST BETWEEN SILTSTONE AND GREYWACKE. METALS DEPOSITED BY TEMPERATURE/DISTANCE FACTORS FROM SOURCE AND ASSOCIATED WITH IRON RICH CHLORITES.
D3	SINISTRAL STRIKE SLIP DEFORMATION AND WEST BLOCK UP MOVEMENT PRODUCES PERVASIVE DUE EAST DIPPING CLEAVAGE. SULFIDES REMOBALISED AND STRETCHED OUT. METAMORPHIC PROCESSES PRODUCE QUARTZ VEINS THAT FILL ALL STRUCTURES. QUARTZ VEINING MAY REMOBILISE GOLD FROM BASEMENT ROCKS. LATE STAGE Mg RICH SHEARS DEVELOPE AND QUARTZ FILLED STRUCTURES LIKE D ZONE CREATED.

CHAPTER 9

CONCLUSIONS

During the course of the above text many geological issues related to the Cobar Basin and the mineralisation it contains have been raised. This began with a detailed structural analysis of the CSA deposit using both surface and underground mapping. The observed structural components were then compared to the findings of Robertson (1974) for the upper part of the CSA deposit, Glen (1990, 1988, 1987) for the Cu-Au deposits and regional data, and Hinman and Scott (1990) for the Peak deposit. By doing this it was found that the structural components observed at the CSA deposit were typical of the components observed in the other deposits found within Zone 1 of the Cobar Basin.

However, as a result of the detailed structural analysis there were a number of timing relationships between mineralisation, structure and quartz veining that required clarification. This has been achieved by recognising three deformation events within Zone 1. These include

1) D1, a basin closure event producing tight subhorizontal folds and no mineralisation,
2) a D2 event resulting from a change in the horizontal stress field from NE to SE which sheared and cleaved the rocks of Zone 1 producing pipe like fracture zones through which metal bearing fluids moved and deposited mineralisation, and finally
3) a post mineralisation D3 event which contained strike slip

west block up movement allowing the injection of quartz into the mineralised zones.

In developing this new structural model for Zone 1 of the Cobar Basin it was then possible to re-examine the problem of sulfide source and quartz veining. By representing the isotopic data and conclusions of Brill and Seccombe (unpub), Brill and Seccombe and Chivas (unpub), Seccombe (unpub) and Seccombe (1990) it was shown that the sulfides of Zone 1 deposits could be of sedimentary or igneous origin but not of metamorphic origin like the quartz which has remobilised and displaced mineralisation. Based on S:Se data the mineralisation could be either igneous and/or hydrothermal in origin, but it is not known if this method of determination of source is accurate. As for the source of the quartz veining, a metamorphic origin is accepted based on the work of Brill, Seccombe and Chivas (unpub) and Phillips and Powell (1992).

Three other key points evolved from reassessing the isotopic data. Firstly, sulfide disequilibrium was noted for the quartz veined CSA and Cu-Au deposits and not for the Elura deposit, implying that the quartz veining was later than the mineralisation. This was already confirmed by the detailed structural analysis of Chapter 4 and the observation by Robertson (1974) that sulfides had been mechanically remobilised. Secondly, the quartz and calcite isotopic data of mineralised areas differs from unmineralised areas, suggesting some mixing and contamination, loosely implying the quartz is later than the mineralisation. Finally, the isotopic dating of Glen, Dallmeyer and Black (1986, 1992) has the low grade metamorphic cleavage forming event occuring at around 404Ma. Rejuvenation of detrital micas and feldspars occurred during this event making the sulfide emplacement date difficult to determine given the quartz is injected late in the deformation history.

With these observations came the realisation through the work of Phillips and Powell (1992) that the chemistry of the Cobar quartz veins is typical of those found in 90% of all gold deposits. Given that this fluid is ideal for gold transportation and that the quartz is found late in the structural history, then it becomes possible to separate a sulfide mineralising D2 phase from a gold bearing D3 event. This suggests that the gold may have been stripped from the basement rocks, and in the case of the Peak deposit only found close to the source rocks.

Incorporated in this study was an appraisal of gravity as a tool for understanding the structure of the Cobar Basin on both a regional and local scale. Prior to the models being created, the data from a survey conducted between 1972 and 1974 was retrieved and computerised by the author and later reprocessed to a density of 2.2gm/cc. From this, models were generated that have assisted in understanding basement/basin contact depths, shear locations, and possibly the depths to which mineralisation extends at the CSA deposit (ie to 2km below surface) given some of the geological assumptions made. The gravity models may also assist in understanding the structural models presented by Glen (1990) and assist subsequent workers since this data is now accessible for the first time.

ACKNOWLEDGEMENTS

The author wishes to thank Cobar Mines Pty. Ltd. for their support in researching this paper and allowing access to historical, exploration, and unpublished reports. Mr C. Smith is thanked for partaking in discussions related to this paper and Dr David Leaman is thanked for assistance with the gravity corrections. Many thanks to the three unknown reviewers for their comments. Mrs M. Jeffrey is also thanked for making the time available to type the manuscript.

This document was completed as part requirements for a Masters Of Economic Geology Degree for the University Of Tasmania, Hobart, Australia.

REFERENCES

Adams, R.L. and Schmidt,B.L., 1980. Geology of the Elura Zn/Pb/Ag deposit. Bill. Aust. Soc. Explor. Geophys., v.11, no. 4.

Andrews, E.C., 1913. Report on the Cobar Copper and Goldfield. *Geol. Surv. N.S.W. Mineral Resources 17.*

Baker, C.J., 1975. Geology of the Cobar 1:100000 Sheet, 8035. Geol. Surv. N.S.W.

Brill, B.A. and Seccombe, P.K., unpub. Conditions of ore formation at the CSA Cu/Pb/Zn/ Mine , Cobar, Australia, as indicated by fluid inclusions and composition of chlorites.

Brill, B.A., Seccombe, P.K., Chivas, A., unpub. An oxygen, hydrogen, carbon and sulfur isotope study of the CSA Cu/Pb/Zn Mine Cobar Australia

Brooke, W.J.L., 1975. Cobar Mining Field, in Economic Geology of Australia and Papua New Guinea: 1 Metals. Aust. Inst. Min. Metall. Monograph 5, pp 683-694.

Connor, A.G., 1985, unpub. Ore Potential of the Cobar Trough.

De Mark, P.L., inprep. The geology of the Western Gossan Area, CSA mine, Cobar. Hons. project University of Technology, Sydney.

De Roo, J.A., 1989. The Elura Ag/Pb/Zn Mine in Australia: Ore Genesis in a slate belt by syndeformational metasomatism along hydrothermal fluid conduits. Econ. Geol. 84, pp 256-278.

Fritz, P., 1976. Oxygen and carbon isotopes in ore deposits in sedimentary rocks. In Wolf, K.H. (ed.), Handbook of strata-bound and stratiform ore deposits 2: 191-217.

Gilligan, L.B. and Supple, D.W., 1978. Mineral deposits in the Cobar Supergroup and their structural setting. N.S.W. Geol. Surv. Qt. Notes no.33.

Glen, R.A., 1982. The Amphitheatre Group, Cobar N.S.W. Preliminary results of the new mapping and implications for ore search. N.S.W. Geol. Surv. Qt. Notes no.49, pp1-14.

Glen, R.A. and Black, L.P., 1983. Cobar geochronology. In BMR '83,pp 107-708. Aust. Govt. Pub. Serv., Canberra.

Glen R.A., 1985. Basement control on the deformation of cover basins: an example from the Cobar district in the Lachlan Fold Belt, Australia. Jour. Struct. Geol. Vol.7, nos.3/4, pp 301-315.

Glen, R.A., Dallmeyer, R.D., Black, L.P., 1986. Preliminary report on new isotopic evidence for and implications of an early Devonian deformation at Cobar. Geol. Surv N.S.W. Qt. Notes no. 64.

Glen, R.A., 1987. Copper and gold rich deposits in deformed turbidites at Cobar, Australia; their structural control and hydrothermal origin. Econ. Geol. Vol. 82, pp 124-140.

Glen, R.A., 1988. Basin inversion, thrusts and ore deposits at Cobar N.S.W. A preliminary report. Geol. Surv. Qt. Notes 73, pp 21-26.

Glen, R.A., 1990. Formation and inversion of transtensional basins in the western part of the Lachlan Fold Belt, Australia, with emphasis on the Cobar Basin. Journ. Struct. Geol. vol. 12, no. 5, pp 601-602.

Glen, R.A., 1992. ACORP deep seismic profiling of the Cobar Basin. Minfo no. 35.

Glen, R.A., Dallmeyer, R.D., Black, L.P., 1992. Isotopic dating of basin inversion; the Palaeozoic Cobar Basin, Lachlan Orogen, Australia. Tectonophysics 214, pp 249-268.

Harland, W.B., Cox, A.V., Llewellyn, P.G., Pickton, C.A.G., Smith, A.C., Walters, R., 1989. Subdivisions of Phanerozoic Time. Cambridge Press, Cambridge. 263pp.

Harvey, T.V. and Clarke, G.F., 1972, unpub. Cobar area gravity survey. Mines Exploration P/L report.

Hinman, M.C. and Scott, A.K., 1990. The Peak gold deposit, Cobar. In geology of the mineral deposits of Australia and Papua New Guinea (Eb. F.E. Hughes). Aust. Inst. Min. Metall. pp 1345-1351.

Kapelle, K, 1970. Geology of the CSA Mine, Cobar, N.S.W. Proc. Aust. Inst. Min. Metall., 233, pp 79-94.

Kirk, B.I., 1983. A review of the geology and ore genesis of the Cobar mining field. Aust. Inst. Min. Metall. Conf. Broken Hill, pp 183-185.

Knight, C.L., 1958, unpub. CSA prospect, Cobar: Report on drilling test which terminated December 1957. Report for Enterprise Exploration Co. P/L.

Kreulen, R., 1980. CO2 rich fluids during metamorphism on Naxos, Greece: Carbon isotopes and fluid inclusions. Amer. J. Sci. 280: 745-771.

Marshall, B., etal, 1981. Genetic aspects of the CSA and QTS mineralisation, Cobar, N.S.W. Abstr. Geol. Soc. Aust. 3:4.

Mulholland, C. St J. and Rayner, E.O., 1958. The gold-copper deposits of Cobar, N.S.W., central section (Great Cobar to Occidental). Tech. Rep. Dep. Mines N.S.W., 6, pp 23-47.

Ohmoto, H., and Rye, R.O., 1979. Isotopes of sulfur and carbon. In Barnes, H. (ed.), Geochemistry of hydrothermal ore deposits. Wiley and Sons, new York, 509-556.

Pegum, D.M., 1962, unpub. Gravity survey over CSA area, Cobar N.S.W. Geol. Surv. N.S.W. Dept. of Mines Rep.

Phillips, G.N. and Powell, R., 1992. Gold only province and their common features. EGRU contribution 43, James Cook University, Queensland Aust.

Pogson, D.J. and Felton, E.A., 1978. Reappraisal of geology Cobar-Canbelego-Mineral Hill region, central western N.S.W. Geol. Surv. N.S.W. Qt. Notes 33, pp 1-4.

Rayner, E.O., 1969. The copper ores of the Cobar region. Mem. Geol. Surv. N.S.W. No. 10.

Roach, M., 1992. Interactive 2D gravity and magnetic modelling programme for IBM PC compatible computers, version 3. Centre for Ore Deposit and Exploration Studies, University of Tasmania, Hobart, Australia.

Robertson, I.D.M., 1982a, unpub. The geochemistry and mineralogy of fresh wallrocks at Cobar N.S.W. (Cobar primary dispersion project). Vol 1-3.

Robertson, I.D.M., 1982b, unpub. Alkali, alkaline earth and base metal haloes in fresh wallrocks at Cobar N.S.W. (Cobar primary

dispersion project).
Robertson, I.D.M., 1983, unpub. A fresh rock halo geochemical assessment of some exploration targets at Cobar N.S.W. (Cobar primary dispersion project).
Robertson, I.D.M., 1984, unpub. A depletion mechanism for the Cobar haloes and a proposed Cobar ore model.
Robertson, I.D.M., 1985, unpub. Auger bedrock hydrocarbon halo geochemistry over the CSA Mine and Peak and Dapville prospects Cobar N.S.W.
Robertson, I.G., 1974, unpub. The environmental features and petrogenesis of the mineral zones of Cobar, N.S.W. PhD. Thesis, Armidale University, New England.
Rose, W.J., 1974, unpub. Bedrock geochemistry EL 402, Cobar.
Schmidt, B.L., 1983. Aspects of mineralisation at Elura. Lithosphere dynamics and evolution of continental crust. Sixth Geol. Soc. Aust. Abstr. pp 313-315.
Schofield, N., 1990, unpub. Mapping the distribution of copper grade in QTS South, CSA Mine, Cobar.
Scott, A.K., and Phillips, K.G., 1990. CSA copper-lead-zinc deposit, Cobar. In Geology of the Mineral Deposits of Australia and Papua New Guinea (Ed. F.E. Hughes). Aust. Inst. Min. Metall., pp 1337-1343.
Seccombe, P.K., 1990. Fluid inclusion and sulfur isotope evidence for syntectonic mineralisation at the Elura mine, southeastern Australia. Mineral Deposita 25, pp 304-312.
Seccombe, P.K., unpub. Sulfur isotope and fluid inclusion geochemistry of metamorphic Cu-Au vein deposits Cobar, N.S.W., Australia.
Smith, J.V., 1992. Experimental kinematic analysis of en echelon structures in relation to the Cobar basin, Lachlan Fold Belt. Tectonophysics, 214, pp 296-276.
Smith, J.V. and Marshall, B., 1992. Patterns of folding and fold interference in oblique contraction of layered rocks of the inverted Cobar basin, Australia. Tectonophysics, 215, pp 319-334.
Stanton, R.L., 1972. Ore Petrology. Mc Graw Hill.
Sullivan, C.J., 1950. Mineralisation in the Cobar-Nymagee province and its significance. Proc. Aust. Inst. Min. Metall. No. 156-157, pp 154-176.
Sullivan, C.J., 1951. Geology of New Occidental, New Cobar and Chesney Mines, Cobar N.S.W. B.M.R. Rep. 6.
Sun, S.S., 1983. Implications of S and Pb isotope data to genesis of massive sulfides in the Cobar area. Geol. Soc. Aust. Abstr. 9, pp 307-309.
Suppel, D.W. and Scheibner, E., 1990. Lachlan fold belt in New South Wales: Regional geology and mineral deposits. In Geology of the Mineral Deposits of Australia and Papua New Giunea (Ed. F.E. Hughes, Aust. Inst. Min. Metall. pp 1321-1327.
Trueman, N.A., 1972, unpub. Quartz-feldspar porphyry from EL 219, Cobar. Mines Exploration P/L report.
Walshe, J.L., 1986. A six component chlorite solid solution model and the conditions of chlorite formation in hydrothermal and

geothermal systems. Econ. Geol. 81, pp 681-703.
Wilkins, R.W.T., and Barkas, J.P., 1978. Fluid inclusions, deformation and recrystallisation in granite tectonites. Contrib. Min. Pet. 65: 293-299.

APPENDIX 1
WESTERN ZONE SURFACE STRUCTURAL DATA

CSA SURFACE WESTERN ZONE
DATA COLLECTOR DATE
0
DIP/DIPDIRECTION
0
NO QUANTITY
1 EXTRA DATA COLUMN

number	;DIP	;DIRECTION	;TYPE
1	80	255	BED
2	80	242	BED
3	80	60	BED
4	80	85	BED
5	85	80	BED
6	80	87	BED
7	65	130	BED
8	85	235	BED
9	75	87	BED
10	80	268	BED
11	80	88	BED
12	70	85	BED
13	80	265	BED
14	80	255	BED
15	59	92	BED
16	85	50	BED
17	79	47	BED
18	75	78	BED
19	60	90	BED
20	76	87	BED
21	55	70	BED
22	64	88	BED
23	44	91	BED
24	56	87	BED
25	75	80	BED
26	80	91	BED
27	55	90	BED
28	60	95	BED
29	49	295	BED
30	45	60	BED
31	15	110	BED
32	85	280	BED
33	70	88	BED
34	80	60	BED
35	80	80	BED
36	50	63	BED
37	35	70	BED
38	60	80	BED
39	46	280	BED
40	50	280	BED
41	80	91	BED
42	85	90	BED
43	80	95	BED
44	80	265	BED
45	85	270	BED
46	85	265	BED
47	80	270	BED

A1.2

48	85	268	BED
49	80	260	BED
50	80	78	BED
51	72	80	BED
52	48	80	BED
53	50	75	BED
54	50	260	BED
55	50	240	BED
56	58	60	BED
57	44	275	BED
58	46	250	BED
59	50	260	BED
60	50	260	BED
61	80	80	BED
62	85	235	BED
63	80	240	BED
64	70	80	BED
65	80	230	BED
66	80	60	BED
67	50	230	BED
68	65	250	BED
69	70	245	BED
70	80	60	BED
71	80	260	BED
72	70	265	BED
73	85	90	CLEAV
74	65	70	CLEAV
75	80	92	CLEAV
76	80	92	CLEAV
77	80	90	CLEAV
78	80	85	CLEAV
79	70	60	CLEAV
80	75	90	CLEAV
81	75	90	CLEAV
82	75	70	CLEAV
83	72	65	CLEAV
84	70	65	CLEAV
85	56	40	CLEAV
86	75	70	CLEAV
87	77	70	CLEAV
88	85	91	CLEAV
89	85	91	CLEAV
90	88	310	CLEAV
91	87	90	CLEAV
92	86	90	CLEAV
93	85	90	CLEAV
94	60	110	CLEAV
95	65	100	CLEAV
96	55	95	CLEAV
97	75	95	CLEAV
98	60	120	CLEAV
99	60	120	CLEAV
100	55	105	BED
101	70	65	CLEAV
102	85	245	BED
103	85	75	CLEAV

104	85	290	BED
105	75	70	BED
106	80	80	BED
107	55	20	CLEAV
108	55	50	CLEAV
109	85	70	CLEAV
110	85	245	BED
111	75	250	BED
112	90	240	BED
113	90	260	BED
114	75	90	BED
115	85	250	BED
116	55	160	BED
117	80	75	BED
118	70	95	CLEAV
119	65	255	BED
120	75	266	BED
121	75	115	BED
122	60	160	BED
123	80	260	BED
124	65	265	BED
125	85	255	BED
126	80	265	BED
127	80	245	BED
128	80	85	CLEAV
129	75	245	BED
130	55	95	CLEAV
131	55	85	CLEAV
132	65	95	CLEAV
133	65	95	CLEAV
134	80	85	CLEAV
135	55	115	CLEAV
136	80	100	CLEAV
137	80	85	CLEAV
138	70	55	CLEAV
139	70	100	CLEAV
140	65	95	CLEAV
141	80	265	BED
142	75	85	CLEAV
143	65	60	BED
144	75	270	BED
145	80	280	BED
146	80	290	BED
147	75	85	CLEAV
148	80	270	BED
149	80	80	CLEAV
150	74	125	BED
151	77	265	BED
152	80	235	BED
153	70	145	BED
154	71	195	BED
155	80	85	BED
156	78	275	BED
157	80	275	BED
158	75	118	BED
159	56	115	BED

160	51	145	BED
161	66	120	BED
162	80	270	BED
163	55	185	BED
164	61	170	BED
165	63	155	BED
166	66	155	BED
-1			

APPENDIX 2
EASTERN ZONE SURFACE STRUCTURAL DATA

CSA SURFACE EASTERN ZONE

DATA COLLECTOR DATE
0
DIP/DIPDIRECTION
0
NO QUANTITY
1 EXTRA DATA COLUMN

number	;DIP	;DIRECTION	;TYPE
1	85	250	BED
2	85	90	CLEAV
3	88	250	BED
4	86	90	CLEAV
5	75	225	BED
6	85	90	CLEAV
7	90	320	CLEAV
8	87	265	BED
9	78	215	BED
10	85	110	CLEAV
11	85	260	BED
12	80	270	BED
13	87	90	CLEAV
14	88	90	CLEAV
15	75	245	BED
16	90	320	CLEAV
17	76	200	BED
18	88	120	CLEAV
19	85	50	CLEAV
20	78	254	BED
21	88	90	CLEAV
22	80	255	BED
23	80	90	CLEAV
24	70	250	BED
25	70	255	BED
26	70	250	BED
27	90	320	CLEAV
28	80	270	BED
29	80	120	CLEAV
30	85	90	CLEAV
31	80	265	BED
32	80	260	BED
33	80	120	CLEAV
34	88	320	CLEAV
35	86	90	CLEAV
36	80	115	CLEAV
37	80	270	BED
38	80	270	BED
39	80	290	BED
40	90	330	CLEAV
41	90	40	CLEAV
42	70	265	BED
43	85	120	CLEAV
44	90	320	CLEAV
45	90	30	CLEAV
46	85	90	CLEAV
47	80	120	CLEAV

A2·2

48	72	260	BED
49	80	265	BED
50	90	40	CLEAV
51	90	320	CLEAV
52	87	260	BED
53	88	90	CLEAV
54	70	260	BED
55	90	40	CLEAV
56	90	320	CLEAV
57	80	255	BED
58	90	320	CLEAV
59	85	270	BED
60	85	90	CLEAV
61	80	260	BED
62	60	250	BED
63	80	230	BED
64	70	240	BED
65	80	250	BED
66	80	245	BED
67	80	260	BED
68	70	240	BED
69	60	260	BED
70	75	270	BED
71	75	270	BED
72	80	270	BED
73	80	265	BED
74	80	265	BED
75	80	260	BED
76	80	260	BED
77	80	265	BED
78	25	270	BED
79	76	260	BED
80	70	270	BED
81	88	260	BED
82	70	265	BED
83	70	260	BED
84	70	255	BED
85	75	250	BED
86	88	265	BED
87	80	90	CLEAV
88	88	90	CLEAV
89	88	310	CLEAV
90	80	90	CLEAV
91	88	300	CLEAV
92	85	90	CLEAV
93	88	110	CLEAV
94	88	325	CLEAV
95	88	30	CLEAV
96	85	113	CLEAV
97	80	88	CLEAV
98	75	92	CLEAV
99	85	92	CLEAV
-1			

APPENDIX 3
UNDERGROUND STRUCTURAL DATA

A301

CSA UNDERGROUND
BEDDING
0
dip/dipdirection
0
no quantity
1
number ;dip ;direction;type ;

number	dip	direction	type
1	84	265	11
2	88	255	11
3	85	255	11
4	85	255	11
5	80	260	11
6	82	270	11
7	88	260	11
8	85	260	11
9	85	90	11
10	88	90	11
11	87	90	11
12	50	255	11
13	55	240	11
14	80	270	11
15	80	270	11
16	81	256	11
17	80	250	11
18	70	275	11
19	80	275	11
20	90	255	11
21	85	260	11
22	85	260	11
23	85	260	11
24	90	255	11
25	85	260	11
26	87	270	11
27	85	85	11
28	89	260	11
29	85	265	11
30	85	270	11
31	65	230	11
32	85	270	11
33	85	240	11
34	75	270	11
35	89	275	11
36	83	90	11
37	70	260	11
38	89	75	11
39	85	265	11
40	85	85	11
41	85	85	11
42	82	90	11
43	85	100	11
44	80	90	11
45	85	80	11
46	75	258	11
47	88	260	11
48	90	84	11
49	88	270	11
50	85	260	11
51	85	245	11
52	75	250	11
53	66	75	11
54	75	70	11
55	88	75	11
56	81	80	11
57	74	72	11
58	86	56	11
59	68	70	11
60	78	75	11
61	90	255	11
62	82	80	11
63	80	80	11
64	65	90	11
65	88	250	11
66	83	91	11
67	82	62	11
68	77	73	11
69	90	250	11
70	75	85	11
71	75	85	11
72	87	64	11
73	80	45	11
74	55	86	11
75	84	73	11
76	85	80	11
77	85	80	11
78	85	80	11
79	78	80	11
80	85	90	11
81	80	250	11
82	80	240	11
83	85	230	11
84	80	240	11
85	85	70	11
86	85	70	11
87	82	80	11
88	78	80	11
89	82	80	11
90	78	80	11
91	84	65	11
92	78	75	11
93	78	75	11
94	80	75	11
95	89	70	11
96	85	75	11
97	85	70	11
98	77	75	11
99	55	90	11
100	80	70	11
101	73	90	11
102	80	260	11
103	70	80	11
104	63	80	11

A3·2

105	76	268	11	161	88	265	11
106	60	98	11	162	80	255	11
107	83	275	11	163	75	240	11
108	89	270	11	164	89	235	11
109	89	275	11	165	87	250	11
110	85	272	11	166	88	215	11
111	85	270	11	167	83	250	11
112	65	260	11	168	85	265	11
113	84	275	11	169	80	222	11
114	84	270	11	170	86	268	11
115	87	275	11	171	87	255	11
116	85	310	11	172	85	260	11
117	82	270	11	173	82	235	11
118	80	240	11	174	85	220	11
119	65	270	11	175	75	230	11
120	86	270	11	176	80	240	11
121	70	265	11	177	88	270	11
122	75	270	11	178	75	257	11
123	75	259	11	179	78	245	11
124	75	260	11	180	82	235	11
125	88	280	11	181	88	245	11
126	75	275	11	182	84	240	11
127	88	270	11	183	85	260	11
128	75	280	11	184	87	260	11
129	72	290	11	185	78	255	11
130	80	270	11	186	80	260	11
131	75	265	11	187	87	281	11
132	80	265	11	188	81	280	11
133	75	320	11	189	71	235	11
134	70	275	11	190	80	185	11
135	70	320	11	191	80	230	11
136	85	265	11	192	72	220	11
137	90	250	11	193	76	230	11
138	88	250	11	194	65	225	11
139	80	260	11	195	77	235	11
140	75	260	11	196	70	240	11
141	80	240	11	197	76	235	11
142	85	275	11	198	78	250	11
143	78	260	11	199	72	240	11
144	76	260	11	200	80	230	11
145	80	260	11	201	75	250	11
146	78	240	11	202	80	265	11
147	85	250	11	203	80	215	11
148	78	260	11	204	78	240	11
149	85	240	11	205	89	255	11
150	87	245	11	206	85	260	11
151	78	260	11	207	90	260	11
152	84	255	11	208	85	80	11
153	80	255	11	209	90	80	11
154	78	255	11	210	85	80	11
155	82	265	11	211	85	80	11
156	78	250	11	212	90	260	11
157	87	230	11	213	85	90	11
158	78	265	11	214	85	90	11
159	80	275	11	215	89	240	11
160	85	260	11	216	90	260	11

A3-3

217	85	80	11	273	80	65	11
218	80	240	11	274	87	45	11
219	80	230	11	275	80	90	11
220	80	230	11	276	84	65	11
221	80	245	11	277	82	75	11
222	80	245	11	278	75	70	11
223	78	230	11	279	60	265	11
224	75	230	11	280	85	255	11
225	75	230	11	281	80	270	11
226	72	230	11	282	86	230	11
227	70	230	11	283	89	235	11
228	80	260	11	284	86	240	11
229	80	185	11	285	89	240	11
230	87	190	11	286	87	245	11
231	78	225	11	287	84	80	11
232	83	180	11	288	84	65	11
233	85	260	11	289	85	60	11
234	85	250	11	290	78	85	11
235	90	250	11	291	82	80	11
236	88	90	11	292	83	250	11
237	85	85	11	293	80	240	11
238	85	75	11	294	84	255	11
239	75	185	11	295	89	230	11
240	78	205	11	296	85	230	11
241	85	215	11	297	85	230	11
242	75	200	11	298	84	220	11
243	80	260	11	299	85	240	11
244	85	26	11	300	89	235	11
245	85	260	11	301	75	220	11
246	80	80	11	302	84	235	11
247	75	70	11	303	89	90	11
248	75	75	11	304	75	90	11
249	85	240	11	305	80	95	11
250	85	110	11	306	80	75	11
251	80	75	11	307	84	70	11
252	85	65	11	308	88	60	11
253	80	240	11	309	88	70	11
254	80	270	11	310	90	240	11
255	75	260	11	311	80	245	11
256	80	270	11	312	85	230	11
257	85	240	11	313	88	255	11
258	80	240	11	314	85	255	11
259	80	240	11	315	85	250	11
260	85	240	11	316	89	90	11
261	80	240	11	317	85	240	11
262	85	225	11	318	85	240	11
263	80	240	11	319	85	240	11
264	80	220	11	320	90	240	11
265	75	220	11	321	80	240	11
266	90	250	11	322	85	240	11
267	85	240	11	323	88	245	11
268	85	240	11	324	85	240	11
269	80	230	11	325	87	250	11
270	88	250	11	326	85	245	11
271	80	65	11	327	85	240	11
272	80	230	11	328	87	245	11

A3.4

329	85	240	11	385	64	225	11
330	85	240	11	386	70	255	11
331	85	240	11	387	70	235	11
332	75	240	11	388	55	270	11
333	25	220	11	389	88	270	11
334	80	240	11	390	88	270	11
335	80	240	11	391	78	240	11
336	70	290	11	392	70	230	11
337	80	240	11	393	75	250	11
338	75	300	11	394	72	220	11
339	77	195	11	395	60	230	11
340	85	255	11	396	82	190	11
341	85	235	11	397	60	210	11
342	86	225	11	398	78	230	11
343	76	200	11	399	60	270	11
344	74	205	11	400	70	260	11
345	82	205	11	401	88	270	11
346	85	205	11	402	70	270	11
347	87	235	11	403	85	270	11
348	86	255	11	404	72	260	11
349	79	235	11	405	80	245	11
350	85	245	11	406	75	265	11
351	86	280	11	407	62	235	11
352	78	235	11	408	65	242	11
353	78	235	11	409	85	215	11
354	84	245	11	410	78	260	11
355	85	240	11	411	75	252	11
356	83	235	11	412	70	255	11
357	74	225	11	413	80	220	11
358	89	255	11	414	75	250	11
359	89	255	11	415	75	250	11
360	89	255	11	416	72	245	11
361	78	245	11	417	76	222	11
362	78	235	11	418	74	241	11
363	89	255	11	419	68	226	11
364	89	225	11	420	77	235	11
365	78	225	11	421	74	249	11
366	70	235	11	422	78	260	11
367	74	230	11	423	72	235	11
368	78	235	11	424	79	241	11
369	90	260	11	425	77	246	11
370	86	245	11	426	73	244	11
371	89	250	11	427	75	242	11
372	84	250	11	428	84	245	11
373	80	245	11	429	87	240	11
374	80	235	11	430	75	240	11
375	82	245	11	431	75	240	11
376	82	235	11	432	76	245	11
377	81	240	11	433	75	240	11
378	82	235	11	434	75	246	11
379	86	250	11	435	76	247	11
380	83	250	11	436	78	250	11
381	80	250	11	437	78	246	11
382	78	250	11	438	85	252	11
383	77	260	11	439	80	250	11
384	87	240	11	440	75	255	11

A3.5

441	75	255	11
442	77	253	11
443	80	250	11
444	75	250	11
445	80	250	11
446	79	265	11
447	80	260	11
448	76	250	11
449	80	250	11
450	80	260	11
451	80	255	11
452	85	270	11
453	75	250	11
454	60	245	11
455	70	255	11
456	80	256	11
457	78	260	11
458	81	260	11
459	80	261	11
460	85	235	11
461	80	245	11
462	80	265	11
463	75	265	11
464	84	270	11
465	85	265	11
466	84	270	11
467	87	270	11
468	85	270	11
469	81	265	11
470	84	270	11
471	79	275	11
472	80	270	11
473	78	270	11
474	78	280	11
475	78	270	11
476	80	270	11
477	82	270	11
478	85	265	11
479	84	260	11
480	86	260	11
481	80	270	11
482	85	260	11
483	80	275	11
484	86	240	11
485	85	270	11
486	85	265	11
487	86	270	11
488	85	268	11
489	80	260	11
490	70	257	11
491	90	264	11
492	85	270	11
493	84	265	11
494	85	275	11
495	73	265	11
496	83	265	11
497	83	255	11
498	80	257	11
499	80	260	11
500	85	260	11
501	78	242	11
502	89	270	11
503	80	270	11
504	84	265	11
505	89	270	11
506	82	265	11
507	85	272	11
508	85	270	11
509	80	260	11
510	85	263	11
511	58	300	11
512	65	260	11
513	80	282	11
514	84	275	11
515	86	275	11
516	88	280	11
517	80	270	11
518	89	270	11
519	85	270	11
520	84	270	11
521	77	260	11
522	80	260	11
523	80	265	11
524	88	260	11
525	80	260	11
526	85	265	11
527	75	260	11
528	85	260	11
529	78	250	11
530	65	270	11
531	70	265	11
532	75	270	11
533	75	260	11
534	75	259	11
535	75	260	11
536	85	270	11
537	88	270	11
538	80	270	11
539	80	250	11
540	78	259	11
541	78	240	11
542	75	260	11
543	85	265	11
544	75	245	11
545	88	270	11
546	88	270	11
547	88	270	11
548	71	260	11
549	65	270	11
550	76	261	11
551	75	265	11
552	85	261	11

A3.6

553	75	259	11	609	70	270	965
554	76	257	11	610	70	270	965
555	81	260	11	611	75	270	965
556	80	258	11	612	80	250	965
557	78	263	11	613	80	260	965
558	80	260	11	614	75	265	965
559	75	260	11	615	70	255	965
560	85	255	11	616	65	280	965
561	89	90	11	617	75	280	965
562	76	257	11	618	75	260	965
563	78	240	11	619	70	270	965
564	88	97	11	620	80	265	965
565	85	285	11	621	85	260	965
566	85	262	11	622	70	260	965
567	80	275	965	623	80	260	965
568	85	275	965	624	80	260	965
569	78	285	965	625	80	260	965
570	78	285	965	626	80	260	965
571	80	290	965	627	80	270	965
572	80	290	965	628	85	270	965
573	80	285	965	629	80	260	965
574	75	255	965	630	70	260	965
575	75	275	965	631	75	260	965
576	80	270	965	632	80	260	965
577	75	270	965	633	70	270	965
578	75	270	965	634	85	270	965
579	81	270	965	635	80	270	965
580	90	270	965	636	80	270	965
581	76	275	965	637	76	265	965
582	85	270	965	638	80	250	965
583	75	270	965	639	80	260	965
584	75	270	965	640	79	260	965
585	75	275	965	641	87	265	965
586	85	270	965	642	80	260	965
587	85	270	965	643	74	260	965
588	78	280	965	644	76	280	965
589	78	280	965	645	85	260	965
590	80	270	965	646	85	260	965
591	85	270	965	647	80	260	965
592	60	270	965	648	75	260	965
593	80	270	965	649	75	265	965
594	70	250	965	650	80	270	965
595	80	280	965	651	75	265	965
596	79	280	965	652	80	270	965
597	85	280	965	653	70	265	965
598	75	270	965	654	85	260	965
599	70	260	965	655	85	260	965
600	70	260	965	656	80	260	965
601	90	290	965	657	80	250	965
602	60	265	965	658	85	255	965
603	80	240	965	659	80	260	965
604	75	260	965	660	75	265	965
605	85	265	965	661	77	270	965
606	80	280	965	662	75	270	965
607	80	280	965	663	85	265	965
608	80	280	965	664	80	265	965

665	75	265	965	721	85	255	810
666	85	265	965	722	80	260	810
667	82	270	965	723	80	265	805
668	80	270	965	724	80	270	805
669	75	270	965	725	75	260	805
670	75	270	965	726	80	270	805
671	75	265	965	727	80	265	805
672	80	265	965	728	80	265	805
673	80	280	965	729	75	265	805
674	75	260	965	730	60	260	805
675	70	265	965	731	85	260	805
676	80	250	965	732	80	260	805
677	80	260	965	733	75	260	805
678	80	270	965	734	80	265	805
679	75	280	965	735	85	270	805
680	80	260	965	736	80	270	805
681	80	265	965	737	80	270	805
682	77	265	965	738	80	270	805
683	78	260	965	739	80	270	805
684	75	260	965	740	85	260	805
685	80	270	965	741	90	260	805
686	80	260	965	742	73	260	805
687	83	250	810	743	85	245	805
688	81	250	810	744	85	270	805
689	81	250	810	745	85	270	805
690	82	250	810	746	77	255	805
691	88	260	810	747	78	270	805
692	86	250	810	748	72	285	805
693	85	260	810	749	72	275	805
694	86	255	810	750	90	280	805
695	85	265	810	751	70	265	805
696	75	275	810	752	85	270	805
697	84	255	810	753	85	270	805
698	86	260	810	754	85	270	805
699	80	255	810	755	85	270	805
700	75	255	810	756	70	250	805
701	70	260	810	757	78	235	805
702	80	260	810	758	74	240	805
703	90	265	810	759	82	285	805
704	87	260	810	760	85	270	805
705	87	255	810	761	74	240	805
706	83	255	810	762	80	95	805
707	85	260	810	763	75	245	805
708	80	255	810	764	70	260	805
709	85	260	810	765	75	260	805
710	82	260	810	766	75	265	805
711	81	260	810	767	80	265	805
712	82	265	810	768	80	280	805
713	80	270	810	769	85	280	805
714	81	260	810	770	85	280	805
715	83	265	810	771	80	270	805
716	87	265	810	772	75	250	805
717	86	265	810	773	80	250	805
718	90	270	810	774	70	250	805
719	80	265	810	775	85	90	805
720	77	265	810	776	85	75	805

A3·8

777	70	250	805
778	85	280	805
779	85	280	805
780	80	280	805
781	75	280	805
782	80	270	805
783	70	250	805
784	75	250	805
785	75	260	805
786	85	260	805
787	80	270	805
788	80	270	805
789	85	265	805
790	85	270	805
791	80	270	805
792	85	270	805
793	85	270	805
794	75	250	805
795	70	260	805
796	85	260	805
797	85	270	805
798	85	270	805
799	85	270	805
800	75	245	805
801	85	245	805
802	75	235	805
803	85	270	805
804	80	270	805
805	90	270	805
806	80	50	805
807	80	270	805
808	75	255	805
809	85	255	805
810	85	270	805
811	90	270	805
-1			

CSA UNDERGROUND
DUE EAST DIPPING CLEAVAGE
0
DIP/DIPDIRECTION
0
NO QUANTITY
1

NUMBER ;	DIP ;	DIRECTION ;	TYPE ;
1	80	90	11
2	75	90	11
3	78	90	11
4	85	90	11
5	85	90	11
6	80	90	11
7	78	90	11
8	65	90	11
9	80	90	11
10	80	90	11
11	55	90	11
12	75	90	11
13	86	90	11
14	85	90	11
15	70	90	11
16	80	90	11
17	80	90	11
18	66	90	11
19	80	90	11
20	85	90	11
21	74	90	11
22	80	90	11
23	80	90	11
24	75	90	11
25	70	90	11
26	80	90	11
27	87	90	11
28	83	90	11
29	84	90	11
30	85	90	11
31	80	90	11
32	86	90	11
33	78	85	11
34	88	90	11
35	80	90	11
36	88	90	11
37	85	90	11
38	75	90	11
39	80	92	11
40	85	90	11
41	85	90	11
42	80	90	11
43	88	90	11
44	80	90	11
45	80	90	11
46	80	90	11
47	85	90	11
48	82	90	11
49	87	90	11
50	83	90	11
51	88	90	11
52	84	90	11
53	82	90	11
54	85	90	11
55	85	90	11
56	78	90	11
57	78	90	11
58	80	90	11
59	85	90	11
60	75	90	11
61	84	90	11
62	83	90	11
63	86	92	11
64	88	90	11
65	80	90	11
66	70	90	11
67	80	90	11
68	89	90	11
69	89	90	11
70	89	90	11
71	88	90	11
72	90	90	11
73	80	90	11
74	80	90	11
75	87	90	11
76	80	90	11
77	80	90	11
78	80	90	11
79	90	90	11
80	90	90	11
81	90	90	11
82	90	90	11
83	82	90	11
84	80	90	11
85	78	95	11
86	88	90	11
87	85	90	11
88	87	90	11
89	85	90	11
90	85	90	11
91	80	90	11
92	70	90	11
93	88	90	11
94	80	90	11
95	80	90	11
96	80	90	11
97	85	90	11
98	80	90	11
99	85	90	11
100	85	90	11
101	87	90	11
102	88	90	11
103	80	90	11

A3·10

104	80	90	11
105	80	90	11
106	80	90	11
107	84	90	11
108	85	90	11
109	84	90	11
110	84	90	11
111	82	90	11
112	84	90	11
113	80	90	11
114	85	90	11
115	90	90	11
116	80	92	11
117	85	92	11
118	85	90	11
119	80	90	11
120	85	90	11
121	87	90	11
122	84	90	11
123	72	90	11
124	85	90	11
125	82	90	11
126	87	90	11
127	87	90	11
128	80	90	11
129	83	90	11
130	86	90	11
131	85	90	11
132	80	90	11
133	87	90	11
134	82	90	11
135	82	90	11
136	88	90	11
137	85	90	11
138	88	270	11
139	88	90	11
140	88	90	11
141	88	90	11
142	88	90	11
143	87	270	11
144	85	270	11
145	80	90	11
146	85	90	11
147	87	90	11
148	85	270	11
149	85	90	11
150	85	90	11
151	85	90	11
152	85	90	965
153	89	90	965
154	85	90	965
155	88	90	965
156	85	90	965
157	90	90	965
158	85	90	965
159	80	90	965
160	85	90	965
161	90	90	965
162	90	90	965
163	90	90	965
164	90	90	965
165	90	90	965
166	90	90	965
167	90	90	965
168	85	90	965
169	85	90	965
170	85	90	965
171	90	90	965
172	85	270	965
173	86	270	965
174	87	90	965
175	86	90	965
176	88	90	965
177	88	90	965
178	85	93	965
179	90	90	965
180	87	90	965
181	85	90	965
182	85	90	965
183	87	90	965
184	80	90	965
185	87	90	965
186	87	90	965
187	88	90	965
188	89	90	965
189	85	90	965
190	87	90	965
191	80	90	965
192	85	90	965
193	80	90	965
194	80	90	965
195	85	90	965
196	80	90	965
197	80	90	965
198	84	90	810
199	84	90	810
200	88	90	810
201	80	90	810
202	85	90	810
203	90	90	805
204	90	90	805
205	90	90	805
206	90	90	805
207	85	90	805
208	86	90	805
209	88	90	805
210	85	90	805
211	90	90	805
212	84	93	805
213	85	270	805
214	86	270	805
215	88	90	805

A3·11

216	85	90	805
217	85	90	805
218	80	90	805
219	85	90	805
220	90	90	805
221	80	90	805
222	90	90	805
223	80	90	805
224	85	90	805
225	80	90	805
226	80	90	805
227	80	90	805
228	75	90	805
−1			

A 3.12

CSA UNDERGROUND

OTHER CLEAVAGES

0

DIP/DIPDIRECTION

0

NO QUANTITY

1

NUMBER	;DIP	;DIRECTION	;TYPE ;
1	80	110	11
2	87	120	11
3	80	100	11
4	85	110	11
5	80	100	11
6	80	100	11
7	85	110	11
8	80	120	11
9	86	110	11
10	75	110	11
11	85	110	11
12	75	100	11
13	80	110	11
14	70	95	11
15	75	120	11
16	80	100	11
17	89	105	11
18	80	100	11
19	85	95	11
20	85	110	11
21	80	108	11
22	75	100	11
23	80	120	11
24	80	120	11
25	65	260	11
26	80	85	11
27	87	94	11
28	80	85	11
29	90	275	11
30	85	95	11
31	82	95	11
32	80	95	11
33	85	100	11
34	85	100	11
35	82	100	11
36	67	95	11
37	75	81	11
38	85	80	11
39	79	84	11
40	85	10	11
41	86	85	11
42	80	100	11
43	70	80	11
44	86	100	11
45	78	80	11
46	88	100	11
47	85	110	11
48	85	100	11
49	85	110	11
50	85	110	11
51	90	100	11
52	85	100	11
53	79	80	11
54	85	100	11
55	80	100	11
56	85	100	11
57	75	100	11
58	85	100	11
59	85	100	11
60	80	80	11
61	85	80	11
62	85	80	11
63	85	85	11
64	90	80	11
65	90	80	11
66	86	85	11
67	80	80	11
68	80	80	11
69	80	80	11
70	85	80	11
71	85	80	11
72	85	95	11
73	85	100	11
74	85	95	11
75	75	70	11
76	82	80	11
77	70	110	11
78	80	95	11
79	88	110	11
80	85	100	11
81	82	80	11
82	85	110	11
83	88	100	11
84	72	120	11
85	80	120	11
86	80	105	11
87	89	105	11
88	88	75	11
89	87	120	11
90	81	83	11
91	71	80	11
92	89	85	11
93	72	80	11
94	85	97	11
95	80	120	11
96	75	50	11
97	88	110	11
98	88	95	11
99	89	280	11
100	80	107	11
101	88	270	11
102	88	145	11
103	84	310	11

A3·13

104	80	110	11
105	86	98	11
106	64	65	11
107	84	86	11
108	87	85	11
109	80	85	11
110	87	94	11
111	84	75	11
112	80	85	11
113	88	97	11
114	86	95	11
115	78	85	11
116	88	110	11
117	88	110	11
118	80	250	11
119	86	82	11
120	89	256	11
121	85	84	11
122	85	103	11
123	85	50	11
124	80	80	11
125	78	80	11
126	85	78	11
127	84	80	11
128	89	120	11
129	85	80	11
130	85	82	11
131	85	98	11
132	90	100	965
133	90	85	965
134	90	100	965
135	87	75	965
136	88	110	965
137	80	100	965
138	86	100	965
139	80	100	965
140	88	95	965
141	88	95	965
142	80	100	965
143	80	100	965
144	90	80	965
145	75	95	965
146	85	85	965
147	90	100	965
148	90	85	965
149	88	70	965
150	90	85	965
151	90	80	965
152	90	95	965
153	90	100	965
154	90	95	965
155	90	85	965
156	90	95	965
157	90	95	965
158	80	100	965
159	90	80	965
160	85	120	965
161	90	80	965
162	90	80	965
163	88	80	965
164	85	100	965
165	87	80	965
166	84	105	965
167	90	95	965
168	85	100	965
169	85	80	965
170	86	80	965
171	85	100	965
172	90	100	965
173	85	110	965
174	87	95	965
175	89	70	965
176	80	95	965
177	80	95	965
178	89	85	965
179	87	110	965
180	89	75	810
181	87	80	810
182	86	85	810
183	75	115	810
184	79	100	810
185	75	100	810
186	85	105	810
187	87	105	810
188	85	100	810
189	85	100	810
190	87	100	810
191	82	95	810
192	76	70	810
193	85	85	810
194	60	305	810
195	85	100	805
196	80	100	805
197	85	100	805
198	85	95	805
199	80	100	805
200	80	100	805
201	85	100	805
202	85	100	805
203	85	100	805
204	85	100	805
205	82	275	805
206	85	275	805
207	90	70	805
208	85	100	805
209	88	105	805
210	85	100	805
211	85	100	805
212	85	100	805
213	90	70	805
214	90	285	805
215	85	80	805

A3·14

216	85	100	805
217	87	215	805
218	87	290	805
219	90	280	805
220	82	75	805
221	87	85	805
222	85	110	805
223	85	95	805
224	90	105	805
225	90	80	805
226	90	100	805
227	90	100	805
228	85	110	805
229	90	100	805
230	85	110	805
231	85	265	805
232	80	100	805
233	85	100	805
234	80	100	805
235	80	80	805
236	85	80	805
237	85	80	805
238	90	100	805
239	85	285	805
240	85	110	805
241	85	100	805
242	80	100	805
243	85	100	805
244	80	110	805
245	90	110	805
246	85	120	805
247	85	110	805
248	90	110	805
249	85	105	805
250	80	110	805
251	85	110	805
252	80	110	805
253	80	110	805
254	85	110	805
255	80	110	805
256	80	105	805
−1			

CSA UNDERGROUND
SHEARS/FAULTS BY LEVELS
0
DIP/DIPDIRECTION
0
NO QUANTITY
1

NUMBER	DIP	DIRECTION	TYPE
1	85	115	11
2	80	110	11
3	85	130	11
4	90	290	11
5	60	250	11
6	25	90	11
7	85	310	11
8	35	30	11
9	85	310	11
10	80	315	11
11	60	250	11
12	65	45	11
13	58	350	11
14	69	83	11
15	60	320	11
16	20	0	11
17	40	320	11
18	25	225	11
19	18	300	11
20	50	275	11
21	60	285	11
22	82	95	11
23	50	140	11
24	85	240	11
25	89	125	11
26	80	60	11
27	35	310	11
28	89	60	11
29	63	300	11
30	90	210	11
31	70	310	11
32	85	300	11
33	70	264	11
34	88	265	11
35	80	242	11
36	45	270	965
37	90	95	965
38	90	245	965
39	87	315	965
40	90	255	965
41	85	250	965
42	75	305	965
43	85	275	965
44	40	275	965
45	89	290	965
46	35	270	810
47	70	245	810
48	30	325	805
49	30	359	805
50	30	310	805
51	30	20	805
52	30	355	805
53	30	5	805
54	45	325	805
55	40	350	805
56	20	350	805
57	45	315	805
58	30	10	805
59	30	310	805
60	20	240	805
61	30	240	805
62	40	245	805
63	40	230	805
64	30	1	805
65	45	220	805
66	90	310	805
67	80	75	805
68	30	325	805
69	90	75	805
70	25	345	805
71	30	330	805
72	35	315	805
73	80	330	805
-1			

CSA FOLDS AXIS (FA) AND STRETCHING LINEATIONS (SL)
CSA AND SPOTTED LEOPARD
0
TREND/PLUNGE
0
NO QUANTITY
1

number	;trend	;plunge	;type	;
1	352	75	fa	
2	180	14	fa	
3	170	78	fa	
4	165	40	fa	
5	165	55	fa	
6	165	60	fa	
7	90	78	fa	
8	155	55	fa	
9	170	60	fa	
10	0	85	sl	
11	177	50	fa	
12	176	53	fa	
13	180	15	fa	
14	175	45	fa	
15	180	10	fa	
16	178	31	fa	
17	175	40	fa	
18	176	44	fa	
19	178	26	fa	
20	180	10	fa	
21	170	49	fa	
22	175	68	fa	
23	178	46	fa	
24	178	15	fa	
25	180	2	fa	
26	180	30	fa	
27	178	35	fa	
28	176	20	fa	
29	198	70	fa	
30	2	78	fa	
31	180	33	fa	
32	120	75	sl	
33	108	78	sl	
34	170	56	fa	
35	177	35	fa	
36	180	17	fa	
37	174	14	fa	
38	176	46	fa	
39	179	10	fa	
40	175	45	fa	
41	170	60	fa	
42	180	1	fa	
43	175	12	fa	
44	2	35	fa	
45	175	38	fa	
46	174	10	fa	
47	180	2	fa	

A3·17

48	180	14 fa
49	170	30 fa
50	176	14 fa
51	180	20 fa
52	178	20 fa
53	180	30 fa
54	175	47 fa
55	175	40 fa
56	178	31 fa
57	180	48 fa
58	179	25 fa
59	2	5 fa
60	178	27 fa
61	176	30 fa
62	178	25 fa
63	178	27 fa
64	178	15 fa
65	103	76 sl
66	130	66 sl
67	100	80 sl
68	130	72 sl
69	130	75 sl
70	112	67 sl
71	110	80 sl
72	124	80 sl
73	115	79 sl
74	128	80 sl
75	180	36 fa
76	180	66 fa
77	0	10 fa
78	175	51 fa
79	166	52 fa
80	160	56 fa
81	167	59 fa
82	178	13 fa
83	157	35 fa
84	174	67 fa
85	4	5 fa
86	160	38 fa
87	170	72 fa
88	168	46 fa
89	165	51 fa
90	174	8 fa
91	170	56 fa
92	171	47 fa
93	172	15 fa
94	174	44 fa
95	175	45 fa
96	172	40 fa
97	170	60 fa
98	168	38 fa
99	167	68 fa
100	172	47 fa
101	171	60 fa
102	170	67 fa
103	174	54 fa

104	165	67 fa
105	167	50 fa
106	175	40 fa
107	170	57 fa
108	165	64 fa
109	170	66 fa
110	120	85 sl
111	114	82 sl
112	110	82 sl
113	115	78 sl
114	105	78 sl
115	175	78 sl
116	112	81 sl
117	105	75 sl
118	125	68 sl
119	97	76 sl
120	105	74 sl
121	110	70 sl
122	128	78 sl
123	140	64 sl
124	116	70 sl
125	105	82 sl
126	95	73 sl
127	50	79 sl
−1		

APPENDIX 4
DENSITY DATA

A4.1

CORE DENSITY MEASURMENTS
TYPE: FRESH ALTERED ROCK

W1 (dry)	W2 (submerged)	BD=W1/W2	%QUARTZ
379.11	138.5	2.737256	40
253.69	92.7	2.736677	15
307.16	108.8	2.823161	15
269.73	97.7	2.760798	15
269.7	95.8	2.815240	10
393.95	139.7	2.819971	15
281.94	99.7	2.827883	5
230.34	82.4	2.795388	5
282.68	101.5	2.785024	20
266.01	95.5	2.785445	5
289.94	103.4	2.804061	1
227.92	81.4	2.8	5
211.2	77.2	2.735751	20
190.83	68.2	2.798093	10
262.23	94.9	2.763224	15
243.76	86.9	2.805063	0
231.49	83.3	2.778991	20
261.61	92.4	2.831277	5
346.08	124.3	2.784231	5
327.47	116.7	2.806083	1
130.02	49.1	2.648065	40
226.43	83.2	2.721514	20
362.03	128.8	2.810791	5
345.3	124.4	2.775723	2
282.25	100.9	2.797324	10
238.68	85.1	2.804700	5
151.85	54.4	2.791360	1
74.05	26.1	2.837164	0
262.28	92	2.850869	10
289.85	102.7	2.822297	5
288.18	101.8	2.830844	5
205.93	73.3	2.809413	10
429.11	152.4	2.815682	2
219.6	77.8	2.822622	2
251.29	88.7	2.833032	1
112.79	39.9	2.826817	10
189.81	67.6	2.807840	5
311.9	112.5	2.772444	10
237.46	84.7	2.803541	10
250.27	88.9	2.815185	5
335.06	122.4	2.737418	8
336.66	127.5	2.640470	20
327.56	121.8	2.689326	80
184.99	65.2	2.837269	5
314.7	111.7	2.817367	10
197.54	70.9	2.786177	10
107.79	38.2	2.821727	15
158.95	55.7	2.853680	10
345.57	123.6	2.795873	80
122.13	43	2.840232	15
224.61	77.9	2.883311	15
353.19	124	2.848306	15

A4.2

268.62	96	2.798125	10
339.72	120.6	2.816915	15
194.22	68.6	2.831195	15
420.06	151.2	2.778174	40
235.13	84.9	2.769493	10
319.31	112.9	2.828255	1
343.53	121.8	2.820443	10
219.86	77.6	2.833247	5
349.42	123.6	2.827022	1
344.71	123	2.802520	5
343.93	122.9	2.798454	3
201.91	72.2	2.796537	5
261.03	94.6	2.759302	5
235.49	83	2.837228	1
362.12	129.5	2.796293	3
361.79	129	2.804573	5
358.44	129.9	2.759353	15
334.86	121.4	2.758319	20
302.38	108	2.799814	15
327.23	116	2.820948	30
113.51	40.2	2.823631	5
358.43	126.7	2.828966	7
138.65	48.7	2.847022	15
303.92	108.1	2.811470	10
267.19	96.4	2.771680	5
285.59	99.9	2.858758	5
173.02	61.1	2.831751	10
263.13	93.2	2.823283	10
298.17	105.3	2.831623	8
201.66	72.1	2.796948	20
224.28	80.4	2.789552	20
257.5	91.7	2.808069	20
325.41	116.1	2.802842	10
109.82	38.9	2.823136	30
351.88	126.8	2.775078	30
243.12	86.3	2.817149	15
330.98	119.2	2.776677	20
204.19	74	2.759324	50
82.02	29.8	2.752348	70
112.91	40.4	2.794801	20
154.95	55.9	2.771914	30
230.98	83.2	2.776201	20
112.07	39.3	2.851653	15
295.17	105.4	2.800474	25
26.26	9.6	2.735416	95
254.55	89.8	2.834632	10
111.22	39.7	2.801511	5
126.22	45.2	2.792477	10
		279.8666	

AVE. DENSITY : 2.798666

CORE DENSITY MEASURMENTS
TYPE: FRESH UNALTERED ROCK
HOLE: DDHSL8

W1 (dry)	W2 (submerged)	BD=W1/W2
376.24	139	2.71
404.62	150	2.70
291.5	107	2.72
146.4	54	2.71
135.91	50	2.72
381.5	139	2.74
291.42	106	2.75
282.98	103	2.75
224.63	82	2.74
280.61	103	2.72
260.47	95	2.74
306.73	112	2.74
257.36	94	2.74
173	64	2.70
280.93	103	2.73
353.09	127	2.78
97.26	36	2.70
185.74	68	2.73
146.63	54	2.72
222.62	82	2.71
330.18	119	2.77
130.16	48	2.71
360.34	131	2.75
274.38	99	2.77
107.06	39	2.75
396.9	144	2.76
122.03	45	2.71
363.25	131	2.77
133.7	49	2.73
157.24	58	2.71
113.41	42	2.70
366.05	134	2.73
352.61	127	2.78
339.25	123	2.76
254.17	92	2.76
155.22	57	2.72
218.42	81	2.70
147.26	54	2.73
1004.9	360	2.79
570.4	208	2.74
499.98	180	2.78
916.8	336	2.73
1322.1	474	2.79
835.7	300	2.79
818.2	295	2.77
683.5	246	2.78
486.32	176	2.76
792.2	286	2.77
949.9	341	2.79
543.63	196	2.77
587.27	209	2.81
545.33	199	2.74

A4.4

819.5	285	2.78
547.74	198	2.77
784.7	282	2.78
210.95	78	2.70
502.32	182	2.76
504.15	182	2.77
253.36	92	2.75
415.63	150	2.77
359.99	132	2.73
438.61	158	2.78
334.86	123	2.72
503.92	182	2.77
391.49	142	2.76
378.61	137	2.76
388.88	141	2.76
306.62	112	2.74
364	135	2.70
515.75	186	2.77
406.03	147	2.76
343.01	126	2.72
225.77	83	2.72
278.1	101	2.75
133.79	49	2.73
234.9	87	2.70
405.44	150	2.70
180.31	66	2.73
324.23	118	2.75
330.07	120	2.75
417.9	151	2.77
297	107	2.78
345.28	125	2.76
389.89	142	2.75
299.76	109	2.75
473.17	172	2.75
257.15	95	2.71
269.61	98	2.75
217.66	79	2.76
333.92	120	2.78
411.32	152	2.71
213.32	78	2.73
374.19	136	2.75
275.5	100	2.76
417.78	152	2.75
493.08	180	2.74
451.04	164	2.75
564.43	206	2.74
450.75	163	2.77
276.11	100	2.76
349.17	126	2.77
472.65	174	2.72
373.94	138	2.71
322.77	117	2.76
509.27	184	2.77
454.11	166	2.74
447.48	162	2.76
240.88	88	2.74

A 4.5

428.82	156	2.75
430.82	157	2.74
362.82	132	2.75
416.58	151	2.76
353.16	129	2.74
358.56	130	2.76
317.2	115	2.76
355.2	128	2.78
385.22	140	2.75
424.1	157	2.70
307.02	113	2.72
308.2	114	2.70
308.11	114	2.70
236.65	86	2.75
366.55	133	2.76
311.15	113	2.75
419.11	153	2.74
220.79	81	2.73
340.25	125	2.72
353.86	129	2.74
373.74	136	2.75
249.66	91	2.74
338.55	122	2.78
346.18	126	2.75
318.82	116	2.75
282.85	103	2.75
230.24	84	2.74
358	129	2.78
259.4	94	2.76
343.47	125	2.75
403.88	146	2.77
446.62	162	2.76
418.23	152	2.75
345.59	125	2.76
474.04	172	2.76
295.79	107	2.76
411.85	149	2.76
355.69	128	2.78
317.89	116	2.74
355.16	129	2.75
302.59	109	2.78
294.43	107	2.75

411.9747

AVE. DENSITY : 2.75

A4.6

CORE DENSITY MEASURMENTS
TYPE: IRONSTONE

W1 (dry)	W2 (submerged)	BD=W1/W2	%QUARTZ
746.2	319	2.339184	0
336.01	132.5	2.535924	0
519.2	223.5	2.323042	0
692.2	272	2.544852	15
664.3	287.2	2.313022	5
448.72	189	2.374179	1
395.82	150.5	2.630033	0
320.04	124.5	2.570602	1
588.13	242.7	2.423279	0
341.51	142.3	2.399929	0
267.24	104	2.569615	0
348.82	125	2.79056	0
432.27	170.2	2.539776	0
277.95	108	2.573611	0
444.24	192.5	2.307740	0
517.74	230	2.251043	0
1150.9	445	2.586292	0
458.82	208.2	2.203746	0
1032.3	406	2.542610	5
508.16	237	2.144135	1
449.67	181	2.484364	1
112.87	44	2.565227	0
187.43	70	2.677571	0
687	256.5	2.678362	0
221.33	79.5	2.784025	0
126.76	54.5	2.325871	0
452.83	175	2.5876	0
207.02	96.5	2.145284	0
333.11	122.7	2.714832	1
155.71	60.5	2.573719	0
545.05	225	2.422444	0
158.76	60	2.646	0
280.49	113	2.482212	0
424.61	183.5	2.313950	1
567.11	217.5	2.607402	0
554.18	258.5	2.143829	1
579.94	269.5	2.151910	2
1201.7	523	2.297705	0
1341.8	517	2.595357	0
999.6	387	2.582945	25
1936.4	830	2.333012	0
1190.9	500	2.3818	0
1525.9	760	2.007763	0

105.4663

AVE. DENSITY : 2.452706

CORE DENSITY MEASURMENTS
TYPE: PORPHYRY

W1 (dry)	W2 (submerged)	BD=W1/W2
145.96	54.9	2.659
286.47	108.2	2.648
149.93	56.6	2.649
260.21	99.2	2.623
258.9	97.2	2.664
166.48	62.7	2.655
198.45	74.8	2.653
77.78	29.2	2.664
317.79	119.8	2.653
165.42	62.2	2.659
69.87	26.4	2.647
253.5	95.8	2.646
187.94	71.5	2.629
389.29	147.6	2.637
397.77	150.3	2.647
228.55	85.7	2.667
135.63	51.2	2.649
308.1	115.7	2.663
265.82	100.1	2.656
200.43	75.1	2.669
129.28	48.5	2.666
226.76	85.9	2.640
299.31	113.6	2.635
130.72	49.5	2.641
220.62	83.6	2.639
281.36	106.7	2.637
244.82	92.8	2.638
220.98	83.8	2.637
429.36	162.4	2.644
331.69	125.5	2.643
222.07	83.6	2.656
341.66	129	2.649
413.35	156.4	2.643
84.28	31.9	2.642
169.52	64.6	2.624
167.89	64	2.623
218.87	83.3	2.627
300.74	114.7	2.622
321.01	122	2.631
230.98	87.9	2.628
264.24	100.6	2.627
298.35	112.6	2.650
352.87	133.9	2.635
429.6	163.4	2.629
133.96	50.7	2.642
443.61	169	2.625
395.79	150.2	2.635
118.89	45.4	2.619
256.19	97.5	2.628
265.67	100.4	2.646
251.47	94.6	2.658
334.08	126.2	2.647

248.69	93.8	2.651
119.6	44.6	2.682
124.54	46.6	2.673
41.05	15.3	2.683
212.82	80.5	2.644
79.59	30	2.653
80.38	30.3	2.653
380.02	144	2.639
159.51	60.5	2.637
376.07	142.5	2.639
231.5	87.7	2.640
63.94	24.4	2.620
144.43	54.6	2.645
134.08	50.7	2.645
264.18	100.4	2.631
57.92	22	2.633
123.55	46.9	2.634
155.83	59.1	2.637
64.39	24.3	2.650
203.34	76.8	2.648
79.44	29.8	2.666
194.68	75.1	2.592
218.4	82.5	2.647
300.69	113.9	2.640
158.69	59.8	2.654
74.91	28.5	2.628
77.26	29.3	2.637
244.43	93.5	2.614
361.18	137.5	2.627
52.33	19.8	2.643
386.7	146.3	2.643
465.28	176	2.644
249.28	94.5	2.638
107.77	40.8	2.641
280.98	106.1	2.648
101.91	38.6	2.640
229.22	86.4	2.653
401.73	151.5	2.652
253.37	95.9	2.642
49.36	18.51	2.667
265.8	100.6	2.642

245.833

AVE. DENSITY : 2.643

A4-9

CORE DENSITY MEASURMENTS
TYPE: RHYOLITE

HOLE	DEPTH(M)	W1 (dry)	W2 (submerged)	BD=W1/W2	%QUARTZ
PP324	0 - 1	94.12	35.3	2.666	5
TRAY 1		185.21	69.5	2.665	7
		210.57	78.6	2.679	5
		163.69	61.5	2.662	5
		145.29	54.7	2.656	0
		150.9	56.8	2.657	5
		94.65	35.5	2.666	1
		156.29	59.4	2.631	0
		68.98	26.2	2.633	0
		158.91	60.4	2.631	7
		71.79	27.2	2.639	5
		70.01	26.6	2.632	2
		55.7	21.2	2.627	0
	1 - 2	98.09	37.2	2.637	1
		106.88	40.6	2.633	7
		132.55	50.6	2.620	0
		104.07	39.5	2.635	0
		116.53	43.6	2.673	8
		122.72	46.5	2.639	5
		99.71	37.7	2.645	2
		91.28	34.2	2.669	2
		101.48	38.11	2.663	5
		177.7	67.4	2.636	0
		56.63	21.3	2.659	0
		55.45	20.8	2.666	0
		232.85	87.5	2.661	0
	2 - 3	147.29	54	2.728	3
		40.69	15	2.713	2
		237.07	87.7	2.703	5
		140.24	52	2.697	3
		231.17	85.9	2.691	0
		251.77	94	2.678	5
		424.42	160.6	2.643	7
		311.83	117.7	2.649	8
		195.15	72.9	2.677	0
	3 - 4	317.27	119.5	2.655	2
		61.11	22.9	2.669	3
		186.87	69.9	2.673	7
		33.6	12.4	2.710	0
		234.73	87.6	2.680	2
		80.71	30	2.690	0
		240.96	89.6	2.689	10
		89.45	33.1	2.702	1
		261.37	96.7	2.703	1
		188.37	69.7	2.703	3
		214.4	80.4	2.667	9
		99.81	37.2	2.683	0
		246.03	91.6	2.686	7
		123.98	45.9	2.701	2
		86.84	32	2.714	0
	4 - 5	133.09	49.5	2.689	0
		66.3	22.7	2.921	1

A 4010

		69.22	25.8	2.683	0
		164.41	60.8	2.704	2
		103.92	38.2	2.720	1
		63.62	23.2	2.742	2
		98.71	36.1	2.734	1
		60.44	20.4	2.963	25
		90.92	33.6	2.706	20
		169.5	62.5	2.712	28
		64.4	23.7	2.717	0
		145.41	53.5	2.718	8
		243.23	91.1	2.670	65
	5 - 6	175.95	65.2	2.699	5
		134.31	49.8	2.697	35
		66.58	24.8	2.685	40
		97.06	35.5	2.734	45
		121.62	44.8	2.715	18
		369.44	136.3	2.710	15
		106.87	39	2.740	2
		317.16	115.9	2.736	1
		103.81	38.4	2.703	80
		121.82	44.9	2.713	40
	6 - 7	180.31	66	2.732	0
		245.39	89.5	2.742	3
		316.04	115.2	2.743	3
		126.32	47.3	2.671	70
		79.04	29.26	2.701	40
		244.21	89.1	2.741	1
		186.31	68.3	2.728	0
		345.62	126.9	2.724	2
		349.63	128.3	2.725	1
	7 - 8	138.19	50.5	2.736	0
		395.89	144.4	2.742	0
		152.93	56.2	2.721	7
		256.66	93.9	2.733	1
		154.85	57	2.717	3
PP246	350-351	311.98	118.5	2.633	2
TRAY 43		358.74	136.6	2.626	0
		227.29	84.6	2.687	1
		267.06	100	2.671	1
	351-352	270.36	102.1	2.648	0
		169.68	63.7	2.664	0
		338.39	127.7	2.650	1
		293.95	111.4	2.639	0
		125.19	47.19	2.653	1
		328.07	123.4	2.659	0
		185.19	70.2	2.638	0
		490.99	185.5	2.647	5
		247.34	94.1	2.628	0
		177.2	67.8	2.614	0
		118.69	44.7	2.655	0
	354-355	199.9	76.6	2.610	0
		372.86	142.8	2.611	0
		322.53	123.3	2.616	0
		401.33	153.3	2.618	0
	355-356	282.39	107.9	2.617	0
		369.57	140.4	2.632	7

A4•11

	169.94	63.9	2.659	0
	205.94	77	2.675	0
	289.11	109.5	2.640	0
	230.52	87.3	2.641	0
356-357	326.3	124.1	2.629	0
	258.93	98.4	2.631	1
357-358	187.27	70.7	2.649	0
	243.23	91.9	2.647	1
	200.08	75.4	2.654	1
	208.02	79	2.633	1
	260.77	98.7	2.642	0
	157.94	59	2.677	1
	398.91	151.8	2.628	1
358-359	278.37	105.8	2.631	0
	198.26	75.7	2.619	0
	50.8	19.44	2.613	0
	211.38	81	2.610	1

334.641

AVE. DENSITY : 2.677

A4.12

CORE DENSITY MEASURMENTS
TYPE: VOLCANIC BRECCIA

HOLE	DEPTH(M)	W1 (dry)	W2 (submerged)	BD=W1/W2	%QUARTZ
P136	109-110	105.91	39.3	2.695	60
TRAY 14		131.91	48.8	2.703	35
		152.4	56.2	2.712	35
		134.07	48.6	2.759	40
		165.94	61.1	2.716	65
	110-111	55	20.2	2.723	45
		390.96	144.9	2.698	30
		297.71	111.8	2.663	20
		379.54	142.4	2.665	40
		330.09	124.8	2.645	30
		305.18	114.9	2.656	55
		339.49	126.6	2.682	40
		269.61	100.2	2.691	50
	111-112	262.43	98.5	2.664	30
		312.92	116.2	2.693	15
		347.1	128.1	2.710	55
		321.4	118.8	2.705	60
		349.43	128.6	2.717	25
		312.7	115.7	2.703	35
		302.46	111.6	2.710	45
		298.71	110.6	2.701	70
		327.31	121.5	2.694	80
	112-113	333.06	123.5	2.697	50
		368.93	136.9	2.695	65
		266.84	99.1	2.693	35
		499.07	187.1	2.667	70
		283.17	105.2	2.692	60
		254.37	94.3	2.697	70
		240.8	89.1	2.703	70
	113-114	408.58	150.8	2.709	50
		299.57	111	2.699	65
		252.14	93.1	2.708	60
		268.63	99.4	2.703	60
		307.96	113.7	2.709	50
		357.26	132.5	2.696	70
		307.03	113.8	2.698	75
		313.47	116.2	2.698	70
		277.54	102.5	2.708	40
	114-115	319.65	118.6	2.695	75
		349.95	128.7	2.719	60
		403.07	149.8	2.691	60
		184.73	68.8	2.685	50
		272.83	103.2	2.644	85
		311.79	117.1	2.663	45
	115-116	382.9	148.3	2.582	90
		262.63	98.7	2.661	60
		81.29	30.5	2.665	60
		122.18	46.3	2.639	65
		367.62	137.2	2.679	60
		471.84	177.4	2.660	55
		376.24	142.4	2.642	65
		266.42	101	2.638	60

A4:13

		226.72	86.1	2.633	70
		374.79	142.6	2.628	65
		367.25	140	2.623	60
		267.48	102.3	2.615	75
		290.03	110.7	2.620	55
	116-117	376.38	142.8	2.636	60
		308.57	118.8	2.597	70
		360.37	137.2	2.627	25
		335.64	125.1	2.683	25
		284.22	106	2.681	70
PP267	119-120	374.93	140.9	2.661	90
TRAY 15		157.21	56.8	2.768	55
		338.69	125.4	2.701	65
		275.66	100.1	2.754	55
		254.55	94.6	2.691	75
		260.91	97.6	2.673	75
		296.24	111.3	2.662	90
		375.43	138.9	2.703	80
		159.63	59.7	2.674	90
		133.66	50.3	2.657	90
	120-121	159.69	60.2	2.653	85
		321.42	120.5	2.667	70
		207.5	79.12	2.623	60
		301.31	114.4	2.634	85
		156.75	58.6	2.675	65
		209.32	78.2	2.677	70
		217.64	82.2	2.648	80
		89.93	33.8	2.661	80
		234.89	89	2.639	95
	121-122	263.06	100.1	2.628	95
		235.47	88.6	2.658	65
		311.27	117.5	2.649	65
		262.7	99.2	2.648	95
		333.79	125.2	2.666	90
	122-123	357.3	134.7	2.653	95
		220.54	84	2.625	95
		305.14	115.3	2.646	95
		358.69	134.4	2.669	95
		336.06	125.2	2.684	80
		401.63	148	2.714	65
		221.89	82.1	2.703	70
		273.69	100.8	2.715	45
		352.35	132.2	2.665	30
	123-124	270.74	102.5	2.641	70
		64.64	24.4	2.649	45
		291.91	110.7	2.637	70
		290.65	109.4	2.657	35
		293	112.4	2.607	75

267.413

AVE. DENSITY : 2.674

A4-14

CORE DENSITY MEASURMENTS
TYPE: WEATHERED ALTERED ROCK

W1 (dry)	W2 (submerged)	BD=W1/W2	%QUARTZ
491.08	186.4	2.634549	2
730.6	279.2	2.616762	40
297.87	120.1	2.480183	3
819	322.2	2.541899	5
441.21	175.4	2.515450	5
283.24	108.5	2.610506	100
294.27	117.3	2.508695	5
799.6	310	2.579354	25
372.25	142.7	2.608619	2
316.37	118.6	2.667537	10
482.77	188.6	2.559756	85
521.48	205.4	2.538851	10
303.92	122.1	2.489107	15
929.9	379.2	2.452267	5
251.26	100	2.5126	5
787.3	308	2.556168	8
259.06	103.2	2.510271	8
53.31	20.9	2.550717	5
83.2	33.2	2.506024	2
137.91	54.5	2.530458	3
196.59	78.8	2.494796	0
395.31	162.7	2.429686	6
237.19	92.4	2.566991	10
843.9	337	2.504154	5
764.6	331.9	2.303705	4
979.2	384.6	2.546021	0
296.43	113.4	2.614021	70
628.3	252	2.493253	15
1044.1	414.7	2.517723	15
151.11	60.5	2.497685	5
830.3	318.7	2.605271	90
1189.8	464.6	2.560912	40
823.6	334.4	2.462918	0
692.2	275.6	2.511611	5
201.97	82.7	2.442200	5
1416.6	560	2.529642	6
1103.4	444.2	2.484016	2
572.69	227.9	2.512900	1
167.29	65.5	2.554045	5
939.5	369	2.546070	2
825	333	2.477477	4
652.3	264.7	2.464299	0
759.2	296.9	2.557089	3
192.22	76.6	2.509399	0

111.1556

AVE. DENSITY : 2.585015

A4:15

CORE DENSITY MEASURMENTS
TYPE: WEATHERED UNALTERED ROCK

W1 (dry)	W2 (submerged)	BD=W1/W2	%QUARTZ
808.8	350	2.310857	0
203.29	86.3	2.355619	0
215.24	95.8	2.246764	0
480.69	220	2.184954	0
161.79	69.7	2.321233	0
432.29	179.3	2.410987	0
311.2	129.9	2.395688	0
386.67	168.2	2.298870	0
321.13	135.4	2.371713	0
546.78	237.9	2.298360	0
117.99	49.4	2.388461	0
509.77	218.5	2.333043	0
123.77	50.5	2.450891	0
180.45	80.6	2.238833	0
309.08	133.8	2.310014	0
506.5	225.7	2.244129	0
328.19	147.5	2.225016	0
317.27	147.7	2.148070	0
221.94	96.3	2.304672	0
434.23	190.4	2.280619	0
163.48	71.8	2.276880	0
148.23	58.5	2.533846	0
531.82	229.5	2.317298	0
274.08	114.1	2.402103	0
265.37	114.8	2.311585	0
165.71	71.2	2.327387	0
167.99	71.3	2.356100	0
383.37	175.3	2.186936	0
178.94	73.7	2.427951	0
175.79	76.3	2.303931	0
181.04	77.8	2.326992	0
92.56	38.3	2.416710	0
120.14	52.5	2.288380	0
275.73	121.7	2.265653	0
104.79	44.2	2.370814	0
60.95	25.9	2.353281	0
134.48	55.7	2.414362	0
197.88	82.4	2.401456	0
252.32	106.3	2.373659	0
213	88.8	2.398648	0
58.08	24.9	2.332530	0
56.48	24.5	2.305306	0
28.5	11.79	2.417302	0
811.6	347.9	2.332854	0
332.92	147.6	2.255555	0
456.9	196.4	2.326374	0
546.81	242	2.259545	0
150.69	66.4	2.269427	0
433.37	197.4	2.195390	0
382.83	167	2.292395	0
315.93	114.1	2.768886	0
424.94	183.9	2.310712	0

A4.16

1035	446	2.320627	0
447.37	190	2.354578	0
165.69	72.2	2.294875	0
696.1	301.5	2.308789	0
395.96	176	2.249772	0
1152	496.3	2.321176	0
266.04	114.2	2.329597	0
302.15	131.2	2.302972	0
376.97	160.5	2.348722	0
373.25	161.5	2.311145	0
174.6	77.5	2.252903	0
418.69	180.5	2.319612	0
203.93	89	2.291348	0
466.27	189	2.467037	0
49.17	22.46	2.189225	0
39.67	16.7	2.375449	0
534.34	227.5	2.348747	0
169.74	72.5	2.341241	0
155.07	66.7	2.324887	0
		165.2917	
	AVE. DENSITY :	2.328053	

APPENDIX 5
REGIONAL GRAVITY MODEL DATA

```
COBAR REGIONAL GRAVITY MODEL
 0              70000          10000
-5000           0              1000
-25             0              5
 0              200            50
 0              70000          200
B
regrav
 0
none
 0
 4

 57600
-62.4
 9
 90
 100

 1
 6
 .08
 0
 0
 0
 0
 10000         -1000
ZONE 2
 1              220

 0             -.01
 19000         -.01
 20000         -2600
 13000         -1800
 0             -1800
 0             -.01


 2
 5
 .08
 0
 0
 0
 0
 25000         -1000
ZONE 1
 2              220

 19000         -.01
 30000         -.01
 29000         -1600
 20000         -2600
 19000         -.01


 3
 10
```

-.12	
0	
0	
0	
0	
45000	-3000
GRANITE/BASEMENT	
3	220
37000	-500
52000	-400
70000	-1300
70000	-5000
0	-5000
0	-1800
13000	-1800
20000	-2600
29000	-1600
37000	-500
4	
7	
.08	
0	
0	
0	
0	
60000	-300
BALLAST BEDS	
4	220
30000	-.01
70000	-.01
70000	-1300
52000	-400
37000	-500
29000	-1600
30000	-.01

REGRAV. OBS.

00000.0	-5.6
12000.0	-8.5
21000.0	-5.2
37000.0	-18.9
52000.0	-20.0
67000.0	-11.8

APPENDIX 6
BASIN WIDE GRAVITY MODEL DATA

```
CSA MODEL
 372000       386000       2000
-5000         0            1000
-13          -4            1
 0            200          50
 372000       386000       200
B
csa
 0
NONE
 0
 34

 57600
-62.4
 9
 90
 100

 1
 5
-.03
 0
 0
 0
 0
 375600      -50
walt
 2            220

 375570      -.01
 375640      -.01
 375650      -110
 375590      -110
 375570      -.01


 2
 5
-.34
 0
 0
 0
 0
 375730      -50
wunalt
 7            220

 375640      -.01
 375675      -.01
 375710      -110
 375650      -110
 375640      -.01


 3
 5
-.09
 0
 0
 0
 0
 375730      -50
walt
 2            220

 375675      -.01
 375740      -.01
 375780      -90
 375710      -110
 375675      -.01


 4
 5
-.34
 0
 0
 0
 0
 375900      -50
wunalt
 7            220

 375740      -.01
 376005      -.01
 376008      -80
 375780      -90
 375740      -.01


 5
 5
-.09
 0
 0
 0
 0
 376020      -50
walt
 2            220

 376005      -.01
 376025      -.01
 376030      -80
 376008      -80
 376005      -.01


 6
 5
-.34
 0
 0
 0
 0
```

```
 376100        -50
wunalt
 7              220

 376025        -.01
 376500        -.01
 376500        -80
 376030        -80
 376025        -.01


 7
 5
-.34
 0
 0
 0
 0
 375550        -50
wunalt
 7              220

 375460        -.01
 375570        -.01
 375590        -110
 375495        -120
 375460        -.01


 8
 5
-.34
 0
 0
 0
 0
 375450        -50
walt
 2              220

 375410        -.01
 375460        -.01
 375495        -120
 375440        -120
 375410        -.01


 9
 5
-.34
 0
 0
 0
 0
 375300        -50
wunalt
 7              220
```

```
 370000        -.01
 375410        -.01
 375430        -80
 370000        -80
 370000        -.01


 10
 11
 .08
 0
 0
 0
 0
 375300        -200
funalt
 5              220

 374175        -80
 375430        -80
 375480        -250
 375520        -460
 375560        -800
 375590        -1150
 375620        -1850
 375620        -2050
 374175        -2250
 374175        -1950
 374175        -80


 11
 15
 .13
 0
 0
 0
 0
 375500        -250
falt
 6              220

 375440        -120
 375495        -120
 375525        -235
 375535        -460
 375585        -800
 375615        -1200
 375645        -2000
 375645        -2050
 375620        -2050
 375620        -2000
 375590        -1200
 375560        -800
 375520        -460
 375480        -250
 375440        -120
```

A6-3

12
15
.08
0
0
0
0

375600	-300

funalt

5	220
375495	-120
375590	-110
375590	-180
375650	-330
375680	-600
375715	-1200
375730	-2000
375730	-2050
375645	-2050
375645	-2000
375615	-1200
375585	-800
375535	-460
375525	-235
375495	-120

13
15
.26
0
0
0
0

375700	-600

falt

6	220
375590	-110
375650	-110
375675	-200
375690	-375
375745	-570
375760	-1200
375780	-2000
375780	-2050
375730	-2050
375730	-2000
375715	-1200
375680	-600
375650	-330
375590	-180
375590	-110

14
14
.08
0
0
0
0

375700	-300

funalt

5	220
375650	-110
375710	-110
375775	-310
375770	-430
375830	-1200
375880	-2000
375880	-2050
375780	-2050
375780	-2000
375760	-1200
375745	-570
375690	-375
375675	-200
375650	-110

15
14
.32
0
0
0
0

375800	-400

falt

6	220
375710	-110
375780	-90
375840	-245
375890	-460
375955	-840
376000	-1200
376050	-2000
376050	-2050
375880	-2050
375880	-2000
375830	-1200
375770	-430
375775	-310
375710	-110

16
13
.08
0
0

0
0
376000 -400
funalt
5 220

375780 -90
376008 -80
376025 -650
376075 -1200
376130 -2000
376130 -2050
376050 -2050
376050 -2000
376000 -1200
375955 -840
375890 -460
375840 -245
375780 -90

17
5
.08
0
0
0
0
376030 -500
falt
6 220

376008 -80
376030 -80
376060 -650
376025 -650
376008 -80

18
10
.25
0
0
0
0
376100 -800
falt
6 220

376025 -650
376060 -650
376145 -830
376180 -1200
376230 -2000
376230 -2050
376130 -2050
376130 -2000
376075 -1200
376025 -650

19
8
.08
0
0
0
0
376200 -400
funalt
5 220

376030 -80
376500 -80
376500 -2000
376230 -2000
376180 -1200
376145 -830
376060 -650
376030 -80

20
18
-.12
0
0
0
0
381000 -2500
GRANITE/BASEMENT
3 220

388000 -650
388000 -5000
370000 -5000
370000 -1350
372000 -1350
374175 -1950
374175 -2250
375620 -2050
376230 -2050
376500 -2000
376600 -2000
377400 -1950
377500 -1950
378900 -1900
379000 -1900
383175 -1450
383175 -950
388000 -650

21
6

A6·5

```
 .08
 0
 0
 0
 0
 373000        -1000
ZONE 2
 4              220

 370000        -80
 374175        -80
 374175        -1950
 372000        -1350
 370000        -1350
 370000        -80


 22
 5
 .08
 0
 0
 0
 0
 384000        -500
BALLAST BEDS
 8              220

 383175        -80
 388000        -80
 388000        -650
 383175        -950
 383175        -80


 23
 5
 .13
 0
 0
 0
 0
 378800        -1500
falt
 9              220

 379000        -80
 379000        -1900
 378900        -1900
 378900        -80
 379000        -80


 24
 5
-.08
 0
 0
 0
 0
 378800        -50
walt
 9              220

 378900        -.01
 379000        -.01
 379000        -80
 378900        -80
 378900        -.01


 25
 5
 .13
 0
 0
 0
 0
 377500        -1500
falt
 9              220

 377500        -80
 377500        -1950
 377400        -1950
 377400        -80
 377500        -80


 26
 5
 .13
 0
 0
 0
 0
 376500        -1500
falt
 9              220

 376600        -80
 376600        -2000
 376500        -2000
 376500        -80
 376600        -80


 27
 5
 .08
 0
 0
 0
 0
 376700        -1000
funalt
```

```
 9           220
 376600     -80
 377400     -80
 377400     -1950
 376600     -2000
 376600     -80


 28
 5
 .08
 0
 0
 0
 0
 378000     -1000
funalt
 9           220

 377500     -80
 378900     -80
 378900     -1900
 377500     -1950
 377500     -80


 29
 6
 .08
 0
 0
 0
 0
 380000     -1000
funalt
 9           220

 379000     -80
 383175     -80
 383175     -950
 383175     -1450
 379000     -1900
 379000     -80


 30
 5
-.08
 0
 0
 0
 0
 376500     -50
walt
 9           220

 376500     -.01
 376600     -.01
 376600     -80
 376500     -80
 376500     -.01


 31
 5
-.08
 0
 0
 0
 0
 377400     -50
walt
 9           220

 377400     -.01
 377500     -.01
 377500     -80
 377400     -80
 377400     -.01


 32
 5
-.34
 0
 0
 0
 0
 377000     -50
wunalt
 9           220

 376600     -.01
 377400     -.01
 377400     -80
 376600     -80
 376600     -.01


 33
 5
-.34
 0
 0
 0
 0
 378000     -50
wunalt
 9           220

 377500     -.01
 378900     -.01
 378900     -80
 377500     -80
 377500     -.01
```

```
 34
 5
-.34
 0
 0
 0
 0
 382000        -50
wunalt
 9              220

 379000        -.01
 388000        -.01
 388000        -80
 379000        -80
 379000        -.01
```

A6·8

CSA.OBS

374373.0	-6.9
374448.0	-6.8
374523.0	-6.7
374673.0	-6.6
374823.0	-6.5
374933.0	-6.4
375003.0	-6.3
375113.0	-6.2
375193.0	-6.1
375268.0	-6.0
375408.0	-5.9
375448.0	-5.9
375458.0	-5.9
375498.0	-5.8
375653.0	-5.7
375668.0	-5.6
375678.0	-5.5
375688.0	-5.4
375773.0	-5.3
375813.0	-5.4
375833.0	-5.5
375858.0	-5.6
375888.0	-5.7
375928.0	-5.8
375973.0	-5.9
376048.0	-6.0
376088.0	-6.0
376218.0	-6.1
376273.0	-6.1
376328.0	-6.0
376373.0	-6.0
376443.0	-6.1
376523.0	-6.2
376593.0	-6.3
376648.0	-6.4
376708.0	-6.5
376748.0	-6.5
376777.0	-6.5
376952.0	-6.6
377032.0	-6.7
377067.0	-6.7
377117.0	-6.7
377207.0	-6.7
377312.0	-6.6
377472.0	-6.6
377507.0	-6.7
377612.0	-6.8
377677.0	-6.9
377767.0	-7.0
377817.0	-7.1
377892.0	-7.2
377972.0	-7.3
378032.0	-7.3
378162.0	-7.4
378272.0	-7.5
378417.0	-7.4
379087.0	-7.4
379132.0	-7.5
379192.0	-7.6
379265.0	-7.7
379310.0	-7.8
379375.0	-7.9
379525.0	-8.0
379605.0	-8.1
379660.0	-8.2
379695.0	-8.3
379755.0	-8.4
379860.0	-8.5

APPENDIX 7
Cu/Au ^S34 DATA

Sulfur isotope compositions, Cobar, Australia

Sample location		$\delta^{34}S$ per mil py	po	cp	Description
1. CHESNEY FORMATION/GREAT COBAR SLATE CONTACT					
East Cobar					
CA9A	269			9.9	3cm qtz-py vein
	353	8.7			20cm qtz vein with w/r inc
New Cobar					
CA18	371		5.2	6.0	irregular 4cm qtz vein
	373		3.8	4.2	20cm cp-qtz vein
	374			5.4	1cm c/p qtz vein
	374			5.8	4mm folded cp vein in slate
	375		6.8	5.8	10cm qtz vein
CA17	404		6.5	5.7	20cm qtz-chl vein
	405		5.6	5.5	10cm c/p brecciated qtz vein
	413		7.0	5.4	15cm qtz vein with w/r inc
	415		5.1	6.0	10cm cp-po-qtz veins in slate
	415.5		4.8	5.3	po-cp-qtz network in slate
Blue Shaft					
CA2C	489			8.4	2cm c/p qtz vein
	496.5			8.2	10cm c/p qtz vein
	496.8			8.2	20cm c/p qtz vein
	543			8.1	5cm c/p qtz vein
Chesney					
CM3	894			9.0	irregular qtz-cp vein in sltst
	896			9.0	qtz-cp vein
	896.5			8.8	qtz-cp vein
	897			9.1	brecciated qtz-carb vein
	969.5			9.9	brecciated silic chl-carb vein
	969.8			9.6	qtz-cp vein
	970			9.2	diss cp in chl silic slate
	971			9.0	3cm c/p qtz-chl vein
CM3D	1114		10.1	10.0	5cm c/p qtz vein
	1118			8.6	irregular cp-carb-qtz vein
	1119			8.1	wispy cp in chl slate
	1123			9.7	wispy cp in silic chl slate
	1127			9.0	qtz-cp vein
	1129			9.6	qtz-cp vein

Mt Pleasant					
CA12	370			7.8	12cm c/p qtz vein with w/r inc
	371.6			7.2	irregular qtz vein
	372.2			9.0	20cm qtz vein with w/r inc
	383			9.0	10cm c/p qtz vein
CA13	311		8.6	9.0	4cm c/p qtz vein
	318			8.6	laminated 5cm c/p qtz vein
	408			7.5	5cm c/p qtz vein with w/r inc
	415			7.9	c/p cp-qtz vein
CA14	77			9.5	qtz-cp vein
	397			7.9	irregular cp-qtz veining
	403			8.5	c/p cp-qtz vein in chl slate
	404.9			8.4	cp vein with w/r inc
	405.5			8.5	irregular qtz vein
	405.8			8.8	qtz veining in chl slate
	536			7.5	qtz-cp vein
Wood Duck					
CA6	312			8.2	2cm c/p qtz vein
	338			8.0	20cm c/p qtz vein
	341			8.2	20cm qtz vein
CA15A	343.8			8.4	irregular qtz-chl-sulfide vein
	344		9.0	8.8	irregular qtz-sulfide vein
	351			8.0	2mm qtz-cp vein
Occidental					
CA22A	423			8.0	20cm qtz vein
	434.6		9.4	9.1	10cm qtz vein
	435.6		8.9		4cm c/p qtz-sulfide vein
DDH155	65			10.8	irregular qtz-chl-carb vein
OD1 dump				6.1	qtz-chl-mt-cp lode
OD2 dump		11.2			chl-py-mt lode
Queen Bee					
CM6	296.5			7.3	diss sulfide in chl slate
	296.9	8.1		8.3	diss cp in chl slate
CM7	421			7.6	irregular cp veinlets in slate
	426			7.1	irregular cp veinlets in slate
	427	7.7		7.4	c/p veins in slate
	437	7.3		7.3	c/p veins in slate
	449	7.9			irregular py vein in slate
	457	7.7		7.5	sulfide veinlets in sltst
	477			7.1	wispy cp in chl slate
CM7D1	425	8.1		7.3	c/p sulfide veinlets in slate
	426	7.7		7.3	c/p sulfide veinlets

2. GREAT COBAR SLATE HOSTROCK

Great Cobar				
DDH256	10	10.5		3mm c/p py-mt vein in slate
DDH259	120		8.8	patchy cp in siltstone
	170		8.7	mt-py-qtz lode
	205		8.4	mt-chl-qtz-sulfide lode
	230		9.4	chl-qtz-sulfide lode
CM1	1282	9.2	7.9	mt-qtz-chl-sulfide lode
	1284	7.8	7.9	mt-qtz-sulfide lode
	1290	8.7	7.9	sulfide-mt veinlets
	1303		8.3	irregular mt-cp-qtz vein
	1318		8.0	10cm chl-cp-qtz vein in slate
Dapville				
DDH2	55	7.4(gl)		2mm gl-qtz veinlets in slate
Gladstone				
GS6	224		7.8	c/p qtz-carb veinlets in slate
	226		8.6	irregular cp veinlets in slate
DDH261	190		8.4	qtz-carb-chl-cp veins in slate

Notes: Drill hole numbers and depths (m) are given for each sample, unless indicated otherwise (see Figs. 1, 4 and 6 for locations). Abbreviations: carb=carbonate, chl=chlorite (chloritic), cp=chalcopyrite, c/p=cleavage-parallel, diss=disseminated, inc=inclusions, mt=magnetite, po=pyrrhotite, py=pyrite, qtz=quartz, silic=silicified, slst=siltstone, w/r=wallrock

Summary of sulfur isotope data, Cobar

Prospect/mine	$\delta^{34}S$ per mil Mean	Range	Number of samples
1. CHESNEY FORMATION/GREAT COBAR SLATE CONTACT			
East Cobar	9.3	8.7 - 9.9	2
New Cobar	5.5	3.8 - 7.0	18
Blue Shaft	8.2	8.1 - 8.4	4
Chesney	9.2	8.1 -10.1	15
Mt Pleasant	8.4	7.2 - 9.5	16
Wood Duck	8.4	8.0 - 9.0	7
Occidental	9.1	6.1 -11.2	7
Queen Bee	7.6	7.1 - 8.3	17
2. GREAT COBAR SLATE HOSTROCK			
Great Cobar	8.6	7.8 -10.5	13
Dapville	-	7.4	1
Gladstone	8.3	7.8 - 8.6	3
Overall data, regions 1 and 2	7.9	3.8 -11.2	103
3. CSA SILTSTONE HOSTROCK (Seccombe and Brill, 1989)			
CSA mine	7.5	4.6 - 9.7	115
Elura mine	8.1	4.7 -12.6	30

APPENDIX 8
CSA DEPOSIT SULFUR AND SELENIUM DATA

A8·1

TOTAL DATA

CU	PB	ZN	SE	BI	S%	%SE	S:SE
0.18	0.03	0.24	19	19	2.2	0.0019	1157.894
1.35	0.87	4.86	60	70	12.1	0.006	2016.666
3.77	2.2	6.89	360	110	30.6	0.036	850
2.81	5.91	14.5	500	160	28.3	0.05	566
0.45	2.24	6.99	110	40	30.5	0.011	2772.727
0.44	2.21	7.03	100	30	34.3	0.01	3430
0.32	1.49	8.39	100	70	32.8	0.01	3280
0.4	0.97	4.62	100	20	43	0.01	4300
0.55	2.06	7.59	250	70	47.1	0.025	1884
0.29	1.93	4.36	60	50	47.6	0.006	7933.333
0.34	1.42	3.98	50	19	44.2	0.005	8840
0.51	7.92	12.7	90	70	42.3	0.009	4700
0.63	5.56	10.7	50	19	44	0.005	8800
1.47	9.75	14	400	60	34.5	0.04	862.5
0.54	13.3	13.6	100	80	36.8	0.01	3680
0.12	7.84	5.51	120	200	8.5	0.012	708.3333
0.05	0.39	0.32	19	19	5.45	0.0019	2868.421
0.1	1.76	4.02	20	30	11.6	0.002	5800
0.21	4.39	8.02	20	19	23.5	0.002	11750
0.38	1.94	5.77	180	50	9.85	0.018	547.2222
0.9	3.88	10.4	320	110	47.4	0.032	1481.25
0.26	4.33	7.8	40	50	32	0.004	8000
2.46	13.9	12.1	1180	350	32.3	0.118	273.7288
0.47	21.8	26.8	70	190	39.2	0.007	5600
0.46	27.9	23.9	20	190	33.6	0.002	16800
0.77	11.9	18.6	60	100	41.8	0.006	6966.666
0.3	9.6	13.9	30	19	43.1	0.003	14366.66
1.93	18.1	9.75	1200	480	40	0.12	333.3333
0.4	5.51	15.9	180	70	47.8	0.018	2655.555
0.38	7.16	16.9	60	60	42.5	0.006	7083.333
0.35	4.07	14.3	160	100	39.8	0.016	2487.5
3	7.89	21.9	1620	630	31	0.162	191.3580
1.06	1.33	21.5	450	130	35.4	0.045	786.6666
0.6	0.65	8.75	330	120	56.1	0.033	1700
2	0.71	9.48	310	160	20.9	0.031	674.1935
0.87	0.53	9.9	250	120	21.2	0.025	848
0.51	0.41	6.3	210	130	21.4	0.021	1019.047
0.46	0.14	4.54	80	50	13.1	0.008	1637.5
0.91	1.63	11.9	220	60	27.6	0.022	1254.545
0.31	3.65	12.6	60	19	35	0.006	5833.333
0.75	4.12	13	230	70	43.6	0.023	1895.652
1.3	1.23	12.3	80	40	45.7	0.008	5712.5
0.38	3.01	12.1	110	50	32.8	0.011	2981.818
0.38	7.18	13.3	120	110	29.4	0.012	2450
0.23	3.42	8.5	40	20	28	0.004	7000
0.23	3.49	9.1	40	19	28	0.004	7000
0.92	2.86	9.2	100	50	28	0.01	2800
0.27	17.8	8.8	130	90	25.8	0.013	1984.615
1.3	3.34	12.4	210	70	25.7	0.021	1223.809
0.55	3.69	10.5	300	90	7.55	0.03	251.6666
0.42	1.84	6.64	150	40	5.35	0.015	356.6666
0.16	1.77	2.67	60	20	5.65	0.006	941.6666

A8•2

1.73	5	22	420	130	37.8	0.042	900
0.52	4.63	13.3	130	30	41.5	0.013	3192.307
0.82	6.43	11.8	120	20	38.4	0.012	3200
0.47	9.24	15.9	20	40	38.1	0.002	19050
0.56	6.55	14.1	60	50	37.6	0.006	6266.666
0.55	17.2	19.6	170	140	32.7	0.017	1923.529
0.25	14.5	24.3	170	130	32.7	0.017	1923.529
0.78	1.89	21.2	530	250	8.3	0.053	156.6037
0.26	0.15	2.36	70	20	9.15	0.007	1307.142
0.13	0.07	1.06	60	19	9.85	0.006	1641.666
0.33	0.15	2.27	90	20	11.2	0.009	1244.444
0.41	0.38	1.64	120	50	9.2	0.012	766.6666
0.19	0.19	0.68	90	50	4.04	0.009	448.8888
0.2	0.1	0.4	80	80	5.95	0.008	743.75
0.8	0.12	1.17	160	180	13	0.016	812.5
1.01	0.08	0.71	140	110	10.9	0.014	778.5714
1.31	0.14	0.62	180	240	10.1	0.018	561.1111
0.83	0.15	1.37	170	200	13.7	0.017	805.8823
0.44	0.17	14.6	270	210	22.9	0.027	848.1481
0.92	0.51	23.8	590	260	26.6	0.059	450.8474
0.77	0.44	13.7	310	260	15.7	0.031	506.4516
1.8	0.71	16.4	790	480	29.1	0.079	368.3544
0.69	0.79	38.6	660	560	32.5	0.066	492.4242
0.63	0.22	38.4	540	350	32.2	0.054	596.2962
0.89	2.89	45.4	690	300	32.1	0.069	465.2173
2.75	0.18	21	390	290	40.2	0.039	1030.769
1.87	0.18	1.5	260	350	27.5	0.026	1057.692
0.08	0.03	0.08	60	20	5.2	0.006	866.6666
0.62	1.14	10.2	720	190	23.6	0.072	327.7777
0.61	4.48	15.7	270	100	23.7	0.027	877.7777
1.25	3.21	29	670	180	28.4	0.067	423.8805
0.68	2.45	21.2	380	140	37.3	0.038	981.5789
1.36	3.29	15.6	260	110	33.1	0.026	1273.076
1.04	5.73	21.5	400	150	38.4	0.04	960
0.72	3.62	23.6	680	170	33.2	0.068	488.2352
0.83	2.6	24.5	530	140	34	0.053	641.5094
0.56	2.26	21.8	310	150	34.2	0.031	1103.225
0.35	1.86	15.4	240	120	26.4	0.024	1100
0.95	1.16	7.04	440	340	11.7	0.044	265.9090
0.56	0.35	5.97	280	190	11.3	0.028	403.5714
1.04	0.18	1.41	190	210	11	0.019	578.9473